UNIVERSITY OF CALIFORNIA,
IRVINE

Identification of Cellular Proteins Important for Jaagsiekte Sheep Retrovirus Transformation

DISSERTATION

submitted in partial satisfaction of the requirements
for the degree of

DOCTOR OF PHILOSOPHY

in Biological Sciences

by

Tom Sih-Yuan Hsu

Dissertation Committee:
Professor Hung Y. Fan, Chair
Professor Paul Gershon
Professor Melanie Cocco
Professor Bert Semler
Professor Suzanne Sandmeyer

2014

DEDICATION

Dedicated to my family

TABLE OF CONTENTS

LIST OF FIGURES

LIST OF TABLES

LIST OF ABBREVIATIONS

DNA	deoxyribonucleic acid
cDNA	complementary deoxyribonucleic acid
RNA	ribonucleic acid
mRNA	messenger ribonucleic acid
HIV-1	human immunodeficiency virus type 1
kb	kilobases
bp	basepairs
kDa	kilodaltons
PR	protease
NC	nucleocapsid protein
RT	reverse transcriptase
IN	integrase
CA	capsid protein
MA	matrix protein
Env	envelope protein
SU	surface protein
TM	transmembrane protein
CT	cytoplasmic tail
LTR	long terminal repeat
U3	region unique to the 3’ end
R	repeat region

U5	region unique to the 5’ end
Gag	group-specific antigen
SD	splice donor
SA	splice acceptor
MSR	membrane spanning region
SP	signal peptide
JSRV	jaagsiekte sheep retrovirus
RSV	Rous sarcoma virus
HTLV (-I or –II)	human T-cell leukemia virus (-I or –II)
MMTV	mouse mammary tumor virus
SFFV	spleen focus forming virus
M-MuLV	Moloney murine leukemia virus
F-MuLV	Friend murine leukemia virus
MPMV	Mason-Pfizer monkey virus
ENTV	enzootic nasal tumor virus
CMV	cytomegalovirus
OPA	ovine pulmonary adenocarcinoma
BAC	bronchioloalveolar carcinoma
AIS	adenocarcinoma in situ
ORF	open reading frame
Rej	translation enhancing factor for JSRV
SPA	surfactant protein A
SPC	surfactant protein C

BASC	bronchioloalveolar stem cells
RK3E	rat kidney epithelial cells
MDCK	Madin-Darby canine kidney cells
en	endogenous
ex	exogenous
PI3K	phosphoinositol-3 kinase
Hyal2	hyaluronidase 2
MAPK	mitogen-activated protein kinase
mTOR	mammalian target of rapamycin
MEK	mitogen-activated protein kinase kinase
ERK	extracellular-signal-regulated kinase
TLR4	toll-like receptor 4
IKAP	IKK complex-associated protein
RRM2	ribonucleotide reductase subunit 2
Zfp111	zinc finger protein 111
KRAB	Krüppel-associated box
TAP	tandem affinity purification
HBH	6xhistidine-biotination site-6xhistidine
shRNA	small-hairpin RNA
Ni^{2+}	nickel
Endo F	endoglycosidase F
Chymo	chymotrypsin
Tx	transformation

Rev	RNA export factor for HIV-1
Rem	RNA export factor for MMTV
NLS	nuclear localization signal
ER	endoplasmic reticulum
ERAD	endoplasmic reticulum-associated protein degradation
GST	glutathione S-transferase
NTA	nitriloacetic acid
MS	mass spectrometry

ACKNOWLEDGEMENTS

To begin, I would like to thank the person who made my graduate career possible: my mentor Dr. Hung Fan. When I am worried about the progress that I am making in my project, he is there to calm me down and help me rationalize things out. He has time and time again helped me find the bright side to my failed experiments, and followed it up with very helpful suggestions and comments that energize me to go further in my research. His patience with his students and his enthusiasm for science helped to make these years of graduate research enjoyable and very enlightening. Now that I am at the end of my graduate career and looking back on it, I realized that I am very blessed to have joined Hung's lab and have him as my mentor. Thank you Hung.

I would also like to thank the Fan Lab, present and past members that I had worked with. These members include post-docs Takayuki Nitta, Andy Hofacre, Chassidy Johnson, Stacey Hull, visiting scientist Jung Woo Kim, my fellow graduate student Maribel Arias, and my master/undergraduate students Parvez Malak and Kevin Choe. Thank you all for your help during my time in the lab. My experiences here would not be as memorable if I have not met all of you and had the privilege of spending time with you all. Although most of us have gone our separate ways, the time that we had to together will forever be our link to each other. I wish everyone the best of luck in their futures.

Other people who have helped my in my graduate studies include my committee members: Dr. Paul Gershon, Dr. Melanie Cocco, Dr. Bert Semler, and Dr. Suzanne Sandmeyer. I am thankful for their helpful suggestions and comments that helped me shape my work and my thinking. In particular, I would like to thank Dr. Gershon and Dr. Cocco for their help in our collaboration on JSRV Env interacting proteins and JSRV Env structure, respectively. Also, thanks to Nita Driscoll, Patty Depetris, and all of the administrators that have passed through CRI and MB&B office that have helped out over the years.

I would like to thank my family. I would like to give my most heartfelt thanks to my parents Jerry and Alice for all of their support and love throughout my entire life. I would like to give deep thanks to my brother Mike for his support and his advice, as well as to my wife An, who motivated me to keep going forward through all of the failures at work. My family has always encouraged me to pursue my dreams and aspirations, and without them I don't think I would be here at this point in my life. Thank you, thank you all so much. Last but not least, I would like to thank God. He has blessed me with having all of these wonderful people in my life, who support me and cares for me.

Financial support was provided by the University of California, Irvine, NIH training grant T32 AI 07319, and NIH grant R01CA094188.

CURRICULUM VITAE

Tom Sih-Yuan Hsu
150 Sprague Hall
Departments of Molecular Biology & Biochemistry
And Cancer Research Institute
University of California, Irvine
Irvine, CA 92697-3905 USA
Phone: (949) 824-6631
Fax: (949) 824-4023
E-Mail: tshsu@uci.edu

EDUCATION:

2006 – 2014	Doctor of Philosophy, Biological Sciences. Program in Cellular and Molecular Biosciences, Molecular Biology and Biochemistry emphasis, University of California, Irvine
2001 – 2005	Bachelor of Arts, Biological Sciences, University of California, Berkeley

PROFESSIONAL EXPERIENCE:

2010 – Current	Graduate Teaching Assistant, Department of Molecular Biology and Biochemistry, University of California, Irvine
2006 – 2007	Graduate Teaching Assistant, Department of Molecular Biology and Biochemistry, University of California, Irvine
2003 – 2005	Research Assistant, Space Science Laboratory, Kunihiko Nishiizumi Laboratory, University of California, Berkeley

HONORS/AWARDS:

2007 – 2010	NIH Predoctoral Training Grant (5 T32 AI 07319) in the field of virology.

PUBLICATION:

- Hsu, T., Phung, A., Kim, J.W., and Fan, H.Y.. 2014. A role for zinc finger protein 111 (Zfp111) in transformation of 208F rat fibroblasts by Jaagsiekte sheep retrovirus envelope protein. (In Preparation)

- Hsu, T., Kim, J.W., and Fan, H.Y.. 2014. Analysis of the role of ribonucleotide reductase subunit 2 (RRM2) in Jaagsiekte sheep retrovirus envelope mediated cell transformation. (In Preparation)

MEETING PRESENTATIONS:

1. West Coast Retrovirus Meeting, Palm Springs, CA. Hsu, T., Kim, J.W., Fan. H.Y., *Ribonucleotide Reductase M2 Knock-down Reduces Oncogenic Transformation by Jaagsiekte Sheep Retrovirus*. Poster Presentation. 2008

2. West Coast Retrovirus Meeting, Palm Springs, CA. Hsu, T., Kim, J.W., Fan. H.Y., *Ribonucleotide Reductase M2 Knock-down Reduces Oncogenic Transformation by Jaagsiekte Sheep Retrovirus*. Oral Presentation. 2009

3. West Coast Retrovirus Meeting, Palm Springs, CA. Hsu, T., Kim, J.W., Fan. H.Y., *Ribonucleotide Reductase M2 and Zinc Finger Protein 111 Knock-down Reduces Oncogenic Transformation by Jaagsiekte Sheep Retrovirus*. Oral Presentation. 2010

4. Retroviral Pathogenesis Meeting, Newport Beach, CA. Hsu, T., Kim, J.W., Fan. H.Y., *Ribonucleotide Reductase M2 and Zinc Finger Protein 111 Knock-down Reduces Oncogenic Transformation by Jaagsiekte Sheep Retrovirus*. Poster Presentation. 2010

5. West Coast Retrovirus Meeting, Palm Springs, CA. Hsu, T., Malek, P., Kim, J.W., Fan. H.Y., *Analyzing the Role of Zfp111 in Transformation by Jaagsiekte Sheep Retrovirus*. Oral Presentation. 2011

6. West Coast Retrovirus Meeting, Palm Springs, CA. Hsu, T., Malek, P., Kim, J.W., Phung, A., Fan. H.Y., *Analyzing the Role of Zfp111 in Transformation by Jaagsiekte Sheep Retrovirus*. Oral Presentation. 2012

ABSTRACT OF THE DISSERTATION

Identification of Cellular Proteins Important for Jaagsiekte Sheep Retrovirus Transformation

By

Tom Sih-Yuan Hsu

Doctor of Philosophy in Biological Sciences

University of California, Irvine, 2014

Professor Hung Y. Fan, Chair

Jaagsiekte sheep retrovirus (JSRV) is the etiologic agent of a contagious lung cancer in sheep, ovine pulmonary adenocarcinoma (OPA). The envelope gene (*env*) also is an oncogene, since it induces cell transformation and tumors on its own. The subject of this thesis was to identify cellular proteins that interact with JSRV Env and to assess their roles in JSRV transformation. A previous yeast two-hybrid screen identified candidate proteins that can interact with the JSRV envelope protein. Two were studied here: Zinc Finger Protein 111 (Zfp111) and Ribonucleotide Reductase subunit 2 (RRM2).

For Zfp111, shRNA knockdown of endogenous zfp111 in rat 208F fibroblasts reduced transformation by JSRV Env but not by another viral oncogene *v-mos*. Env transformation was restored by a knockdown-resistant Zfp111 cDNA, and over-expression of zfp111 increased transformation by Env but not *v-mos*. Knockdown of zfp111 decreased proliferation rates of Env transformed cells but not untransformed cells.

Zfp111 bound to a smaller form of Env ($P70^{env}$); while the Env polyprotein ($Pr80^{env}$) is cytoplasmic, $P70^{env}$ is nuclear. $P70^{env}$ and $Pr80^{env}$ have the same polypeptide backbone, so they differ in glycosylation. Co-expression of Zfp111 with JSRV Env stabilizes both proteins. Selected alanine scanning mutants in the Env cytoplasmic tail (CT) were co-transfected with Zfp111; there was a strong correlation between mutant transformation efficiencies and levels of $P70^{env}$ and Zfp111 detected. The results suggested a putative interaction region for Zfp111 in the Env CT.

With regard to RRM2, endogenous RRM2 co-localized with Env by re-localization to the plasma membrane in transfected NIH 3T3 cells. In rat 208F cells, RRM2 knockdown decreased Env transformation, but there was also a decrease (significantly less) in *v-mos* transformation. RRM2 knockdown cells showed a decrease in overall growth rates, which might explain the effect on *v-mos* transformation.

Progress towards tandem affinity purification (TAP) of JSRV Env-associated cellular proteins is also described. JSRV Env with a C-terminal TAP tag (HBH) was generated. The HBH-tagged Env could transform cells, and it could be successfully purified over Ni^{2+} and streptavidin columns; JSRV Env peptide sequences (SU and TM) were identified in preliminary TAP/MS experiments.

CHAPTER 1: INTRODUCTION

Retroviruses: Features, Genomic Organization, and Life Cycle

Retroviruses have been of great interest as molecular and pathogenic infectious agents. Retroviruses contain a virus core that consists of two identical positive-stranded viral RNA genomes encapsidated with virus-coded enzymes in a spherical or conical protein capsid (Fig. 1.1) (81). This virus core is surrounded by a viral envelope consisting of host-derived plasma membrane lipid and viral glycoproteins that mediates host cell receptor recognition. Retroviruses are commonly classified into one of two major categories based on the organization of their genome: simple or complex (117). Simple retroviruses contain only the three fundamental coding domains necessary for retroviral life cycle: *gag*, which encodes for the viral capsid, nucleocapsid, and matrix protein; *pol*, which encodes for reverse transcriptase, integrase, and protease enzymes; and *env*, which encodes for the viral surface (SU) and transmembrane (TM) proteins that is essential for viral entry into host cell (Fig. 1.2A). Complex retroviruses have *gag*, *pol*, and *env* genes along with additional genes that encode regulatory proteins. Retroviruses, both simple and complex, are organized into 7 groups, highlighted in Table 1.1, with 5 members of the 7 groups known to have oncogenic properties (alpha, beta, gamma, delta, and epsilonretrovirus).

The *gag* gene encodes the structural proteins of the viral core, which include nucleocapsid (NC), matrix (MA), capsid (CA), and others, depending on the virus. The *pol* gene encodes the viral enzymes reverse transcriptase (RT), integrase (IN) and protease (PR), whose functions will be described below (118). The *env* protein includes the surface (SU) and

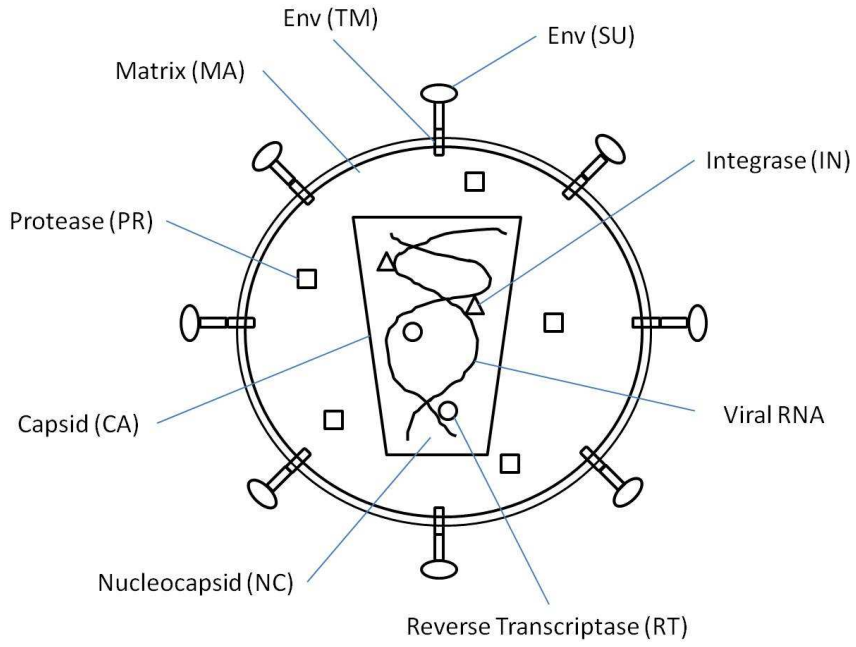

Fig. 1.1: The structure of a typical retrovirus. All retroviruses contain a viral core composed of viral RNA and structural proteins Nucleocapsid (NC) and Capsid (CA) and enzymes Reverse Transcriptase (RT) and Integrase (IN). Surrounding the viral core are the Matrix (MA) structural protein and Protease (PR) enzyme. The very outer lipid membrane contains the envelope proteins Surface (SU) / Transmembrane (TM).

transmembrane (TM) domains, which are necessary for virus entry into host cell. At the 5' and 3' ends of the viral RNA genome are non-coding sequences U5 and U3 respectively, flanked by short repeated sequences (R) (118). An example of a simple retrovirus' genome is shown in Figure 1.2B, which is the Jaagsiekte sheep retrovirus (JSRV) genome. JSRV is a simple retrovirus, containing only the essential retroviral genes *gag*, *pro-pol*, and *env* for retroviral replication. More information about JSRV will be presented in the sections below and in the other chapters of this thesis.

For all retroviruses, the lifecycle begins with attachment of the virus to the host cell by specific interaction between the viral SU glycoprotein domain and a cognate host cell

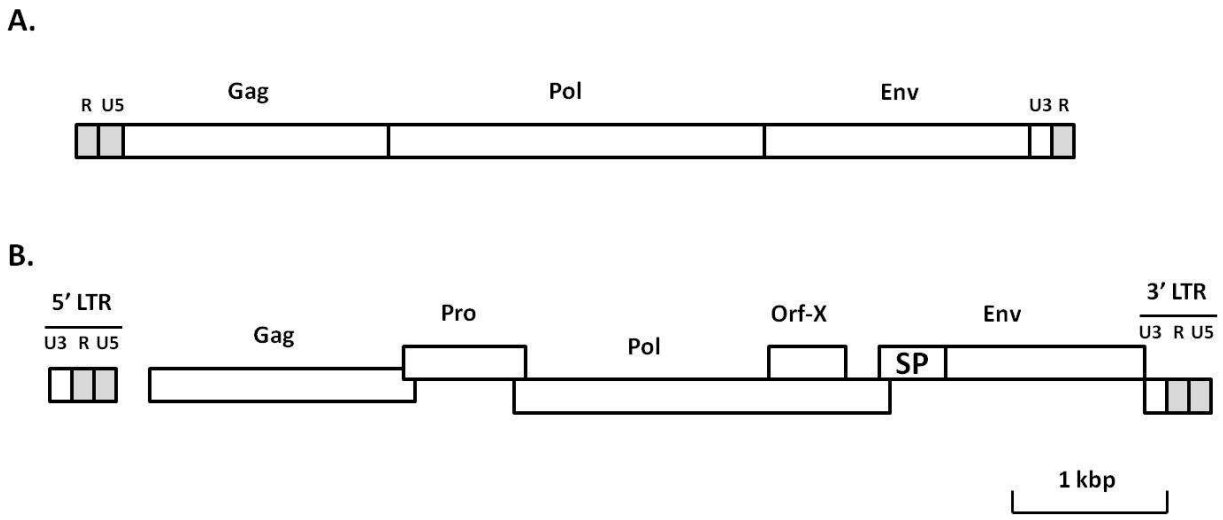

Fig. 1.2: Retrovirus genomes. (A) An example of a simple retrovirus' genome. The essential genes for simple retroviruses -- *gag*, *pol* and *env* are shown here. The terminal regions at 5' and 3' ends contain direct repeats (R), and U5 and U3 sequence unique sequences. The boxes represent open reading frames. (B) The JSRV provirus resembles a simple retrovirus' genome. It contains *gag*, *pro*, *pol*, and *env* genes. It also includes an open reading frame X (*orf-x*) of unknown function, and the signal peptide (SP) region of *env* encodes Rej, which can enhance viral mRNA translation (11, 45). The LTR (long terminal repeats) are found at both ends of the genome integrated provirus, each containing U3, R and U5 elements.

receptor (Fig. 1.3). This is followed by membrane fusion of the viral envelope and host cell plasma membrane. TM facilitates the fusion of the viral and cellular membranes at the cell surface or in internal compartments such as lysozomes (18, 48). The virus core is then released into the cell cytoplasm, where the viral RNA is used as a template for reverse transcriptase (RT) to generate double stranded viral DNA. The viral DNA contains long terminal repeats (LTRs) at either end, with duplicated U3 and U5 regions. After reverse transcription, viral DNA often gains entry into the host cell nucleus during mitosis, when the nuclear membrane is temporarily dissolved. For the lentiviruses sub-class, viral DNA can access the nucleus using nuclear localization signals found on proteins in the pre-integration complex, which contain viral

Table 1.1: Retrovirus classifications. Some parts are adapted from (16).

Genus	Example	Genome
Alpharetrovirus	Rous sarcoma virus	Simple
Betaretrovirus	Jaagsiekte sheep retrovirus	Simple
Gammaretrovirus	Moloney murine leukemia virus	Simple
Deltaretrovirus	Human T-cell leukemia virus	Complex
Epsilonretrovirus	Walleye dermal sarcoma virus	Complex
Lentivirus	Human immunodeficiency virus	Complex
Spumavirus	Human foamy virus	Complex

proteins such as integrase (IN) and perhaps some cellular proteins as well. Viral DNA insertion into the host cell genome is mediated by IN, and the insertion sites are selected virtually at random although there may be preferred for chromosomal regions for some retroviruses (10) (e.g. start sites of genes for gammaretroviruses). The viral DNA that has been integrated into the host genome is referred to as the provirus. Proviral DNA is transcribed by host cell RNA polymerase II and associated factors to give full-length viral RNA identical to genomic RNA. Viral transcription is driven by enhancer and promoter sequences located in the LTR (79, 91). The newly synthesized viral RNA can either remain as the full length viral transcript or be spliced (Fig. 1.4). Full length viral transcripts are exported to the cytoplasm where they are either directly incorporated into virions or translated into viral Gag and Gag-Pol polyproteins. The Gag-Pol polyprotein is generated when the translational machinery bypasses

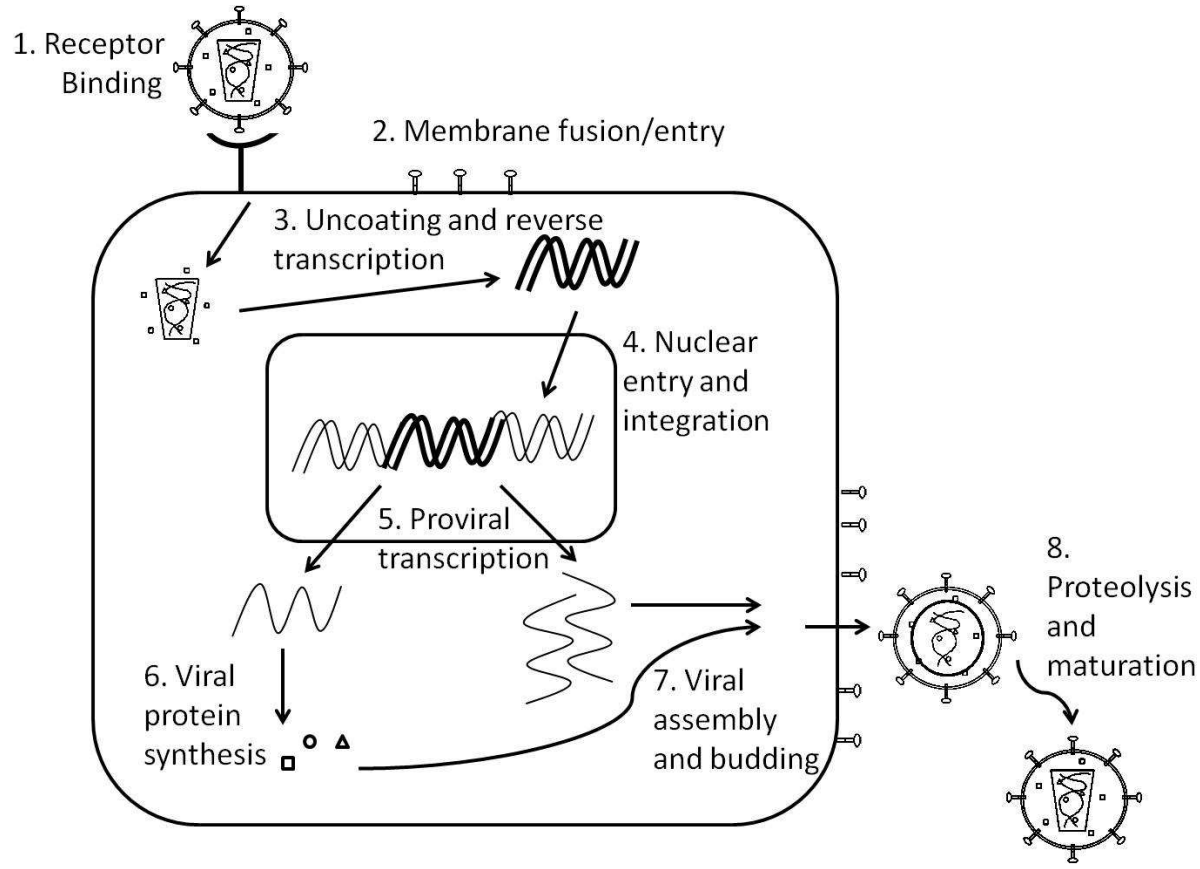

Fig 1.3: The retrovirus life cycle.

the termination codon at the end of *gag*. The bypass can occur in two ways: readthrough suppression or -1 frameshift. In readthrough suppression, the termination codon at the end of *gag* is suppressed by insertion of an amino acid at the amber stop codon (glutamine for murine leukemia virus), leading to continued translation into the *pro-pol* regions. In -1 frameshifting, ribosomes slip backward by one nucleotide near the end of the Gag coding sequences without releasing the growing polypeptide chain, leading to a shift in the reading frame and continued translation into the *pro-pol* regions (91). Spliced viral RNA is exported to the cytoplasm and translated into viral Env polyprotein (e.g. $Pr80^{env}$ for gammaretroviruses) (91). The Env polyprotein is then cleaved in the Golgi by a cellular protease (furin) to give the mature SU and

TM domains. Retroviral core assembly occurs either in the cytoplasm or at the plasma membrane during budding. For betaretroviruses, viral core assembly occurs in the perinuclear compartment of the cell, after which the cores are transported to the plasma membrane for budding and release (81). Upon release of the virion, proteolytic cleavage of the viral polyprotein (Gag-Pol-Pro) by the viral protease converts the immature, non-infectious virion into a mature, infectious virus (110) (Fig. 1.3).

Retroviral Pathogenesis

In addition to being classified as simple or complex, some retroviruses are pathogenic in susceptible hosts. Different retroviruses cause cancers, neurological disease or immunodeficiency (96). Oncogenic retroviruses have great historical significance, as studies on them helped to elucidate mechanisms of cancer development in humans and animals (96). Oncogenic retroviruses are divided into two classes based on their mechanism of cell

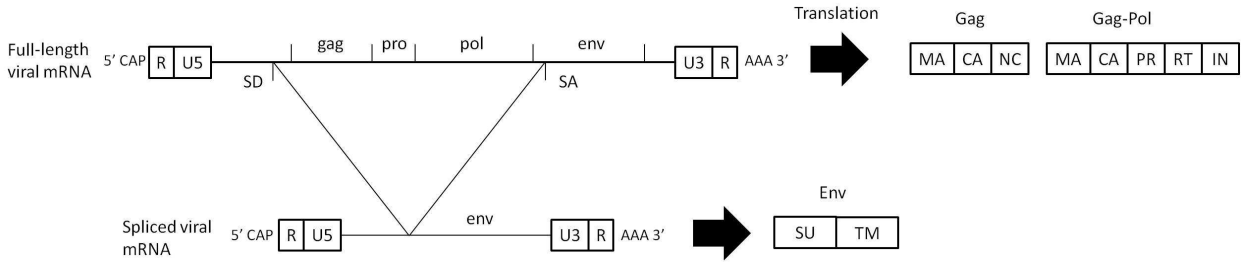

Fig. 1.4: Translation of retroviral mRNA transcripts. Full length retroviral mRNA is shown at the top, with the U5 and R regions behind the 5' cap and U3 and R regions before the 3' poly (A) tail. The full length mRNA contains the *gag*, *pro*, *pol*, and *env* genes. The full length mRNA is spliced at the splice donor (SD) and splice acceptor (SA) sites. The spliced retroviral mRNA transcript is shown at the bottom, containing only the *env* gene. Translation of full length mRNA results in the formation of the Gag and Gag-Pol polypeptides shown to the right of the full length mRNA. Translation of spliced mRNA results in the formation of Env polypeptide shown to the right of the spliced mRNA.

transformation and the speed of tumorigenesis: acute transforming and non-acute retroviruses.

The subject of this thesis is Jaagsiekte sheep retrovirus, the causative agent of a transmissible lung cancer in sheep called ovine pulmonary adenocarcinoma (OPA), and a brief overview is provided here. JSRV is classified by phylogeny as a betaretrovirus; other betaretroviruses include murine mammary tumor virus and Mason-Pfizer monkey virus. Betaretroviruses are simple retroviruses with genomes containing only essential genes for the retroviral lifecycle (*gag*, *pro-pol*, and *env*) (Fig. 1.2B) (37, 43, 59). However in addition to the essential genes, the JSRV genome also contains an open reading frame *orf-x* that overlaps the *pol* gene in a different reading frame, with a predicted amino-acid sequence that shows weak homology to a G protein coupled receptor (8, 95). The exact function of *orf-x* is still unknown, but it does not appear to be necessary for in vivo replication or transformation (19, 66). The signal peptide of Env protein also encodes Rej, which can enhance viral mRNA translation (11, 45). JSRV is able to induce lung tumors in newborn sheep in as little as 10 days (116), which typically indicates the presence of an oncogene in its genome in order to induce rapid transformation. This is surprising, given that there are no apparent oncogenes present in JSRV genome (see below). Deletion analysis of the JSRV genome reveals that the native *env* gene also acts as an oncogene (66). Analysis of JSRV transformation is the main focus of this thesis, with an emphasis on the mechanism of transformation.

Acute Transforming Retroviruses

Acute transforming retroviruses are characterized by rapid development of tumors when they are infected in susceptible host animals. In addition, infection by many acute transforming retroviruses can morphologically transform cells in culture. These rapid tumorigenesis and

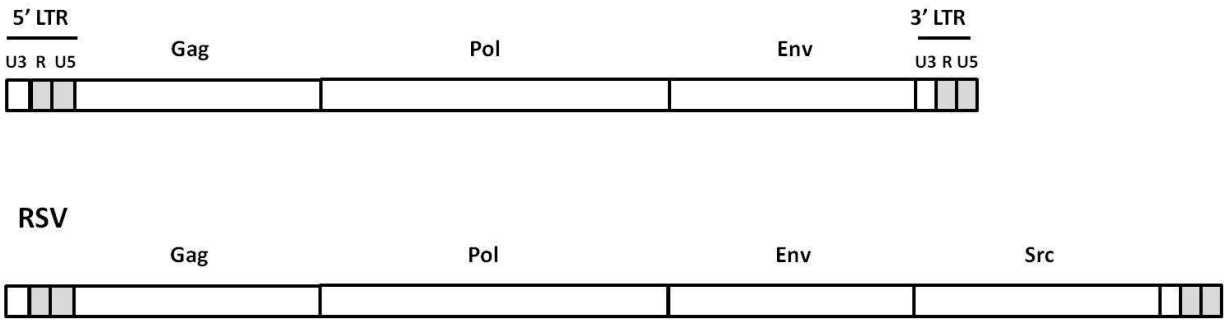

Fig. 1.5: Genome of the acute transforming retrovirus Rous sarcoma virus. A typical simple retrovirus's genome is shown in DNA form at the top, complete with 5' and 3' LTR elements, *gag*, *pol*, and *env* genes. The Rous sarcoma virus (RSV) genome is shown at the bottom, which contains all of the genomic information found in a simple retrovirus genome plus an extra viral *src* gene. The viral *src* gene in RSV was found to be derived from celluar *src*, a proto-oncogene in mammalian cells. The viral *src* allows for rapid transformation of cells, which is the main characteristic of acute transforming retroviruses.

transformation properties are typically due to additional genetic information in the form of oncogenes (96). Retroviral oncogenes were derived from normal cell genes that were incorporated into the viral genome by virus-cell recombination events (Fig. 1.5) (17). The normal cell genes are referred to as proto-oncogenes, with the first cellular proto-oncogenes being identified as the cellular analogs of viral oncogenes in acute transforming retroviruses (107). Retroviral oncogenes are typically modified and constitutively expressed at high levels compared to the parental cellular proto-oncogenes (107). To accommodate the incorporated proto-oncogene into the viral genome, parts of the viral genes in acute transforming retroviruses are typically lost due to a limit to the total length of viral RNA that can be packaged into a retroviral particle (118). As a result acute transforming retroviruses are generally replication defective; acute transforming retroviruses replicate by co-infection with a replication-competent (helper) virus that encodes all of the viral proteins necessary for making infectious particles (96). However, a few acute transforming retroviruses contain all of the viral structural genes as well as

an oncogene (HTLV I and II, Rous sarcoma virus), so they are replication competent (96, 103). As it will be discussed below, the Env gene of JSRV also serves as an oncogene (2, 66, 96). The tumors formed by acute transforming retroviruses tend to be polyclonal in that they arise from multiple transformed cells (59).

Non-acute retroviruses

Non-acute retroviruses cause tumors slowly compared with acute-transforming retroviruses, and they do not transform cells in culture. These viruses are typically replication-competent retroviruses and they do not carry oncogenes. Rather, oncogenic transformation results from insertion of a provirus near a cellular proto-oncogene in an infected cell, leading to over-expression of the proto-oncogene via the strong enhancers and promoters in the viral LTR (96). There are two mechanisms for the insertional activation of proto-oncogenes: promoter insertion and enhancer activation. In promoter insertion, the provirus is integrated upstream of the proto-oncogene in the same transcriptional orientation (Fig. 1.6A). Transcription from the viral LTR (upstream or downstream) leads to read-through into the downstream proto-oncogene (39). Since retroviral LTRs are constitutively highly active this leads to over-expression of the proto-oncogene, which can lead to tumor development. The first demonstration of the promoter-insertion mechanism was described for avian leukosis virus-induced B-lymphomas in chickens, where activation of the *c-myc* proto-oncogene occurred (39). In enhancer activation, the enhancers sequences in the proviral LTR activate a nearby proto-oncogene's own promoter, often from many nucleotides away (Fig. 1.6B) (86). In enhancer activation the retroviral provirus may be inserted upstream or downstream from the proto-oncogene, in the same or opposite transcriptional orientation. In contrast to promoter insertion, where the over-expressed proto-oncogene results from a hybrid viral-proto-oncogene transcript, in tumors with enhancer

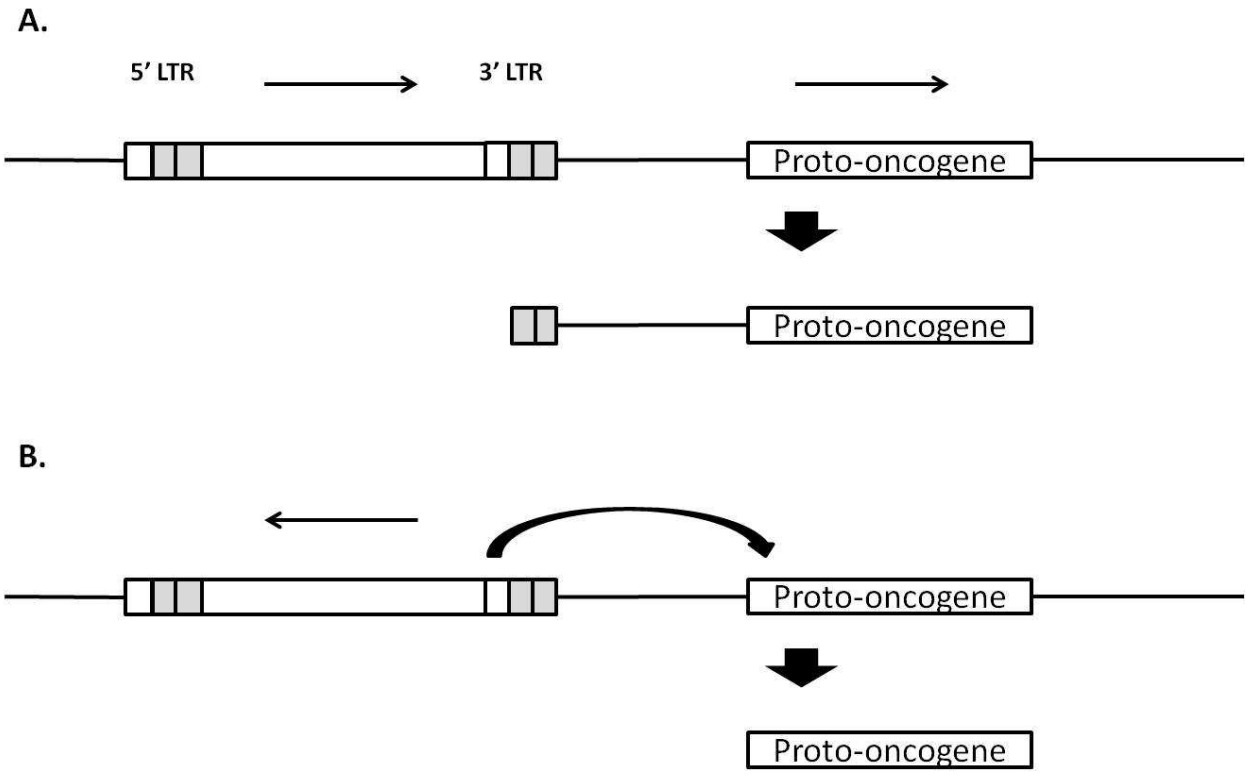

Fig. 1.6: Activation of proto-oncogenes by proviral insertion. (A) In promoter insertion, provirus inserts upstream of a cellular proto-oncogene in the same transcriptional orientation. The DNA organization of the integrated viral DNA and adjoining proto-oncogene is shown at the top. The promoter elements in the 3' LTR can act as a promoter to initiate the transcription of the downstream proto-oncogene. The transcript is shown at the bottom. (B) In enhancer activation, provirus can insert both upstream or downstream of a cellular proto-oncogene in the opposite transcriptional orientation (top). The provirus increases expression of the normal proto-oncogene transcript due to the strong enhancer sequence in the U3 region (bottom).

activation there is over-expression of the native proto-oncogene transcript. Early examples of enhancer activation of proto-oncogenes include ALV-induced B-lymphomas and activation of *c-myc* in chickens (86) and mouse mammary tumor virus (MMTV)-induced mammary tumors and activation of *wnt*-1 in mice (76). Other mechanisms of insertional activation include the disruption of the control elements on proto-oncogenes and disruption of tumor suppressor genes. In SL3-3 murine leukemia virus, which does not contain an oncogene, the proto-oncogene *gfi1* is

commonly activated by the viral LTR elements. In addition, the provirus insertion can also disrupt the control element for *gfi1* by inserting itself into the micro RNA binding sites for *gfi1* at the 3' untranslated region, leading to the deregulation of the proto-oncogene when the miRNAs can no longer bind and inhibit gfi1 (21). The spleen focus forming virus (SFFV) is an acute transforming retrovirus with the oncogene *spi-1*. In addition to transformation with the viral oncogene, SFFV provirus can also inserts itself into the p53 tumor suppressor gene, disrupting the p53 expression in infected cells (9).

As mentioned, non-acute retroviruses induce tumors relatively slowly (months – years), although they still induce specific cancers with high efficiency. For instance Moloney murine leukemia virus will induce T-lymphomas in 100% of susceptible mice with a mean latency of 3-4 months (32). Integration of retroviral DNA into host cells is relatively random with respect to the host DNA, so in an infected animal multiple cycles of infection in different cells (and time) are necessary before a provirus is inserted nearby a proto-oncogene in one cell; this cell eventually develops into a tumor. In contrast, every cell infected by an acute transforming retrovirus will express the oncogene, so tumors will develop much more rapidly. The tumors formed by non-acute retroviruses also tend to be clonal or oligoclonal in origin, meaning that they originate from a single or small number of transformed cells (96). Tumors induced by non-acute retroviruses tend to exhibit activation of specific proto-oncogenes – e.g. *c-myc* in ALV-induced B-lymphomas and *Wnt-1* in MMTV-induced mammary tumors. In some cases, multiple proto-oncogenes can be activated – e.g. M-MuLV-induced T-lymphomas show activation of *c-myc*, *pim-1*, *pim-2* and others.

It is well-understood that carcinogenesis is a multi-step process (33), and insertional activation of a proto-oncogene may be just one step in the oncogenic process, which further

lengthens the time for tumor development. In fact in some non-acute retrovirus-induced tumors, more than one proto-oncogene may be activated in the same tumor cell (e.g. *c-myc* and *pim-1* in some M-MuLV – induced T-lymphomas), reflecting collaborative steps in tumorigenesis, both virus driven.

The LTRs in non-acute retroviruses play an important role in the virus' ability to induce specific diseases. While the availability of viral receptors on a cell is an important factor in determining cell tropism, retrovirus strains that share cell tropisms were found to induce disease only in a specific type of cell, despite having identical cell tropism. For example, murine leukemia viruses (MuLV) strains such as Friend MuLV and Moloney MuLV cause very different hematological malignancies. Friend MuLV induces erythroleukemia, while Moloney MuLV induces T-lymphoma. The importance of the viral LTR in tissue-specific disease induction was demonstrated when the LTR of Moloney MuLV was replaced with the LTR from Friend MuLV, and this switch in LTR caused the resulting virus to induce erythroleukemia instead of T-lymphoma (13). This shows that although Moloney MuLV was able to infect erythrocytes as well, there was no disease induction until the viral LTR from Friend MuLV replaced its original LTR. This cell specificity of the viral LTR can be partly explained by the specificity of the enhancer sequences in the LTR. The enhancer sequences in the LTR are often cell-specific, such that if the non-acute retrovirus infects the wrong cell type, the cellular transcription factors will not bind to the viral enhancer elements. This can be due to either the transcription factors not recognizing this viral enhancer motif or the transcription factors specific for this viral enhancer are not expressed in this particular cell type (33). The activity of the viral LTR is an additional factor to be considered with the points mentioned above. If the viral LTR is very active, such as

when the viral enhancer motif is tandemly repeated, the non-acute retrovirus is better at inducing tumors by activation of proto-oncogenes or disruption of tumor suppressor genes (33).

A molecular hallmark of non-acute retrovirus-induced tumors is that multiple independent tumors show common sites for proviral insertion reflective of activation of nearby proto-oncogenes. Indeed these common insertion sites (CISs) have led to discovery of novel proto-oncogenes that had not previously been captured in acute transforming retroviruses – e.g. *Wnt-1 (36)* and *pim-1* (20) and many more. More recently with the availability of the genomic sequences for mice, as well as high-throughput techniques such as inverse PCR cloning (55) and deep sequencing (52, 68) researchers have used banks of tumors induced by different MuLVs to identify multiple CISs associated with particular tumors. This has led to both identification of previously unknown proto-oncogenes, as well implication of previously known genes in tumorigenesis.

Ovine Pulmonary Adenocarcinoma

Ovine pulmonary adenocarcinoma (OPA) is a contagious form of lung cancer that affects sheep (85). When OPA is clinically diagnosed it is generally lethal, and this inevitably leads to economic consequences in areas where JSRV is endemic, such as Europe and Africa (27, 101). The late stages of OPA are characterized by fluid build-up in the lungs, resulting from secretions from oncogenically transformed type II pneumocytes or Clara cells, which are secretory epithelial cells of the lung (88, 99). Type II pneumocytes and Clara cells secrete specific markers that allow their identification in the lungs. Type II pneumocytes are located in the alveolar sacs of the lung and secrete surfactant protein C (37). Clara cells are located further up the airways in the bronchiole tubes of the lungs and secrete Clara cell-specific protein (37). The

excess lung fluid secreted by Type II pneumocytes and Clara cells causes respiratory problems for the affected sheep, which pant after exercise. The Afrikaans name "Jaagsiekte" means "driving sickness," since animals with OPA appear to be out of breath after being driven/herded. In 1983 it was reported that when OPA lung fluid was passed through a 0.45 micron filter and injected intratracheally into newborn lambs, it could rapidly induce OPA (100, 116). This suggested that OPA is caused by a virus, and that OPA lung fluid contains infectious virus that can presumably be the route of spread to susceptible sheep (83). In addition, retrovirus-like particles were observed in OPA tumor cells by electron microscopy, and OPA lung fluid showed reverse transcriptase activity, which suggested that the infectious agent was a retrovirus (41, 88, 100).

OPA is histologically similar to a type of human pulmonary adenocarcinoma called bronchioalveolar carcinoma [BAC, more recently designated Adenocarcinoma in situ (AIS) (114)]. AIS/BAC is defined as a non-invasive form of lung adenocarcinoma (cancer of epithelial cell origin) that has a pure bronchio-alveolar growth pattern. That is, the tumor cells line the alveoli or bronchioles and spread laterally along the surfaces (lepidic spread) (71). OPA differs slightly from AIS/BAC, in that acinar and papillary growth patterns are observed in addition to the lepidic bronchio-alveolar growth pattern. Both OPA and AIS/BAC tumor cells are derived from Clara and type II pneumocytes (or potentially common progenitor cells [bronchiolo-alveolar stem cells [BASCs (51)]); OPA tumors are often multi-focal (71, 82). AIS/BAC and OPA are both considered non-small cell lung cancer; human AIS/BAC tends to be less associated with smoking than other forms of lung cancer such as small-cell lung cancer, which is highly associated with smoking (54, 71, 109). Thus OPA is an animal model (and the only viral model) for studying non-small cell human lung cancer.

JSRV and OPA

The evidence for a retroviral etiology for OPA was further strengthened by western blotting of the lung fluid and tumor extracts. Antibodies specific for the Gag proteins of two betaretroviruses, Mason-Pfizer monkey virus (MPMV) and MMTV, identified retroviral Gag in the lung fluid and tumors (102). These antisera allowed monitoring and optimization of purification procedures of virus from OPA lung fluid, and in particularly separation of betaretroviral particles away from sheep lentivirus (visna/maedi) that was also present in many of the OPA tumor samples. Isolation of RNA from the purified virus followed by cDNA synthesis using an oligo(dT) primer resulted in generation of a cDNA probe that could detect viral RNA from partially purified OPA lung fluid. The cDNA probe was also used as a hybridization probe in molecular cloning of betaretroviral cDNAs from OPA lung fluid, and this allowed deduction of the genomic sequence of the retrovirus (121, 122). This retrovirus was named Jaagsiekte sheep retrovirus (JSRV). While multiple lines of evidence supported a retroviral etiology in OPA, including identification of the JSRV genome in the lung fluids, a major impediment in confirming an etiologic role of JSRV in OPA was the fact that the cloned JSRV (or virus from lung fluid) could not be grown in tissue culture. In 1999 our laboratory was able to establish a causal role for JSRV in OPA (85). First, using hybridization probes from cloned JSRV, a complete integrated JSRV provirus was molecularly cloned in lambda phage from DNA of an OPA tumor from the United Kingdom. A plasmid version of the JSRV genome was generated, in which the promoter and enhancer sequences in the upstream LTR were replaced with human cytomegalovirus (CMV) immediate early promoter, to give the plasmid pCMV2JS21 (Fig. 1.7). Since the U3 region in the upstream LTR of a retroviral provirus is not transcribed, pCMV2JS21 would encode native JSRV RNA when transfected into cells.

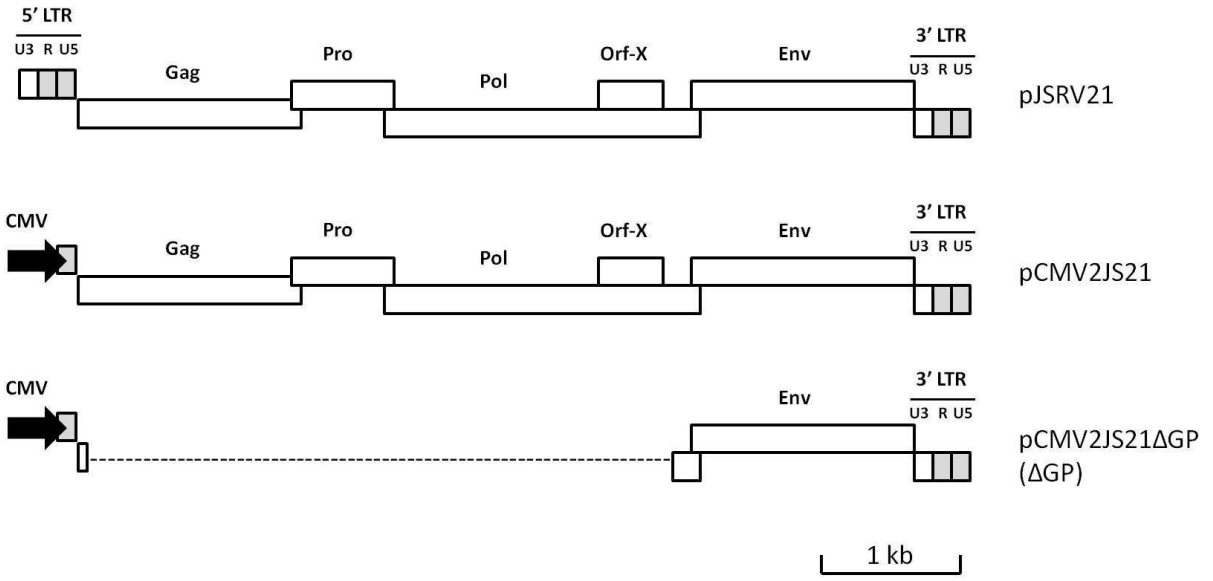

Fig. 1.7: Molecular clones of JSRV. In pJSRV21, the full length JSRV proviral genome was cloned into pBluescript plasmid. For pCMV2JS21, the 5' LTR was replaced with the human CMV promoter. pCMV2JS21ΔGP (ΔGP) was generated by the deletion of *gag*, *pro*, and *pol* genes from the JSRV genome to express only JSRV *env*. Some parts of the *gag* and *pol* genes were retained in ΔGP for efficient *env* RNA splicing and expression.

Transfection of pCMV2JS21 into human 293T embryonic kidney cells (which support high levels of transcription from the CMV enhancer/promoter and which also amplify plasmids such as pCMV2JS21 that contain an SV40 origin of replication) resulted in efficient JSRV production, as measured by release of mature virus particles (with cleaved CA protein). JSRV virions produced from the transfected 293T cells were inoculated intratracheally into newborn lambs, and OPA developed in 2/4 animals within 4 months; the tumors were positive for JSRV DNA and proteins (85). This provided proof that JSRV is necessary and sufficient to induce OPA.

Interestingly, immunohistochemistry using polyclonal antisera raised against bacterially expressed JSRV capsid protein showed positive reactivity in 30% of human BAC tissues, while non-pulmonary adenocarcinomas, other tumor types and normal lung tissues did not show

reactivity (26). While these results would be consistent with the involvement of a JSRV-like retrovirus in human lung cancer of the BAC type, more specific tests for such a virus (i.e. PCR or RT-PCR with JSRV-specific oligonucleotide primers) have not detected such a virus in human BAC (42, 72, 123). Thus the role of a human retrovirus in development of non-small cell lung cancer remains in doubt.

JSRV Env is an Oncogene

Once JSRV was cloned and shown to be the causative agent of OPA, the mechanism of oncogenesis was of primary interest. The fact that JSRV can induce OPA in newborn lambs within as little as 10 days suggested that JSRV is an acute transforming retrovirus and therefore it should carry an oncogene (116). However sequencing of the JSRV genome indicated that it carries only the basic retroviral genes: *gag*, *pol*, *pro*, and *env* and, with the exception of the alternate *OrfX* reading frame, lacks any additional sequences with the hallmark of an oncogene (e.g. non-retroviral sequences with homology to a cellular gene) (Fig 1.2B). A major breakthrough was the observation that the CMV-driven pCMV2JS21 plasmid will give rise to foci of morphologically transformed cells when transfected into murine NIH-3T3 fibroblasts (66); this observation has been confirmed in transfection of rat 208F fibroblasts (92) and other cell systems (4, 64). The ability to morphologically transform cells in culture is a hallmark of retroviral oncogenes, so even though sequence analysis did not suggest the presence of an oncogene in JSRV, it apparently does carry one.

The next question was to identify the functional oncogene in the JSRV genome. For these experiments it was possible to use the morphological transformation assay as the read-out for oncogene activity. Removal of the alternate reading frame *orf-X* did not inhibit cell

transformation, eliminating it as the oncogene (66). Deletion of *gag*, *pro*, *pol* and *Orf-X* from the pCMV2JS21 vector gave rise to the pCMV2JS21ΔGP vector, or simply known as ΔGP (Fig. 1.8A). ΔGP contains only JSRV *env*, and epitope tagged versions of this vector were constructed in later studies (46, 65). This new vector was able to induce cell transformation in rodent cell lines with high efficiency, indicating that JSRV *env* functions as the oncogene (Fig. 1.8B) (66). Thus JSRV Env not only facilitates viral entry into host cells but it also transforms them. The transformation ability by JSRV Env has been suspected to be advantageous for viral replication *in vivo*, perhaps by stimulating division of the infected cells (34, 80, 82). In addition to being able to transform cells in culture, JSRV Env can also induce tumors in vivo.

Replication-defective adeno-associated virus vectors expressing JSRV *env* induce lung tumors in immunodeficient and normal mice (56, 119). Two independent efforts in generating

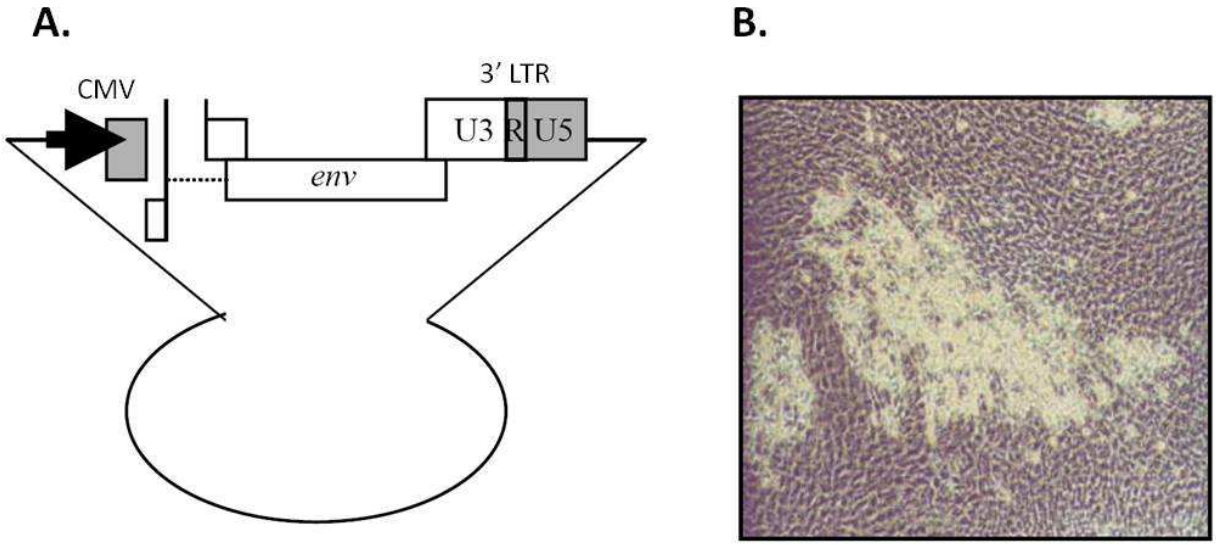

Fig. 1.8: Transformation of mouse fibroblast cells NIH 3T3 by JSRV Env. (A) The JSRV *env* expression vector (ΔGP) contains full-length env, wild type 3' LTR, and a constitutively active CMV promoter. (B) An example of a transformed focus seen in NIH 3T3 cells, 6 weeks post-transfection with ΔGP. Adapted from (66)

mouse models for OPA consisted of generating immunocompetent transgenic mice that express JSRV Env under the control of the mouse lung-specific Surfactant Protein A (SPA) promoter (22) or Surfactant Protein C (SPC) promoter (14). In the SPA transgenic mice there was low but lung-specific expression of the SPA-Env transgene (22). This SPA-Env transgene also induced lipomas in some of the transgenic animals. In the SPC transgenic mice there were spontaneous lung tumors formed, with the tumors resembling OPA (14). Also as described above, laboratory-produced JSRV was able to infect newborn sheep and induce OPA (85).

Oncogenesis by native *env* genes is almost unprecedented for retroviruses. To date oncogenic envelope proteins have been found only for enzootic nasal tumor virus (ENTV-1 and -2) (2, 30, 77), viruses closely related to JSRV that induce nasal epithelial tumors in sheep and goats, and avian hemangioma retrovirus (3). In addition the oncogene of the acute transforming replication-defective spleen focus-forming virus (SFFV) of the Friend murine leukemia virus complex is an internally deleted Env protein that no longer functions as a viral entry molecule (97).

Domains in JSRV Env Involved in Transformation

The JSRV Env polyprotein is a type-I transmembrane protein of 615 amino acids in length prior to cleavage (29, 85, 122). As described above Env is cleaved by furin protease into the surface (SU) and the transmembrane (TM) proteins, which are linked by disulfide bonds (Fig. 1.9A). SU is involved in reception recognition and binding, while TM is involved in viral-cell membrane fusion. The receptor for JSRV is the glycosylphosphatidylinositol anchored protein hyaluronidase 2 (92). The JSRV TM domain contains a membrane spanning region, followed by an amphipathic helix, and ends in a short 44 amino acid cytoplasmic tail. The cytoplasmic tail

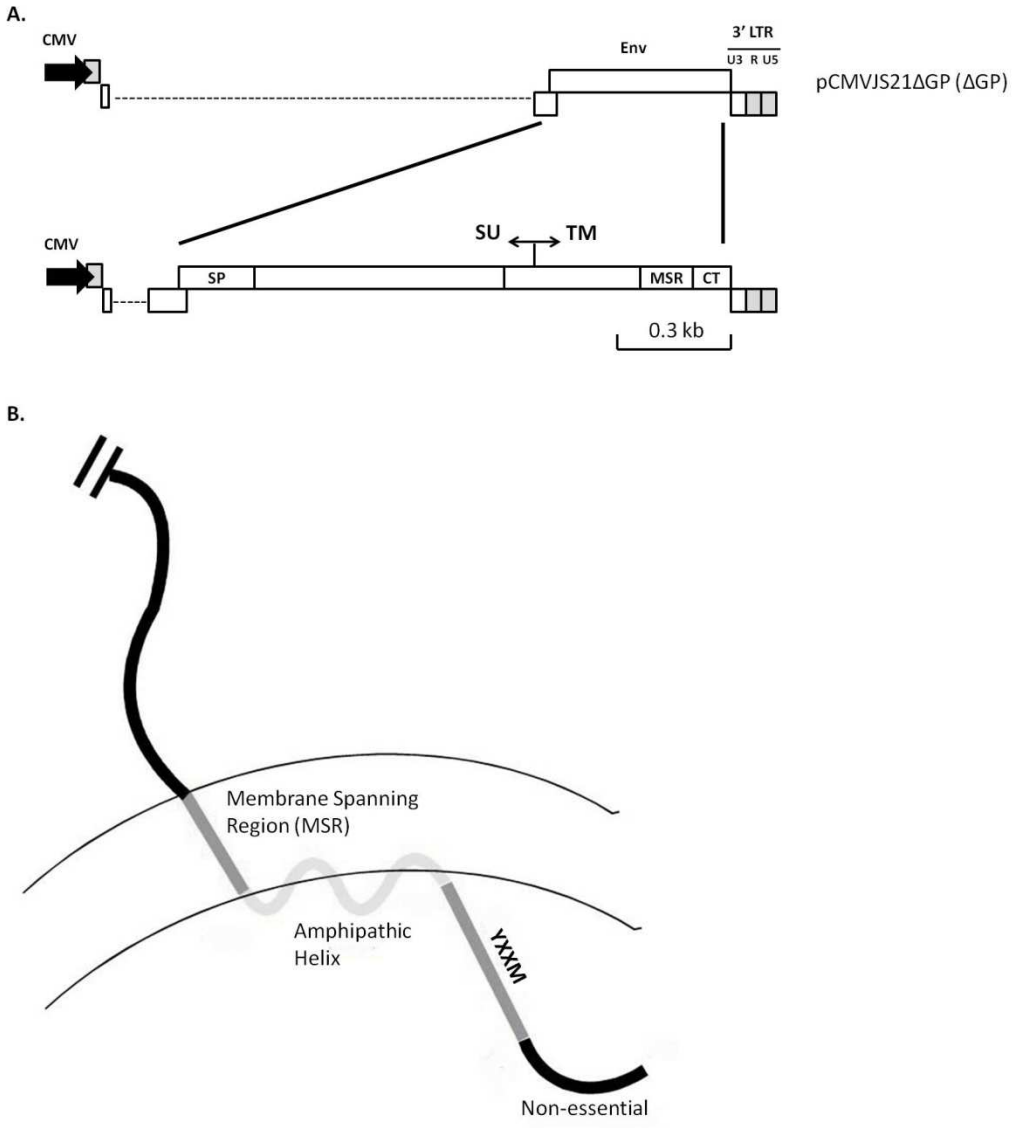

Fig. 1.9: Domains of JSRV Env. (A) JSRV Env is a type I transmembrane protein, 615 amino acids in length. It is composed of two subunits, surface (SU) and tranmembrane (TM). SP is signal peptide, MSR is membrane spanning region, CT is cytoplasmic tail. (B) Domains of the cytoplasmic tail. The membrane spanning region leads into an amphipathic helix, which stretches from residues 570 to 587. The YXXM domain is spanning from residue 590 (Y590) to 593 (M593). C-terminal residues from 607 to 615 are not essential for transformation. Adapted from (46).

contains an internal domain that is important for transformation, while the C-terminal 10 residues are dispensable for transformation (46).

Changes in the CT, such as chimeras or deletion, lead to the elimination of transformation across different cell lines and suggest that CT is necessary for transformation (4, 47, 58, 61, 84). Chimeras were generated by combining an endogenous JSRV (enJSRV) genome with exogenous JSRV (exJSRV) genome. Distinguishing between the two versions of JSRV was accomplished through differences in their restriction digest and hybridization patterns (78). enJSRVs are found in multiple copies in the sheep genome (40, 122), and their envelope proteins do not have oncogenic properties but can interfere exogenous JSRV infection (7, 73, 74, 106). Only this exogenous JSRV *env* acts as an oncogene. This was verified when the OPA tumor cells only contained exogenous JSRV DNA without changes in enJSRV DNA (78). Chimeras of the exJSRV Env were made by replacing regions of JSV *env* with enJSRV *env* sequences. In particular, it was shown that by replacing the TM domain of JSRV Env with the TM of an enJSRV Env JSRV transformation was abolished (84), suggesting that the TM domain of exJSRV Env is necessary for JSRV transformation. An additional JSRV Env chimera was constructed by replacing the carboxy-terminal of TM with enJSRV Env sequences, and this exJSRV Env chimera showed that the carboxy-terminal of TM, which consists of the membrane-spanning region of Env and a cytoplasmic tail (CT), is important for transformation (84). In particular, the internal domain of CT was found to contain an YXXM motif. The importance of CT and the YXXM motif will be discussed below.

The cytoplasmic tail of exJSRV Env contains a single tyrosine residue (Y590) while the CT from the non-transforming enJSRV Env lacks tyrosines in the CT (84). Moreover, mutation of the JSRV Env tyrosine (Y590A) abolished JSRV transformation in NIH-3T3 cells (84). Tyrosine residues are important in signal transduction: if phosphorylated, they can serve as docking sites for other signaling proteins that contain SH2 domains (104). The JSRV CT

tyrosine is in a YXXM motif (Y is tyrosine, X is any amino acid, M is methionine) (Fig. 1.9B), which if phosphorylated is a putative interaction site for the p85 regulatory subunit of phosphatidylinositide 3-kinase (PI3K) (104). The PI3K-Akt signaling pathway is well known for its role in oncogenesis (25), and much work has investigated the role of the YXXM motif in JSRV transformation (4, 44, 58, 61, 84). Mutation of the tyrosine residue eliminated transformation in NIH 3T3 cells (44, 84) and reduced transformation levels in rat fibroblast 208F (58), avian fibroblast DF-1 (4), and canine kidney epithelial MDCK cells, as observed through efficiency of focus formation (61). In addition, mutation of the methionine residue was able to eliminate transformation in NIH 3T3 cells (84). Furthermore the downstream Akt kinase is constutively phosphorylated in Env transformed rodent cells (58), and PI3K inhibitors reduce transformation levels in different cells (58, 61, 124). On the other hand mutation of the YXXM methionine had little or no effect in transformation levels for certain cell lines (4, 44, 61). Moreover PI3K has not been found to directly bind to JSRV Env (60), and phosphorylation of JSRV Env on tyrosine, necessary for putative PI3K binding, has not been detected (58, 61).

Alanine scanning mutations along the CT revealed differences in the transformation efficiencies by different mutants when transfected into rodent cell lines (46). The changes in transformation efficiencies can be organized into four categories: 1) wild-type (WT) Env transformation levels, 1) partial transformation levels, 3) no transformation, and 4) above WT transformation levels. Mutations in the tyrosine and methionine residues showed no transformation and partial transformation activity, respectively (46). Thus while the YXXM motif is important for JSRV Env transformation in at least some cells, the mechanism by which it acts is still unclear.

While the CT is the primary determinant for JSRV Env transformation (44), the SU domain also plays a role in Env transformation (Fig. 1.9A). Chimeras of JSRV Env containing SU from the enJSRV showed decreased transformation levels in 208F and NIH 3T3 cells (47). Large or sequential deletions within the SU of JSRV Env also showed abolition or large reduction of JSRV transformation in rodent cells as well (44). Furthermore, co-transfection of a transformation-defective SU mutant and a transformation-defective TM mutant (Y590F) showed complementation and rescue of Env transformation activity (44).

Another mechanism for SU in JSRV Env transformation has been proposed (24). The cellular receptor for JSRV is hyaluronidase 2 (Hyal2), a glycophosphatidyl inositol-linked cell surface membrane protein (92). While SU does not bind to mouse Hyal2 (57), it can bind to human and ovine Hyal2, as demonstrated in human BEAS-2B human bronchial epithelial cells (24). In BEAS-2B cells Hyal2 is found in a complex with the RON receptor tyrosine kinase, and RON is inactive in this complex. In contrast in JSRV Env transformed BEAS-2B cells it has been reported that the binding of Env SU to Hyal2 leads to the release of RON kinase; free RON can then activate downstream signaling pathways such as PI3K/Akt and MAPK pathways after binding its ligand (24). While this mechanism may be applicable to human and ovine cells, JSRV Env SU does not bind to mouse Hyal2 and it binds rat Hyal2 with low affinity (57) but it still transforms rodent cells (66). Thus, at least in rodent cells, JSRV transformation does not involve interaction of SU with Hyal2 as JSRV cannot infect mouse cells, but the mechanisms and Env domains discussed above are likely operative. Many retroviral oncogenes induce transformation through multiple pathways and mechanisms (43), so multiple pathways/mechanisms for JSRV tumorigenesis and transformation are likely.

As a side note, the JSRV Rej protein is also encoded in Env, as the signal peptide upstream of the SU region (11, 45). Rej has been shown to enhance nuclear export of unspliced viral RNA, and/or its translation into Gag polyprotein; it may also prevent Gag degradation and release of JSRV virions from the cell (5, 11, 45). Although Rej is not directly involved in Env transformation, it does facilitate the viral life cycle, which can lead to more JSRV in the infected sheep and greater disease development.

JSRV Signaling Pathways

So far three signaling pathways have been reported to be utilized in JSRV transformation (Fig. 1.10). First, as mentioned above, Akt shows enhanced activation (phosphorylation) in many different JSRV-transformed cell lines including mouse NIH 3T3, rat 208F (2, 15, 64, 65, 82) and avian DF-1 (4) fibroblasts, and canine MDCK and rat RK3E epithelial cells (49, 61). The Akt pathway is famous for its role in oncogenic cell transformation and cell survival (25). In addition, a major downstream effector of Akt signaling is the mammalian target of rapamycin (mTOR) complex MTORC1 and treatment with rapamycin, an MTORC1 inhibitor, reduces the efficiency of Env transformation levels in both NIH 3T3 fibroblasts and RK3E epithelial cells (47, 64).

The mechanism of Akt activation by JSRV Env is complex, and it appears to proceed through both PI3K-dependent and –independent pathways. Inhibitors of PI3K such as LY294002 or wortmannin significantly reduce the levels of Akt phosphorylation in cells, and they reduce the efficiency of JSRV Env transformation in culture, and/or revert the transformed phenotype of JSRV-transformed cells in some but not all studies (49, 58, 61, 65, 124). On the other hand, PI3K-independent activation of AKT by JSRV Env was observed in NIH 3T3 cells

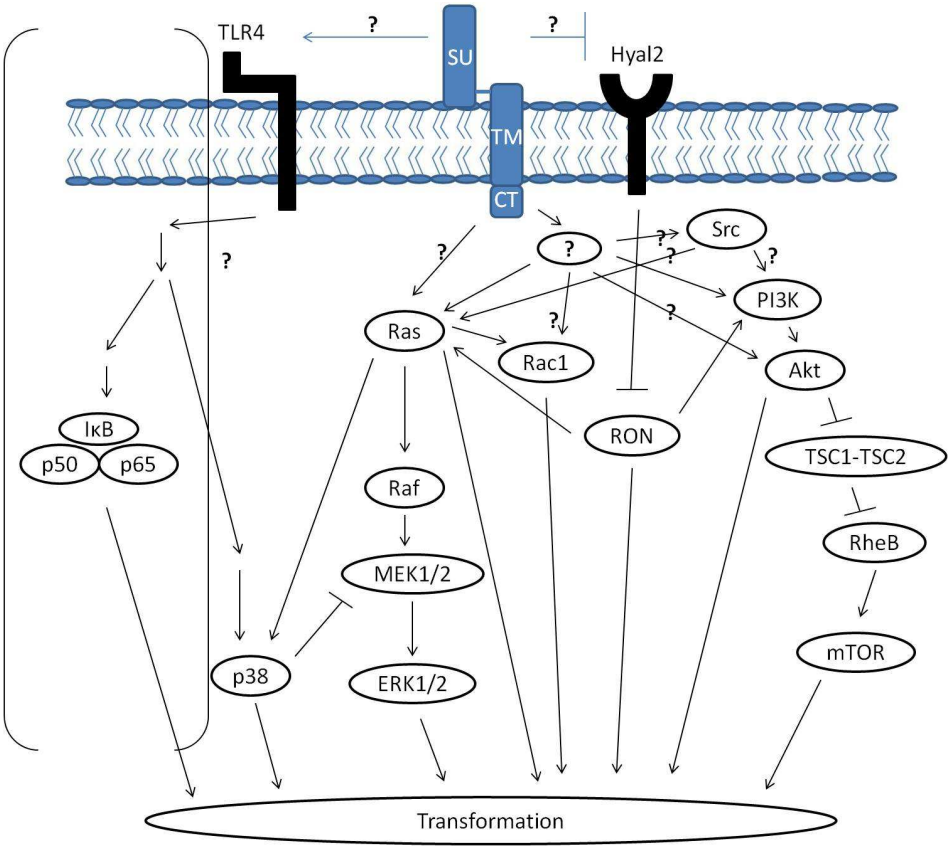

Fig. 1.10: Signaling pathways used in JSRV Env transformation. The three main signaling pathways for JSRV Env transformation are the PI3K-Akt pathway, Ras-Raf-MEK-ERK pathway, and Hyal2-RON pathway. Signaling pathway importance depends on cell line. Pathways that have been shown to affect JSRV Env transformation levels but are not well defined include the TLR4-NFκB pathway and the Rac1 pathway (63). Putative interactions and binding proteins are shown here with question mark (?). With the exception of the Hyal2-RON pathway, JSRV Env does not directly interact with members of the PI3K-Akt pathway or the Ras-Raf-MEK-ERK pathway. Adapted from (43).

stably expressing a dominant negative form of p85, which is the regulatory subunit of PI3K. In these cells, the efficiency of JSRV Env transformation was similar to that of parental NIH 3T3 cells (65). Nevertheless elevated Akt phosphorylation levels were found in the NIH-3T3 cells expressing dominant negative p85 and transformed by JSRV Env. Thus in these cells PI3K was not needed for JSRV Env transformation, indicating an alternate PI3K-independent mechanism

of Akt activation (65). In either case, constitutive Akt activity was observed in the transformed cell lines and also in OPA tumor tissues (108). The differences in Akt activation (PI3K-dependent and –independent) may reflect differences in signaling in different cell types; for other retroviral oncogenes (e.g. *v-src*) it has been shown that the same oncogene may transform using different signaling factors in different cell lines (1).

The second signaling pathway used in transformation by JSRV Env is the Ras-Raf-MEK-ERK1/2 pathway, commonly known as the MAPK (mitogen-activated protein kinase) pathway. The MAPK pathway is well known for its role in cell growth, differentiation, survival, and transformation (87). Inhibitors targeting various steps in MAPK signaling were used to elucidate the role of MAPK signaling in Env transformation. The MEK1/2 inhibitor PD98059 abolished Env transformation in NIH 3T3 cells and it greatly reduced transformation in rat epithelial RK3E cells (64). The H/N-Ras inhibitor FTI-227 also abolished Env transformation in NIH 3T3 cells, but it had minimal effects on transformation in RK3E cells (47, 64). Thus the relative importance of different steps of MAPK signaling in JSRV Env transformation may differ between cell lines. In both experimentally and naturally induced OPA tumors, phosphorylated ERK1/2 was detected in some but not all tumors by immunohistochemistry (28, 64). The p38 MAPK is also involved in Env transformation in that p38 is activated (phosphorylated) and it acts as an inhibitor of MEK1/2 to down-regulate activation of ERK1/2. The p38 inhibitor SB203580 increases Env transformation levels in both NIH 3T3 and RK3E cells (64).

The third signaling pathway reported to be important for JSRV Env transformation is the Hyal2-RON pathway as described above. Activation of RON signaling was described in only one cell line, the human bronchial cell line BEAS-2B; in rodent cell lines JSRV Env and mouse or rat Hyal2 do not interact (24, 57, 61, 70). As previously mentioned, binding of JSRV Env to

human Hyal2 in BEAS-2B cells leads to the release of RON from an inhibitory Hyal-2/RON complex; the free RON can then interact with its ligand (macrophage-stimulating protein) and activate downstream signaling through the PI3K/Akt and MAPK pathways (24). This mechanism suggests that Hyal2 can function as a tumor suppressor. Indeed a dominant-negative kinase-dead RON mutant was able to block Env transformation in BEAS-2B cells (24). However, overexpression of human Hyal2 did not change cell proliferation and morphology in NIH 3T3, 208F, MDCK, and various human lung cancer cells (60), but this could be due to activation of Hyal2 in JSRV Env transformation only. While the Hyal2-RON pathway is not involved in JSRV transformation in rodent cells, RON is over-expressed and constitutively activated in human BAC cells (24), and Hyal-2 maps near a common site for loss of heterozygosity (LOH) in human lung cancers (3p21.3) (92). Sites of LOH are often indicative of lost tumor suppressor genes (113). Moreover sheep cells contain functional JSRV receptors and lung epithelial cells express RON (27).

Other signaling pathways also have been reported be involved in JSRV transformation, including the Src and Toll-like receptor 4 (TLR4) pathways, although they have been less extensively studied. Src, which is a member of a family of non-receptor protein kinases, has been shown to be important in JSRV transformation. Addition of PP2, a Src inhibitor, was able to reduce levels of Env transformation in 208F cells (46, 115). TLR4 is a membrane-bound pathogen-associated molecular pattern (PAMP) receptor involved in innate immunity (53). The Env of the betaretrovirus mouse mammary tumor virus (MMTV) was found to bind to TLR4 in polarized mammary epithelial cells, resulting in the activation of downstream TLR4 signaling pathways (93). JSRV Env was also found to be able to bind to TLR4, although the effect of Env-TLR4 binding has not yet been characterized (43).

It should be noted that direct interaction between JSRV Env and any components of the PI3K-Akt-mTOR pathway or MAPK pathway has not been reported. This suggests that JSRV Env must first interact with another cellular protein(s) to activate these downstream signaling pathways. To fully understand the mechanism of Env transformation, the cellular proteins that interact with JSRV Env must first be identified and tested for their role in JSRV Env transformation.

Yeast Two-Hybrid Screens for Candidate JSRV Env Interacting Proteins

To identify cellular proteins that bind to JSRV Env, previous investigators in the lab performed yeast two-hybrid screens using bait plasmids expressing the bacterial LexA DNA binding domain fused to either the cytoplasmic tail or the entire JSRV Env protein (43). These bait plasmids were stably transformed into *Sachromyces cerevisae*; the resulting strains also contained the *leu2* and *lacZ* genes under LexA transcriptional control. The bait strains were then transfected with human HeLa and mouse NIH 3T3 cDNA libraries in the pJG4-5 vector; this vector expresses the cDNAs as fusion proteins containing the LexA activation domain upon galactose induction. Transformants that could grow in leu- medium after galactose induction were secondarily screened for induction of LacZ by staining with X-gal, the cDNAs were recovered and grown in E. coli, and the identities of the genes were determined by DNA sequencing. Seven different cDNAs were identified, as shown in Table 1.2. Two of the cDNAs were of particular interest due to their interaction strength with the bait protein (as measured by intensity of X-gal staining) and multiple independent isolations in the two-hybrid screening: ribonucleotide reductase subunit 2 (RRM2) and zinc finger protein 111 (Zfp111).

Table 1.2: Candidate JSRV Env-interacting proteins from yeast 2-hybrid screens

Candidates	Bait[a]	Library used[b]	Interaction strength[c]	Number of clones[d]	Normal cell function	Transformation[e]
IKAP	CT	Human	++	1	Component of transcription elongation complex	?
RRM2	CT	Human	++	4	Ribonucleotide reductase regulatory subunit	+
Pontin 52	CT	Human	+	1	Beta-catenin interacting protein (Nuclear); Chromatin remodeling; c-myc interactor	+
Reptin 52	CT	Human	+	1	Beta-catenin interacting protein (Nuclear); Chromatin remodeling; c-myc interactor	+
Nm23-H2/ND PK-B	CT	Human	++	1	Nucleoside Diphosphate Kinase; suppressor or metastasis; transcriptional activator	+
Ferritin	CT	Human	++	1	Fe binding protein	-
Zfp111	Whole Env/ CT	Mouse / Human	++	4	Zinc-finger protein 111; transcriptional suppressor	?

[a] Two different bait proteins in the screens were used, either JSRV Env cytoplasmic tail only (CT) or the whole JSRV Env protein.
[b] cDNA libraries from human (HeLa) and mouse (NIH-3T3) cells were screened.
[c] Interaction strengths were based on the relative blue color of colonies on X-gal plates.
[d] Number of independent clones of the same cDNA that were isolated from the screens.
[e] Previous publications reporting a role in cell transformation or tumorigenesis.

Zinc finger protein 111 (aka rKr2) is a member of a subset of Cys_2/His_2 zinc finger proteins called Krüppel-like transcription factors, members of which have been shown to be involved in cellular processes such as proliferation, differentiation, embryogenesis, and tumorigenesis (23). Not much is currently known about this protein. Studies on rat Zfp111 have shown that it contains 19 Cys_2/His_2 zinc finger domains at the carboxy-terminus, connected by

very well conserved 7 amino acid linkers (HTGEKPY), referred to as H/C links. At the amino-terminus, there is a Krüppel-associated box (KRAB) domain that has been reported to act as a very potent transcriptional repressor (89). High expression levels of zfp111 have been observed in neuronal cells, primarily in oligodendrocyte progenitors, but zfp111 has also been seen in other tissues, including lungs, at lower levels (62, 89). A previous report on another member of the Krüppel-like transcription factor, KLF5, showed a decrease in anchorage-independency of *K-ras* transformed human lung cell lines when it was knocked down, although knockdown did not affect the proliferation of the cells (69). Further investigation of Zfp11 interaction with JSRV Env will help to determine if it plays a role in Env transformation and the studies might reveal a role for Zfp111 in lung tumorigenesis.

Ribonucleotide reductase is a ubiquitous enzyme found in all cellular organisms. Its main function is in the synthesis of the four deoxyribonucleoside triphosphates (dNTPs) that are required for DNA synthesis and repair by reducing ribonucleoside triphosphates (NTPs) on the ribose ring. The enzyme is made up of two subunits: RRM1, an 168 kDa homodimeric subunit that contains an allosteric regulatory site and the catalytic site of the enzyme, and RRM2, an 88 kDa homodimeric subunit that contains a tyrosine free radical that is used by RRM1 in ribonucleotide reduction (75, 112). While RRM1 levels are constant through the cell cycle (31, 67), RRM2 is highly regulated, both transcriptionally and by protein degradation (75). RRM2 levels peak during the S phase of the cell cycle, and RRM2 is rapidly degraded by the end of the cycle (12).

Given the importance of ribonucleotide reductase for cell growth and division, it has been considered an important target for anticancer therapy. Several RR inhibitors (e.g. hydroxyurea and triapine) have been investigated as chemotherapeutic agents in chronic myelogenous

leukemia or *in vitro* in cell lines such as L1210 leukemia cells and human KB nasopharyngeal cells (50, 98). Interestingly a recent drug efficacy study showed that the effectiveness of anti-cancer drugs for patients with advanced lung adenocarcinoma is associated with RRM2 levels, where tumors with lower levels of RRM2 showed higher drug responses (105).

A few studies have also suggested that over-expression of RRM2 by itself can enhance transformation of tumorigenicity independent of ribonucleotide reductase enzyme activity. In an early report, the overexpression of RRM2 enhanced focus formation of activated *H-ras* in NIH 3T3 cells, and this was associated with enhanced Raf protein at the plasma membrane (35). More recently Xu et al. reported that overexpression of RRM2 from the ubiquitously active CMV promoter in transgenic mice specifically induced adenocarcinoma of the lung; this was correlated with increased genetic mutation frequencies in cells cultured from these animals (120). Moreover the lung neoplasms were found to have arisen from type II pneumocytes, the primary target cell of JSRV, and there was detectable mutational activation of *K-ras* in the tumors. Thus RRM2 over-expression may play a role in cancer development, and in particular of lung cancers.

Identification of Cellular Interaction Proteins Through Tandem Affinity Purification of JSRV Env

Yeast two-hybrid screening is a valuable tool to identify proteins that interact with a given bait protein. However, a disadvantage of the yeast two-hybrid system is that some protein interactions require post-translational modifications of the interacting proteins which may not be carried out in yeast (e.g., phosphorylation). As a result the list of JSRV Env candidate interacting proteins obtained from the two-hybrid screen is likely incomplete. To identify

additional JSRV Env interacting proteins, as well as confirming the current candidate proteins, tandem affinity purification followed by mass spectrometry analysis of the purified proteins provides can be employed.

Tandem affinity purification (TAP) is the purification of a protein that has been tagged with a TAP tag that is capable of interacting with multiple different affinity matrices. The TAP-tagged protein and associated proteins would be isolated from cell extracts by first one type of affinity purification and elution, and then the eluates would be subjected to a second round of affinity purification using the second affinity matrix (94). This two-step purification procedure helps to reduce many contaminants that bind non-specifically to one affinity matrix but not the other. TAP tags consist of two different tags linked together, with each of the tags displaying high affinity toward its target matrix. These high affinity tags are quite diverse, with some of the most popular ones being biotinylation, 6-histidine, calmodulin-binding peptide (CBP) tags, and two IgG binding domains of Staphylococcus aureus protein A (ProtA) (6, 90, 94). In addition epitope tags (e.g. HA, FLAG, c-myc, etc.) have been multimerized into TAP tags (6). The use of TAP in identification of cellular interacting proteins has been employed in proteomics (6, 38, 90, 94, 111). In proteomics, TAP-purified proteins are digested with proteolytic enzymes such as trypsin or chymotrypsin, and the resulting masses of the peptides or their secondary cleavage products can be used to determine the sequences of the peptides (and the proteins from which they originated) by tandem mass spectrometry. Proteomics/MS has substantially increased the sensitivity and rate of identification of cellular interacting proteins.

The HB tag, which consists of 6x histidine followed by a biotinylation site, is a powerful TAP tag developed by our colleague Dr. Peter Kaiser (111). This tag, which has high affinity for Ni^{2+} (from the 6xHistidine) and streptavidin (from biotin), was able to allow purification of HB-

tagged proteins under fully denaturing conditions. Moreover, *in vivo* crosslinking allowed for the purification of entire protein complexes containing an HB-tagged protein under denaturing conditions that are ready for analysis by mass spectrometry after reversal of the crosslinking (38, 111). In our lab previous attempts at purification of GST-tagged JSRV Env resulted in large numbers of non-specific contaminants after mass spectrometry (data not shown). In this thesis, a slightly modified version of the HB tag, 6xHis-Biotinylation site-6xHis (HBH), was attached to JSRV Env to allow for tandem purification of JSRV Env.

Studies Described in this Dissertation

The work presented in this dissertation focuses on two candidate cellular proteins identified by the yeast-two hybrid screen to interact with JSRV Env, Zfp111 and RRM2. Chapter 2 examines the role of Zfp111 in JSRV Env transformation, by shRNA knockdown or overexpression of Zfp111 in JSRV Env transformation assays. Zfp111 co-immunoprecipitated with JSRV Env, and knockdown or overexpression of Zfp111 decreased and increased JSRV Env transformation in rat 208F cells, respectively. Chapter 3 describes the identification of a new form of JSRV Env protein, found in the nuclear compartment of cells. This new form of Env, termed $P70^{env}$, was found to be highly associated with Zfp111. Molecular characterization of nuclear Env was also conducted. Chapter 4 examines the role of RRM2 in JSRV Env transformation, by knockdown of RRM2 in JSRV Env transformation assays. Knockdown of RRM2 reduced JSRV Env transformation levels. Chapter 5 details establishment JSRV Env containing the HBH TAP tag. The HBH tagged version of JSRV Env (ΔGP-HBH) was found to transform cells and could be purified using Ni^{2+} and streptavidin beads in tandem.

References

1. **Aftab, D. T., J. Kwan, and G. S. Martin.** 1997. Ras-independent transformation by v-Src. Proc Natl Acad Sci U S A **94:**3028-33.
2. **Alberti, A., C. Murgia, S. L. Liu, M. Mura, C. Cousens, M. Sharp, A. D. Miller, and M. Palmarini.** 2002. Envelope-induced cell transformation by ovine betaretroviruses. J Virol **76:**5387-94.
3. **Alian, A., D. Sela-Donenfeld, A. Panet, and A. Eldor.** 2000. Avian hemangioma retrovirus induces cell proliferation via the envelope (env) gene. Virology **276:**161-8.
4. **Allen, T. E., K. J. Sherrill, S. M. Crispell, M. R. Perrott, J. O. Carlson, and J. C. DeMartini.** 2002. The jaagsiekte sheep retrovirus envelope gene induces transformation of the avian fibroblast cell line DF-1 but does not require a conserved SH2 binding domain. J Gen Virol **83:**2733-42.
5. **Armezzani, A., F. Arnaud, M. Caporale, G. di Meo, L. Iannuzzi, C. Murgia, and M. Palmarini.** 2011. The signal peptide of a recently integrated endogenous sheep betaretrovirus envelope plays a major role in eluding gag-mediated late restriction. J Virol **85:**7118-28.
6. **Arnau, J., C. Lauritzen, G. E. Petersen, and J. Pedersen.** 2006. Current strategies for the use of affinity tags and tag removal for the purification of recombinant proteins. Protein Expr Purif **48:**1-13.
7. **Arnaud, F., P. R. Murcia, and M. Palmarini.** 2007. Mechanisms of late restriction induced by an endogenous retrovirus. J Virol **81:**11441-51.
8. **Bai, J., J. V. Bishop, J. O. Carlson, and J. C. DeMartini.** 1999. Sequence comparison of JSRV with endogenous proviruses: envelope genotypes and a novel ORF with similarity to a G-protein-coupled receptor. Virology **258:**333-43.
9. **Ben-David, Y., A. Lavigueur, G. Y. Cheong, and A. Bernstein.** 1990. Insertional inactivation of the p53 gene during friend leukemia: a new strategy for identifying tumor suppressor genes. New Biol **2:**1015-23.
10. **Brown, P. O.** 1997. Integration. In: Coffin JM, Hughes SH, Varmus HE, editors. Retroviruses. Cold Spring Harbor (NY): Cold Spring Harbor Laboratory Press; 1997. .
11. **Caporale, M., F. Arnaud, M. Mura, M. Golder, C. Murgia, and M. Palmarini.** 2009. The signal peptide of a simple retrovirus envelope functions as a posttranscriptional regulator of viral gene expression. J Virol **83:**4591-604.
12. **Chabes, A. L., C. M. Pfleger, M. W. Kirschner, and L. Thelander.** 2003. Mouse ribonucleotide reductase R2 protein: a new target for anaphase-promoting complex-Cdh1-mediated proteolysis. Proc Natl Acad Sci U S A **100:**3925-9.
13. **Chatis, P. A., C. A. Holland, J. E. Silver, T. N. Frederickson, N. Hopkins, and J. W. Hartley.** 1984. A 3' end fragment encompassing the transcriptional enhancers of nondefective Friend virus confers erythroleukemogenicity on Moloney leukemia virus. J Virol **52:**248-54.
14. **Chitra, E., S. L. Yu, K. N. Hsiao, H. Y. Shao, C. Sia, I. H. Chen, S. Y. Hsieh, J. H. Chen, and Y. H. Chow.** 2009. Generation and characterization of JSRV envelope transgenic mice in FVB background. Virology **393:**120-6.
15. **Chow, Y. H., A. Alberti, M. Mura, C. Pretto, P. Murcia, L. M. Albritton, and M. Palmarini.** 2003. Transformation of rodent fibroblasts by the jaagsiekte sheep retrovirus envelope is receptor independent and does not require the surface domain. J Virol **77:**6341-50.
16. **Coffin, J. M., Hughes, S.H., Varmus, H.E., editors.** 1997. The Place of Retroviruses in Biology. Retroviruses. Cold Spring Harbor (NY): Cold Spring Harbor Laboratory Press.
17. **Cooper, G. M.** 1995. Retroviral Oncogenes, 37-65. In G. M. Cooper (ed.), Oncogenes. Jones and Barlett Publishers, Sudbury, Massachusetts.

18. **Cote, M., Y. M. Zheng, and S. L. Liu.** 2009. Receptor binding and low pH coactivate oncogenic retrovirus envelope-mediated fusion. J Virol **83:**11447-55.
19. **Cousens, C., N. Maeda, C. Murgia, M. P. Dagleish, M. Palmarini, and H. Fan.** 2007. In vivo tumorigenesis by Jaagsiekte sheep retrovirus (JSRV) requires Y590 in Env TM, but not full-length orfX open reading frame. Virology **367:**413-21.
20. **Cuypers, H. T., G. Selten, W. Quint, M. Zijlstra, E. R. Maandag, W. Boelens, P. van Wezenbeek, C. Melief, and A. Berns.** 1984. Murine leukemia virus-induced T-cell lymphomagenesis: integration of proviruses in a distinct chromosomal region. Cell **37:**141-50.
21. **Dabrowska, M. J., K. Dybkaer, H. E. Johnsen, B. Wang, M. Wabl, and F. S. Pedersen.** 2009. Loss of MicroRNA targets in the 3' untranslated region as a mechanism of retroviral insertional activation of growth factor independence 1. J Virol **83:**8051-61.
22. **Dakessian, R. M., Y. Inoshima, and H. Fan.** 2007. Tumors in mice transgenic for the envelope protein of Jaagsiekte sheep retrovirus. Virus Genes **35:**73-80.
23. **Dang, D. T., J. Pevsner, and V. W. Yang.** 2000. The biology of the mammalian Kruppel-like family of transcription factors. Int J Biochem Cell Biol **32:**1103-21.
24. **Danilkovitch-Miagkova, A., F. M. Duh, I. Kuzmin, D. Angeloni, S. L. Liu, A. D. Miller, and M. I. Lerman.** 2003. Hyaluronidase 2 negatively regulates RON receptor tyrosine kinase and mediates transformation of epithelial cells by jaagsiekte sheep retrovirus. Proceedings of the National Academy of Sciences of the United States of America **100:**4580-4585.
25. **Datta, S. R., A. Brunet, and M. E. Greenberg.** 1999. Cellular survival: a play in three Akts. Genes Dev **13:**2905-27.
26. **De las Heras, M., S. H. Barsky, P. Hasleton, M. Wagner, E. Larson, J. Egan, A. Ortin, J. A. Gimenez-Mas, M. Palmarini, and J. M. Sharp.** 2000. Evidence for a protein related immunologically to the jaagsiekte sheep retrovirus in some human lung tumours. Eur Respir J **16:**330-2.
27. **De las Heras, M., L. Gonzalez, and J. M. Sharp.** 2003. Pathology of ovine pulmonary adenocarcinoma. Curr Top Microbiol Immunol **275:**25-54.
28. **De Las Heras, M., A. Ortin, A. Benito, C. Summers, L. M. Ferrer, and J. M. Sharp.** 2006. In-situ demonstration of mitogen-activated protein kinase Erk 1/2 signalling pathway in contagious respiratory tumours of sheep and goats. J Comp Pathol **135:**1-10.
29. **DeMartini, J. C., J. V. Bishop, T. E. Allen, F. A. Jassim, J. M. Sharp, M. de las Heras, D. R. Voelker, and J. O. Carlson.** 2001. Jaagsiekte sheep retrovirus proviral clone JSRV(JS7), derived from the JS7 lung tumor cell line, induces ovine pulmonary carcinoma and is integrated into the surfactant protein A gene. J Virol **75:**4239-46.
30. **Dirks, C., F. M. Duh, S. K. Rai, M. I. Lerman, and A. D. Miller.** 2002. Mechanism of cell entry and transformation by enzootic nasal tumor virus. J Virol **76:**2141-9.
31. **Engstrom, Y., S. Eriksson, I. Jildevik, S. Skog, L. Thelander, and B. Tribukait.** 1985. Cell cycle-dependent expression of mammalian ribonucleotide reductase. Differential regulation of the two subunits. J Biol Chem **260:**9114-6.
32. **Fan, H.** 1997. Leukemogenesis by Moloney murine leukemia virus: a multistep process. Trends Microbiol **5:**74-82.
33. **Fan, H., and C. Johnson.** 2011. Insertional oncogenesis by non-acute retroviruses: implications for gene therapy. Viruses **3:**398-422.
34. **Fan, H., M. Palmarini, and J. C. DeMartini.** 2003. Transformation and oncogenesis by jaagsiekte sheep retrovirus. Curr Top Microbiol Immunol **275:**139-77.
35. **Fan, H., C. Villegas, and J. A. Wright.** 1996. Ribonucleotide reductase R2 component is a novel malignancy determinant that cooperates with activated oncogenes to determine transformation and malignant potential. Proc Natl Acad Sci U S A **93:**14036-40.

36. **Gallahan, D., C. Kozak, and R. Callahan.** 1987. A new common integration region (int-3) for mouse mammary tumor virus on mouse chromosome 17. J Virol **61:**218-20.
37. **Griffiths, D. J., H. M. Martineau, and C. Cousens.** 2010. Pathology and pathogenesis of ovine pulmonary adenocarcinoma. J Comp Pathol **142:**260-83.
38. **Guerrero, C., C. Tagwerker, P. Kaiser, and L. Huang.** 2006. An integrated mass spectrometry-based proteomic approach: quantitative analysis of tandem affinity-purified in vivo cross-linked protein complexes (QTAX) to decipher the 26 S proteasome-interacting network. Mol Cell Proteomics **5:**366-78.
39. **Hayward, W. S., B. G. Neel, and S. M. Astrin.** 1981. Activation of a cellular onc gene by promoter insertion in ALV-induced lymphoid leukosis. Nature **290:**475-80.
40. **Hecht, S. J., K. E. Stedman, J. O. Carlson, and J. C. DeMartini.** 1996. Distribution of endogenous type B and type D sheep retrovirus sequences in ungulates and other mammals. Proc Natl Acad Sci U S A **93:**3297-302.
41. **Herring, A. J., J. M. Sharp, F. M. Scott, and K. W. Angus.** 1983. Further evidence for a retrovirus as the aetiological agent of sheep pulmonary adenomatosis (jaagsiekte). Vet Microbiol **8:**237-49.
42. **Hiatt, K. M., and W. E. Highsmith.** 2002. Lack of DNA evidence for jaagsiekte sheep retrovirus in human bronchioloalveolar carcinoma. Hum Pathol **33:**680.
43. **Hofacre, A., and H. Fan.** 2011. Jaagsiekte sheep retrovirus biology and oncogenesis. Viruses **2:**2618-48.
44. **Hofacre, A., and H. Fan.** 2004. Multiple domains of the Jaagsiekte sheep retrovirus envelope protein are required for transformation of rodent fibroblasts. J Virol **78:**10479-89.
45. **Hofacre, A., T. Nitta, and H. Fan.** 2009. Jaagsiekte sheep retrovirus encodes a regulatory factor, Rej, required for synthesis of Gag protein. J Virol **83:**12483-98.
46. **Hull, S., and H. Fan.** 2006. Mutational analysis of the cytoplasmic tail of jaagsiekte sheep retrovirus envelope protein. Journal of virology **80:**8069-8080.
47. **Hull, S., J. Lim, A. Hamil, T. Nitta, and H. Fan.** 2012. Analysis of jaagsiekte sheep retrovirus (JSRV) envelope protein domains in transformation. Virus Genes.
48. **Hunter, E.** 1997. Viral Entry and Receptors. In: Coffin JM, Hughes SH, Varmus HE, editors. Retroviruses. Cold Spring Harbor (NY): Cold Spring Harbor Laboratory Press.
49. **Johnson, C., K. Sanders, and H. Fan.** 2010. Jaagsiekte sheep retrovirus transformation in Madin-Darby canine kidney epithelial cell three-dimensional culture. J Virol **84:**5379-90.
50. **Kennedy, B. J.** 1992. The evolution of hydroxyurea therapy in chronic myelogenous leukemia. Semin Oncol **19:**21-6.
51. **Kim, C. F., E. L. Jackson, A. E. Woolfenden, S. Lawrence, I. Babar, S. Vogel, D. Crowley, R. T. Bronson, and T. Jacks.** 2005. Identification of bronchioalveolar stem cells in normal lung and lung cancer. Cell **121:**823-35.
52. **Kool, J., A. G. Uren, C. P. Martins, D. Sie, J. de Ridder, G. Turner, M. van Uitert, K. Matentzoglu, W. Lagcher, P. Krimpenfort, J. Gadiot, C. Pritchard, J. Lenz, A. H. Lund, J. Jonkers, J. Rogers, D. J. Adams, L. Wessels, A. Berns, and M. van Lohuizen.** 2010. Insertional mutagenesis in mice deficient for p15Ink4b, p16Ink4a, p21Cip1, and p27Kip1 reveals cancer gene interactions and correlations with tumor phenotypes. Cancer Res **70:**520-31.
53. **Kopp, E. B., and R. Medzhitov.** 1999. The Toll-receptor family and control of innate immunity. Curr Opin Immunol **11:**13-8.
54. **Leroux, C., N. Girard, V. Cottin, T. Greenland, J. F. Mornex, and F. Archer.** 2007. Jaagsiekte Sheep Retrovirus (JSRV): from virus to lung cancer in sheep. Vet Res **38:**211-28.
55. **Li, J., H. Shen, K. L. Himmel, A. J. Dupuy, D. A. Largaespada, T. Nakamura, J. D. Shaughnessy, Jr., N. A. Jenkins, and N. G. Copeland.** 1999. Leukaemia disease genes: large-scale cloning and pathway predictions. Nat Genet **23:**348-53.

56. **Linnerth-Petrik, N. M., L. A. Santry, D. L. Yu, and S. K. Wootton.** 2012. Adeno-associated virus vector mediated expression of an oncogenic retroviral envelope protein induces lung adenocarcinomas in immunocompetent mice. PLoS One **7:**e51400.
57. **Liu, S. L., F. M. Duh, M. I. Lerman, and A. D. Miller.** 2003. Role of virus receptor Hyal2 in oncogenic transformation of rodent fibroblasts by sheep betaretrovirus env proteins. J Virol **77:**2850-8.
58. **Liu, S. L., M. I. Lerman, and A. D. Miller.** 2003. Putative phosphatidylinositol 3-kinase (PI3K) binding motifs in ovine betaretrovirus Env proteins are not essential for rodent fibroblast transformation and PI3K/Akt activation. J Virol **77:**7924-35.
59. **Liu, S. L., and A. D. Miller.** 2006. Oncogenic transformation by the jaagsiekte sheep retrovirus envelope protein. Oncogene.
60. **Liu, S. L., and A. D. Miller.** 2007. Oncogenic transformation by the jaagsiekte sheep retrovirus envelope protein. Oncogene **26:**789-801.
61. **Liu, S. L., and A. D. Miller.** 2005. Transformation of madin-darby canine kidney epithelial cells by sheep retrovirus envelope proteins. J Virol **79:**927-33.
62. **Lovas, G., W. Li, U. Pott, T. Verga, and L. D. Hudson.** 2001. Expression of the Kruppel-type zinc finger protein rKr2 in the developing nervous system. Glia **34:**110-120.
63. **Maeda, N., and H. Fan.** 2008. Signal transduction pathways utilized by enzootic nasal tumor virus (ENTV-1) envelope protein in transformation of rat epithelial cells resemble those used by jaagsiekte sheep retrovirus. Virus Genes **36:**147-55.
64. **Maeda, N., W. Fu, A. Ortin, M. de las Heras, and H. Fan.** 2005. Roles of the Ras-MEK-mitogen-activated protein kinase and phosphatidylinositol 3-kinase-Akt-mTOR pathways in Jaagsiekte sheep retrovirus-induced transformation of rodent fibroblast and epithelial cell lines. J Virol **79:**4440-50.
65. **Maeda, N., Y. Inoshima, D. A. Fruman, S. M. Brachmann, and H. Fan.** 2003. Transformation of mouse fibroblasts by Jaagsiekte sheep retrovirus envelope does not require phosphatidylinositol 3-kinase. J Virol **77:**9951-9.
66. **Maeda, N., M. Palmarini, C. Murgia, and H. Fan.** 2001. Direct transformation of rodent fibroblasts by jaagsiekte sheep retrovirus DNA. Proc Natl Acad Sci U S A **98:**4449-54.
67. **Mann, G. J., M. Dyne, and E. A. Musgrove.** 1987. Immunofluorescent quantification of ribonucleotide reductase M1 subunit and correlation with DNA content by flow cytometry. Cytometry **8:**509-17.
68. **Mattison, J., J. Kool, A. G. Uren, J. de Ridder, L. Wessels, J. Jonkers, G. R. Bignell, A. Butler, A. G. Rust, M. Brosch, C. H. Wilson, L. van der Weyden, D. A. Largaespada, M. R. Stratton, P. A. Futreal, M. van Lohuizen, A. Berns, L. S. Collier, T. Hubbard, and D. J. Adams.** 2010. Novel candidate cancer genes identified by a large-scale cross-species comparative oncogenomics approach. Cancer Res **70:**883-95.
69. **Meyer, S. E., J. R. Hasenstein, A. Baktula, C. S. Velu, Y. Xu, H. Wan, J. A. Whitsett, C. B. Gilks, and H. L. Grimes.** Kruppel-Like Factor 5 Is Not Required for K-RasG12D Lung Tumorigenesis, but Represses ABCG2 Expression and Is Associated with Better Disease-Specific Survival. Am J Pathol.
70. **Miller, A. D.** 2008. Hyaluronidase 2 and its intriguing role as a cell-entry receptor for oncogenic sheep retroviruses. Semin Cancer Biol **18:**296-301.
71. **Mornex, J. F., F. Thivolet, M. De las Heras, and C. Leroux.** 2003. Pathology of human bronchioloalveolar carcinoma and its relationship to the ovine disease. Curr Top Microbiol Immunol **275:**225-48.

72. **Morozov, V. A., S. Lagaye, J. Lower, and R. Lower.** 2004. Detection and characterization of betaretroviral sequences, related to sheep Jaagsiekte virus, in Africans from Nigeria and Cameroon. Virology **327:**162-8.
73. **Mura, M., P. Murcia, M. Caporale, T. E. Spencer, K. Nagashima, A. Rein, and M. Palmarini.** 2004. Late viral interference induced by transdominant Gag of an endogenous retrovirus. Proc Natl Acad Sci U S A **101:**11117-22.
74. **Murcia, P. R., F. Arnaud, and M. Palmarini.** 2007. The transdominant endogenous retrovirus enJS56A1 associates with and blocks intracellular trafficking of Jaagsiekte sheep retrovirus Gag. J Virol **81:**1762-72.
75. **Nordlund, P., and P. Reichard.** 2006. Ribonucleotide reductases. Annu Rev Biochem **75:**681-706.
76. **Nusse, R., and H. E. Varmus.** 1982. Many tumors induced by the mouse mammary tumor virus contain a provirus integrated in the same region of the host genome. Cell **31:**99-109.
77. **Ortin, A., C. Cousens, E. Minguijon, Z. Pascual, M. P. Villarreal, J. M. Sharp, and L. Heras Mde.** 2003. Characterization of enzootic nasal tumour virus of goats: complete sequence and tissue distribution. J Gen Virol **84:**2245-52.
78. **Palmarini, M., C. Cousens, R. G. Dalziel, J. Bai, K. Stedman, J. C. DeMartini, and J. M. Sharp.** 1996. The exogenous form of Jaagsiekte retrovirus is specifically associated with a contagious lung cancer of sheep. J Virol **70:**1618-23.
79. **Palmarini, M., S. Datta, R. Omid, C. Murgia, and H. Fan.** 2000. The long terminal repeat of Jaagsiekte sheep retrovirus is preferentially active in differentiated epithelial cells of the lungs. J Virol **74:**5776-87.
80. **Palmarini, M., P. Dewar, M. De las Heras, N. F. Inglis, R. G. Dalziel, and J. M. Sharp.** 1995. Epithelial tumour cells in the lungs of sheep with pulmonary adenomatosis are major sites of replication for Jaagsiekte retrovirus. J Gen Virol **76 (Pt 11):**2731-7.
81. **Palmarini, M., and H. Fan.** 2003. Molecular biology of jaagsiekte sheep retrovirus. Curr Top Microbiol Immunol **275:**81-115.
82. **Palmarini, M., and H. Fan.** 2001. Retrovirus-induced ovine pulmonary adenocarcinoma, an animal model for lung cancer. J Natl Cancer Inst **93:**1603-14.
83. **Palmarini, M., H. Fan, and J. M. Sharp.** 1997. Sheep pulmonary adenomatosis: a unique model of retrovirus-associated lung cancer. Trends in microbiology **5:**478-483.
84. **Palmarini, M., N. Maeda, C. Murgia, C. De-Fraja, A. Hofacre, and H. Fan.** 2001. A phosphatidylinositol 3-kinase docking site in the cytoplasmic tail of the Jaagsiekte sheep retrovirus transmembrane protein is essential for envelope-induced transformation of NIH 3T3 cells. J Virol **75:**11002-9.
85. **Palmarini, M., J. M. Sharp, M. de las Heras, and H. Fan.** 1999. Jaagsiekte sheep retrovirus is necessary and sufficient to induce a contagious lung cancer in sheep. J Virol **73:**6964-72.
86. **Payne, G. S., J. M. Bishop, and H. E. Varmus.** 1982. Multiple arrangements of viral DNA and an activated host oncogene in bursal lymphomas. Nature **295:**209-14.
87. **Pearson, G., F. Robinson, T. Beers Gibson, B. E. Xu, M. Karandikar, K. Berman, and M. H. Cobb.** 2001. Mitogen-activated protein (MAP) kinase pathways: regulation and physiological functions. Endocr Rev **22:**153-83.
88. **Perk, K., I. Hod, and T. A. Nobel.** 1971. Pulmonary adenomatosis of sheep (jaagsiekte). I. Ultrastructure of the tumor. J Natl Cancer Inst **46:**525-37.
89. **Pott, U., H. J. Thiesen, R. J. Colello, and M. E. Schwab.** 1995. A new Cys2/His2 zinc finger gene, rKr2, is expressed in differentiated rat oligodendrocytes and encodes a protein with a functional repressor domain. Journal of neurochemistry **65:**1955-1966.

90. **Puig, O., F. Caspary, G. Rigaut, B. Rutz, E. Bouveret, E. Bragado-Nilsson, M. Wilm, and B. Seraphin.** 2001. The tandem affinity purification (TAP) method: a general procedure of protein complex purification. Methods **24:**218-29.
91. **Rabson, A.** 1997. Synthesis and Processing of Viral RNA. In: Coffin JM, Hughes SH, Varmus HE, editors. Retroviruses. Cold Spring Harbor (NY): Cold Spring Harbor Laboratory Press; 1997.
92. **Rai, S. K., F. M. Duh, V. Vigdorovich, A. Danilkovitch-Miagkova, M. I. Lerman, and A. D. Miller.** 2001. Candidate tumor suppressor HYAL2 is a glycosylphosphatidylinositol (GPI)-anchored cell-surface receptor for jaagsiekte sheep retrovirus, the envelope protein of which mediates oncogenic transformation. Proc Natl Acad Sci U S A **98:**4443-8.
93. **Rassa, J. C., J. L. Meyers, Y. Zhang, R. Kudaravalli, and S. R. Ross.** 2002. Murine retroviruses activate B cells via interaction with toll-like receptor 4. Proc Natl Acad Sci U S A **99:**2281-6.
94. **Rigaut, G., A. Shevchenko, B. Rutz, M. Wilm, M. Mann, and B. Seraphin.** 1999. A generic protein purification method for protein complex characterization and proteome exploration. Nat Biotechnol **17:**1030-2.
95. **Rosati, S., M. Pittau, A. Alberti, S. Pozzi, D. F. York, J. M. Sharp, and M. Palmarini.** 2000. An accessory open reading frame (orf-x) of jaagsiekte sheep retrovirus is conserved between different virus isolates. Virus Res **66:**109-16.
96. **Rosenberg, N., Jolicoeur, P. .** 1997. Retroviral Pathogenesis. In: Coffin JM, Hughes SH, Varmus HE, editors. Retroviruses. Cold Spring Harbor (NY): Cold Spring Harbor Laboratory Press; 1997.
97. **Ruscetti, S. K.** 1999. Deregulation of erythropoiesis by the Friend spleen focus-forming virus. Int J Biochem Cell Biol **31:**1089-109.
98. **Shao, J., B. Zhou, B. Chu, and Y. Yen.** 2006. Ribonucleotide reductase inhibitors and future drug design. Curr Cancer Drug Targets **6:**409-31.
99. **Sharp, J. M.** 1987. Sheep pulmonary adenomatosis: a contagious tumour and its cause. Cancer Surv **6:**73-83.
100. **Sharp, J. M., K. W. Angus, E. W. Gray, and F. M. Scott.** 1983. Rapid transmission of sheep pulmonary adenomatosis (jaagsiekte) in young lambs. Brief report. Arch Virol **78:**89-95.
101. **Sharp, J. M., and J. C. DeMartini.** 2003. Natural history of JSRV in sheep. Curr Top Microbiol Immunol **275:**55-79.
102. **Sharp, J. M., and A. J. Herring.** 1983. Sheep pulmonary adenomatosis: demonstration of a protein which cross-reacts with the major core proteins of Mason-Pfizer monkey virus and mouse mammary tumour virus. J Gen Virol **64 (Pt 10):**2323-7.
103. **Smith, M. R., and W. C. Greene.** 1991. Molecular biology of the type I human T-cell leukemia virus (HTLV-I) and adult T-cell leukemia. J Clin Invest **87:**761-6.
104. **Songyang, Z., S. E. Shoelson, M. Chaudhuri, G. Gish, T. Pawson, W. G. Haser, F. King, T. Roberts, S. Ratnofsky, R. J. Lechleider, and et al.** 1993. SH2 domains recognize specific phosphopeptide sequences. Cell **72:**767-78.
105. **Souglakos, J., I. Boukovinas, M. Taron, P. Mendez, D. Mavroudis, M. Tripaki, D. Hatzidaki, A. Koutsopoulos, E. Stathopoulos, V. Georgoulias, and R. Rosell.** 2008. Ribonucleotide reductase subunits M1 and M2 mRNA expression levels and clinical outcome of lung adenocarcinoma patients treated with docetaxel/gemcitabine. Br J Cancer **98:**1710-5.
106. **Spencer, T. E., M. Mura, C. A. Gray, P. J. Griebel, and M. Palmarini.** 2003. Receptor usage and fetal expression of ovine endogenous betaretroviruses: implications for coevolution of endogenous and exogenous retroviruses. J Virol **77:**749-53.
107. **Stehelin, D., R. V. Guntaka, H. E. Varmus, and J. M. Bishop.** 1976. Purification of DNA complementary to nucleotide sequences required for neoplastic transformation of fibroblasts by avian sarcoma viruses. J Mol Biol **101:**349-65.

108. **Suau, F., V. Cottin, F. Archer, S. Croze, J. Chastang, G. Cordier, F. Thivolet-Bejui, J. F. Mornex, and C. Leroux.** 2006. Telomerase activation in a model of lung adenocarcinoma. Eur Respir J **27:**1175-82.
109. **Sun, S., J. H. Schiller, and A. F. Gazdar.** 2007. Lung cancer in never smokers--a different disease. Nat Rev Cancer **7:**778-90.
110. **Swanstrom, R., Wills, J. W.** 1997. Synthesis, Assembly, and Processing of Viral Proteins. In: Coffin JM, Hughes SH, Varmus HE, editors. Retroviruses. Cold Spring Harbor (NY): Cold Spring Harbor Laboratory Press; 1997.
111. **Tagwerker, C., K. Flick, M. Cui, C. Guerrero, Y. Dou, B. Auer, P. Baldi, L. Huang, and P. Kaiser.** 2006. A tandem affinity tag for two-step purification under fully denaturing conditions: application in ubiquitin profiling and protein complex identification combined with in vivocross-linking. Mol Cell Proteomics **5:**737-48.
112. **Thelander, M., A. Graslund, and L. Thelander.** 1985. Subunit M2 of mammalian ribonucleotide reductase. Characterization of a homogeneous protein isolated from M2-overproducing mouse cells. J Biol Chem **260:**2737-41.
113. **Thiagalingam, S., R. L. Foy, K. H. Cheng, H. J. Lee, A. Thiagalingam, and J. F. Ponte.** 2002. Loss of heterozygosity as a predictor to map tumor suppressor genes in cancer: molecular basis of its occurrence. Curr Opin Oncol **14:**65-72.
114. **Travis, W. D., E. Brambilla, M. Noguchi, A. G. Nicholson, K. R. Geisinger, Y. Yatabe, D. G. Beer, C. A. Powell, G. J. Riely, P. E. Van Schil, K. Garg, J. H. Austin, H. Asamura, V. W. Rusch, F. R. Hirsch, G. Scagliotti, T. Mitsudomi, R. M. Huber, Y. Ishikawa, J. Jett, M. Sanchez-Cespedes, J. P. Sculier, T. Takahashi, M. Tsuboi, J. Vansteenkiste, I. Wistuba, P. C. Yang, D. Aberle, C. Brambilla, D. Flieder, W. Franklin, A. Gazdar, M. Gould, P. Hasleton, D. Henderson, B. Johnson, D. Johnson, K. Kerr, K. Kuriyama, J. S. Lee, V. A. Miller, I. Petersen, V. Roggli, R. Rosell, N. Saijo, E. Thunnissen, M. Tsao, and D. Yankelewitz.** 2011. International association for the study of lung cancer/american thoracic society/european respiratory society international multidisciplinary classification of lung adenocarcinoma. J Thorac Oncol **6:**244-85.
115. **Varela, M., M. Golder, F. Archer, M. de las Heras, C. Leroux, and M. Palmarini.** 2008. A large animal model to evaluate the effects of Hsp90 inhibitors for the treatment of lung adenocarcinoma. Virology **371:**206-15.
116. **Verwoerd, D. W., A. L. Williamson, and E. M. De Villiers.** 1980. Aetiology of jaagsiekte: transmission by means of subcellular fractions and evidence for the involvement of a retrovirus. Onderstepoort J Vet Res **47:**275-80.
117. **Vogt, P. K.** 1997. Historical Introduction to the General Properties of Retroviruses. In: Coffin JM, Hughes SH, Varmus HE, editors. Retroviruses. Cold Spring Harbor (NY): Cold Spring Harbor Laboratory Press; 1997.
118. **Vogt, V. M.** 1997. Retroviral Virions and Genomes. In: Coffin JM, Hughes SH, Varmus HE, editors. Retroviruses. Cold Spring Harbor (NY): Cold Spring Harbor Laboratory Press; 1997.
119. **Wootton, S. K., C. L. Halbert, and A. D. Miller.** 2005. Sheep retrovirus structural protein induces lung tumours. Nature **434:**904-907.
120. **Xu, X., J. L. Page, J. A. Surtees, H. Liu, S. Lagedrost, Y. Lu, R. Bronson, E. Alani, A. Y. Nikitin, and R. S. Weiss.** 2008. Broad overexpression of ribonucleotide reductase genes in mice specifically induces lung neoplasms. Cancer Res **68:**2652-60.
121. **York, D. F., R. Vigne, D. W. Verwoerd, and G. Querat.** 1991. Isolation, identification, and partial cDNA cloning of genomic RNA of jaagsiekte retrovirus, the etiological agent of sheep pulmonary adenomatosis. J Virol **65:**5061-7.

122. **York, D. F., R. Vigne, D. W. Verwoerd, and G. Querat.** 1992. Nucleotide sequence of the jaagsiekte retrovirus, an exogenous and endogenous type D and B retrovirus of sheep and goats. J Virol **66:**4930-9.
123. **Yousem, S. A., S. D. Finkelstein, P. A. Swalsky, A. Bakker, and N. P. Ohori.** 2001. Absence of jaagsiekte sheep retrovirus DNA and RNA in bronchioloalveolar and conventional human pulmonary adenocarcinoma by PCR and RT-PCR analysis. Hum Pathol **32:**1039-42.
124. **Zavala, G., C. Pretto, Y. H. Chow, L. Jones, A. Alberti, E. Grego, M. De las Heras, and M. Palmarini.** 2003. Relevance of Akt phosphorylation in cell transformation induced by Jaagsiekte sheep retrovirus. Virology **312:**95-105.

CHAPTER 2: A ROLE FOR ZINC FINGER PROTEIN (ZFP111) IN TRANSFORMATION OF 208F RAT FIBROBLASTS BY JAAGSIEKTE SHEEP RETROVIRUS ENVELOPE PROTEIN

Abstract

Jaagsiekte Sheep Retrovirus (JSRV) is the etiologic agent of a contagious lung cancer in sheep, ovine pulmonary adenocarcinoma. The native envelope gene (*env*) also acts as an oncogene. To investigate the mechanism of transformation we performed yeast 2-hybrid screening for cellular proteins that interact with Env. We identified Zinc Finger Protein 111 (*zfp111*), a member of the Krüppel family of zinc finger proteins, as a candidate. The interaction between Env and Zfp111 was confirmed through *in vivo* co-immunoprecipitation assays. Knockdown of endogenous zfp111 in rat 208F fibroblasts caused a decrease in cell transformation by JSRV Env but not another viral oncogene (*v-mos).* Env transformation levels could be restored by addition of a knockdown-resistant Zfp111 mutant. Over-expression of zfp111 also increased overall transformation levels by Env. Knockdown of zfp111 decreased the proliferation rates of Env transformed cells, but not untransformed cells. These results supported a role for Zfp111 in JSRV transformation.

Introduction

Jaagsiekte sheep retrovirus (JSRV) is a betaretrovirus that causes ovine pulmonary adenocarcinoma (OPA), a contagious lung cancer in sheep that reflects malignant transformation of lung secretory epithelial cells (19, 22). OPA is morphologically similar to human bronchio-alveolar carcinoma [BAC, more recently designated as Adenocarcinoma in situ (AIS)] (28), a

type of lung cancer that is less associated with cigarette smoke, and is a good model for this type of human lung cancer (20).

JSRV is a simple retrovirus that contains the standard retroviral genes *gag*, *pro*, *pol*, and *env* (33). While JSRV does not carry a transduced cellular oncogene, in experimental inoculation of lambs it induces tumors rapidly (as early as 10 days), similar to acute transforming retroviruses that carry viral oncogenes (25, 30). Interestingly we and others have shown that JSRV envelope protein (Env) also functions as an oncogene in that expression of JSRV Env alone can transform cells in culture (16) and induce lung cancer in mice (10, 32). Thus JSRV Env has the rare feature of acting as both the envelope protein for the virus as well as an oncogene for cell transformation. This rare feature is shared only by a closely related retrovirus enzootic nasal tumor virus (ENTV), which causes epithelial tumors in the nasal passages of infected animals (4).

JSRV Env is initially translated from spliced viral mRNA into a polyprotein that is a type-I transmembrane protein of approximately 615 amino acids (5, 22, 33). The Env polyprotein is cleaved by cellular furin protease into the surface (SU) and transmembrane (TM) proteins. The SU protein is responsible for receptor binding and TM is responsible for the fusion of viral and cellular membranes upon infection. TM contains a 45 amino acid cytoplasmic tail (CT) region that extends into the cytoplasm of the cell. The CT of Env contains the sequence YRNM, a putative binding site for the regulatory subunit (p85) of phosphatidyl inositol 3-kinase (PI3K) if the tyrosine residue is phosphorylated (26). Mutations in the YRNM tyrosine residue (Y590F or Y590D) inhibited Env transformation in mouse NIH 3T3 fibroblasts (8, 21) and tumorigenesis in sheep (3). However, tyrosine phosphorylation has not been detected in TM in JSRV-transformed cells (11) and pull-down experiments have not demonstrated direct

interaction between JSRV Env and PI3K (12). Nevertheless a downstream substrate of PI3K, Akt, is constitutively phosphorylated in JSRV-transformed cells and PI3K inhibitors revert JSRV-transformed cells back towards the non-transformed phenotype (11, 27, 34). Thus the CT of TM (and the YRNM motif in particular) is necessary for JSRV transformation, although this may not result directly from binding of PI3K.

The signaling pathways activated by JSRV Env transformation have also been studied. Both the PI3K-Akt-mTOR and Ras-MEK-MAPK pathways appear to be important for JSRV transformation (11, 14, 21, 34). Inhibitors of the Ras-MEK-MAPK pathway were used in JSRV transformed NIH 3T3 mouse fibroblasts and RK3E rat epithelial cells. Transformed NIH 3T3 cells showed a stronger dependence on Ras-MEK-MAPK compared RK3E cells (14). In contrast treatment with an inhibitor of PI3K-Akt-mTOR signaling, rapamycin, indicated that this pathway was more important for RK3E than NIH-3T3. Thus the relative importance of these pathways for JSRV transformation differs among different cell lines. So far, none of the proteins/enzymes in these signaling pathways have been found to directly interact with JSRV Env. Thus it will be important to identify the cellular proteins that interact with JSRV Env and ultimately activate the downstream signaling pathways such as PI3K-Akt-mTOR and Ras-MEK-MAPK.

In this chapter, a yeast 2-hybrid screen was performed using both full length JSRV Env and cytoplasmic tail (CT) of JSRV Env to identify candidate cDNAs that interact with JSRV Env protein. Seven candidate cDNAs were identified, and among those candidate proteins we identified a zinc finger protein of the Krüppel family, zinc finger protein 111 (Zfp111) that showed strong interaction with both bait proteins and multiple independent cDNA clones being

isolated. Validation of Zfp111 binding with Env *in vivo*, and evidence for a role in JSRV transformation are described in this chapter.

Materials and Methods

Cell Lines. Human embryonic kidney cells 293T and rat fibroblast 208F cells were grown in Dulbecco's modified Eagle's medium supplemented with 10% fetal bovine serum, penicillin (100 U/mL) and streptomycin (100 µg/mL)

Plasmid constructs. The JSRV Env expression plasmid (ΔGP) and the Flag-tagged version have been previously been described (15, 16).

HA-tagged mouse zfp111 expression vector was generated by PCR amplifying mouse zfp111 cDNA from Open Biosystems with the primers 5' –TCCCCGGTCGACAGAACAATGA CCAAGTTA and 5' –TCCCCGGCGGCCGCTTAAGCGTAGTCCGGAACGTCGTACGGGT AATCGGAAGTGTGAGGCCTGAT which was then cloned into pCMV-SPORT6 (Open Biosystems) using SalI and NotI. HA-tagged rat zfp111 expression vector was generated by collecting total RNA from rat 208F cells and converting RNA into cDNA using a 5'/3' RACE Kit (Roche) as per manufacturer's instructions. The cDNA was amplified using 5' –CGCGGC CGGTCCTTTCTAG and 5' –CCACACTGCTAACCGTGAGGG and the PCR product was cloned into the pGEM-T vector (Promega). The rat cDNA was subcloned into pCMV-SPORT6 by using the following primers 5' –TCCCCGGTCGACAGAACGATGACCA AGTTA and 5' – TCCCCGGCGGCCGCTTAAGCGTAGTCCGGAACGTCGTACGGGTAACCGTGCAG GGTTTTTTCTCC and using SalI and NotI. Mutant zfp111 was generated via site-directed mutagenesis at the target site of r36-2 shRNA and was accomplished with two sets of primers (5'

–AGCGCTACTGGTGCCACGA with 5’ –TCGTGGCACCAGTAGCGGT and 5’ –AGCGATATTGGTGCCACGA with 5’ –TCGTGGCACCAATATCGCT).

Yeast two-hybrid Screen. pEG 202 [developed by Brent and coworkers (7)], was used as the vector to express the LexA-JSRV Env fusion protein. It contains the *his3* selectable marker, yeast 2u origin, Escherichia coli pBR origin, and LexA DNA-binding domain. These plasmids (containing the Env fusions) were used as baits.

A human HeLa cell cDNA library and also a mouse liver cDNA library were constructed in the transcription activator B42 fusion vector, pJG4-5 (7). Plasmid pJG4-5 contains the TRP1 selectable marker, yeast 2μ origin, and E. coli pUC origin. Expression of the fusion protein in this plasmid is under the control of GAL1, a galactose-inducible promoter. For the first screen the yeast strain EGY48/pEGLex-JSRV Env was transformed with the HeLa cell cDNA library by the lithium acetate method. Transformants were selected for tryptophan prototrophy on synthetic agar medium containing 2% glucose. All of the transformants were pooled and re-spread on synthetic medium containing 2% galactose for induction. Cells growing on the selection media were retested on the synthetic medium containing 2% galactose (inducing condition) and 2% glucose (non-inducing condition) to confirm their growth dependence on galactose. Cells growing only on the galactose media were subjected to further characterization. The selected cells were also streaked on synthetic medium containing 2% galactose or 2% glucose with 5-bromo-4-chloro-3-indolyl-D-Galactoside (X-gal) to test for β-galactosidase activity. The cells expressing both reporter genes only in the presence of galactose were finally chosen for plasmid isolation. The isolated plasmids were transformed into the E. coli K12 strain KC8, and transformants containing the recombinant cDNAs were selected by their growth on M9 minimal medium containing ampicillin. The plasmids were then isolated from Trp+ E. coli

transformants and used to confirm the selection results and cDNA inserts were sequenced in vitro.

Immunoprecipitation. 293T cells were seeded at 2 X 10^6 cells in 10-cm dishes overnight and transfected with 28 µg total DNA using the CalPhos Mammalian transfection kit (Clontech) as per manufacturer's instructions. Cells were incubated for 48 hours prior to cell lysis. Cells were lysed by sonication in 1% NP-40 lysis buffer [50mM Tris-HCl, pH 8, 150 mM NaCl, 1% NP-40 Substitute, and 1 tablet of Complete Mini EDTA Free (Roche)]. Lysates were cleared by centrifugation and pre-cleared by adding 50 µL of Protein A-Agarose beads (Roche). Supernatants were incubated overnight at 4 °C with 2 µL of Rabbit anti-HA antibody (Cell Signaling) or with 50 µL of Anti-FLAG M2 Affinity Gel (Sigma). An immunoprecipitation (IP) control was done by adding 2 µL of Normal Rabbit IgG (Santa Cruz Biotechnology). Next day, 50 µL of Protein A-Agarose beads was added to the samples incubating with Rabbit anti-HA antibody or with Normal Rabbit IgG and incubated for 4 hours. The incubations were separated into bound (pellet) and unbound (supernatant) fractions by centrifiguation in a microfuge for 5 minutes. After washing of the pellets with lysis buffer the immunoprecipitated material was eluted from the washed pellets by boiling in 2X Laemmli buffer. Proteins were resolved on 10% SDS-polyacrylamide gels and probed with primary antibodies rabbit anti-FLAG or mouse anti-HA antibodies (Cell Signaling), and secondary antibodies goat anti-rabbit HRP or goat anti-mouse HRP(Pierce), respectively. Blot was visualized by chemiluminescence with SuperSignal Femto Maximum Sensitivity Substrate (Pierce).

Zfp111 knockdown and transformation. Construction of the lentiviral shRNA vectors were based the LVTHm vectors [Wiznerowicz & Trono (31)]. The sense sequences for the shRNAs used here are as follows: r27-1 is 5' –ACACTGTCTGCAGACTCTG, r36-2 is 5' –

AGCGCTACTGGTGTCATGA, Scrambled control is 5' –CCTAAGGTTAAGTCG CCCT. Vectors stocks were generated by transiently transfecting the vector plasmids along with pCMV-dR.8.74 (HIV gag-pol) and pMD2G (VSV G protein) helper plasmids into 293T cells, and supernatants were collected after 48 hrs. The lentiviral vector stocks were titered by infection of 208F cells, followed by counting foci of EGFP fluorescence (present in the LVTHm vector) after 4 days. For transduction with the lentiviral vectors, rat fibroblast 208F cells were seeded in 6-well plates at Multiplicities of Infection of 10 or greater with polybrene (final concentration of polybrene: 8 µg/mL), then incubated for 24 hours with the lentiviral vectors. At 24 hours post-transduction, transduced cells were trypsinized and seeded for transformation assays. Transformation assays with the transduced 208F cells were as follows: 208F cells were seeded at 3 X 10^5 cells in 6-cm dishes and transfected with 5 µg of ΔGP using Fugene 6 Transfection Reagent (Promega). In the transformation restoration assay, transduced 208F cells were co-transfected with 5 µg of ΔGP and either WT rat zfp111 or Mutant shRNA-resistant rat zfp111 expression vector. Cells were examined under phase-contrast microscopy at 4 to 5 weeks and and the number of transformed foci were counted. The number of foci relative to those in LVTHm (empty vector)-transduced cells in the same experiment were calculated, and the results from at least three independent experiments were averaged. Statistical significance was determined by Student's t-test.

Zfp111 overexpression and transformation. 208F cells were seeded at 3 X 10^5 cells in 6-cm dishes and transfected with Fugene 6. A total of 10 µg of DNA was transfected into cells, 5 µg ΔGP and up to 5 µg of mouse zfp111 expression vector. Cells were examined under phase-contrast microscopy at 4 to 5 weeks and scored for foci. Statistical significance was determined by Student's t-test.

Quantitative real-time PCR. Total RNA was isolated from cells using Trizol Reagent (Life Technologies) and 2 µg of RNA was digested with DNase I and converted to cDNA using qScript cDNA Synthesis Kit (Quantas) as per manufacturer's instructions. Resulting cDNAs were diluted to a final concentration of 20 ng/µL. Primers for amplification of target genes are as follows: rat zfp111, 5' –GAAGCCATTCAAATGCAATGCATGCCA and 5' –CTCTGATGGATTTGAAGACTGGACC ; mouse zfp111, 5' –GAAGCCATTCAAATGCAATGCATGCCA and 5' –GGAGACCAGACCTCTGGCCAAAGG ; rat β-actin, 5' –CACCAGTTCGCCATGGATGACGAT and 5' –TCTCTTGCTCTGGGCCTCGTCG. Quantitative real-time PCR reactions were performed using Power SYBR Green PCR Master Mix in the 7900HT Fast Real-Time PCR System (Applied Biosystems) as per manufacturer's instructions. All qPCR reactions were run in triplicate. The RNA expression levels were determined by both absolute standard curve and relative comparative C_t methods.

Cell Proliferation Assay. 208F cells (parental or Env transformed) transduced with control or zfp111 shRNA knockdown vectors were seeded at 2.5 X 10^4 cells in 6-cm dishes. The cells were removed from replicate dishes daily by trypsinization and the number of cells was determined by counting in a hemacytometer, using trypan blue exclusion to score only live cells.

Results

Yeast 2-hybrid system screening for cellular proteins interacting with JSRV Env. To identify candidate cellular proteins that interact with JSRV Env, two yeast 2-hybrid screens were performed, with bait plasmids containing either the cytoplasmic tail (CT) of Env or full length JSRV Env, as described in Materials and Methods. In one screen, the bait plasmid was the JSRV Env CT fused to the LexA DNA binding domain, which was stably transfected into

cells along with a *his3* gene driven by a promoter with LexA binding sites. They were then transformed with plasmids from a cDNA library from human HeLa cells; the cDNAs were fused to the activation domain of B42. Colonies with candidate interacting proteins were identified by growth on medium selective for *His* expression. In the second screen, the bait plasmid consisted of the entire JSRV Env protein, and the cDNA library was from mouse liver. The candidate interactor proteins are shown in Table 2.1. Two candidates were of particular interest based on the strength of the interactions with the bait and isolation of multiple interacting cDNA clones, *RRM2* and *zfp111*. These candidates correspond to the ribonucleotide reductase regulatory subunit and a zinc-finger protein with transcriptional repressor activity (24), respectively. Studies on the potential role of RRM2 in JSRV transformation will be reported in Chapter 4. Currently, there are few reports regarding *zfp111* function, especially in the area of cancer. It has been shown that *zfp111* contains 19 zinc finger domains, as well as a Krüppel-associated box domain that suggests function as a transcriptional repressor, and it is highly expressed in neuronal tissue (but expressed at low level in many other tissues) (24). While Zfp111 was identified as a candidate interacting partner in the screen with full-length JSRV Env protein, interaction of zfp111 cDNAs was also found in a subsequent yeast 2-hybrid assay where the bait plasmid contained only the CT domain (not shown). Thus the putative area of Zfp111 interaction is in the cytoplasmic tail of the Env TM protein, which is also the crucial domain for Env-induced cell transformation.

***In vivo* interaction between *Zfp111* and JSRV Env.** To examine the interaction between Zfp111 and JSRV Env in mammalian cells, an HA epitope-tagged zfp111 expression vector was co-transfected along with a FLAG eptitope-tagged JSRV Env expression vector (ΔGP-FLAG, which is a JSRV Env expression vector that has a FLAG epitope tag attached to

Table 2.1: Candidate JSRV Env-interacting proteins from yeast 2-hybrid screens

Candidates	Bait[a]	Library used[b]	Interaction strength[c]	Numberof clones[d]	Normal cell function	Transformation[e]
IKAP	CT	Human	++	1	Component of transcription elongation complex	?
RRM2	CT	Human	++	4	Ribonucleotide reductase regulatory subunit	+
Pontin 52	CT	Human	+	1	Beta-catenin interacting protein (Nuclear); Chromatin remodeling; c-myc interactor	+
Reptin 52	CT	Human	+	1	Beta-catenin interacting protein (Nuclear); Chromatin remodeling; c-myc interactor	+
Nm23-H2/NDPK-B	CT	Human	++	1	Nucleoside Diphosphate Kinase; suppressor or metastasis; transcriptional activator	+
Ferritin	CT	Human	++	1	Fe binding protein	-
Zfp111	Whole Env/ CT	Mouse / Human	++	4	Zinc-finger protein 111; transcriptional suppressor	?

[a] Two different bait proteins in the screens were used, either JSRV Env cytoplasmic tail only (CT) or the whole JSRV Env protein.
[b] cDNA libraries from human (HeLa) and mouse (NIH-3T3) cells were screened.
[c] Interaction strengths were based on the relative blue color of colonies on X-gal plates.
[d] Number of independent clones of the same cDNA that were isolated from the screens.
[e] Previous publications reporting a role in cell transformation or tumorigenesis.

the C-terminus of JSRV Env) into HEK 293T cells and the total cell lysate was incubated with either anti-FLAG or anti-HA antibody-conjugated agarose beads for co-immunoprecipitation. In Fig. 2.1 left panel (middle three lanes), 293T cells that were co-transfected with ΔGP-FLAG and Zfp111-HA and then immunoprecipitated with anti-FLAG showed that anti-FLAG was able to

successfully pull down JSRV Env and also co-immunoprecipitate Zfp111-HA (the eluate lane), demonstrating interaction between Zfp111 and JSRV Env *in vivo*. The control samples, which included transfection of Zfp111-HA only (left three lanes) and co-transfection of ΔGP -FLAG and Zfp111-HA but immunoprecipitation with normal rabbit IgG (right three lanes), did not show co-precipitation between the two proteins. (Note that for all immunoprecipitations in this figure, 20X more eluate volume was loaded compared to total cell lysate and flow-thru.) In the right panel, the reciprocal co-immunoprecipitation using anti-HA was also successful in immunoprecipitating Zfp111-HA and co-precipitating JSRV Env in the samples that were transfected with both expression vectors. The control cells transfected with ΔGP-FLAG showed no co-precipitation of Env. Doubly transfected cell lysates immunoprecipitated with normal rabbit IgG only showed some Env in the eluate, but it was less than when the lysates were immunoprecipitated for Zfp111. In fact, two bands of JSRV Env were observed in lysates from cells transfected with both JSRV Env and Zfp111, and only the lower (more rapidly migrating) band of Env was co-precipitated with Zfp111. The appearance of this lower band will be discussed in Chapter 3. In summary, co-immunoprecipitation of JSRV Env and Zfp111 was observed in transfected 293T cells, suggesting *in vivo* interaction between the two proteins.

Effects of zfp111 knockdown and restoration on JSRV Env transformation. To investigate the potential role of Zfp111 in JSRV Env transformation, lentiviral shRNA vectors were constructed containing shRNA sequences targeting different areas of rat zfp111 mRNA. Lentiviral transduction was chosen since long-term knockdown of zfp111 was needed during the course of *in vitro* transformation assays (4-5 weeks). The control lentiviral vectors (LVTHm and

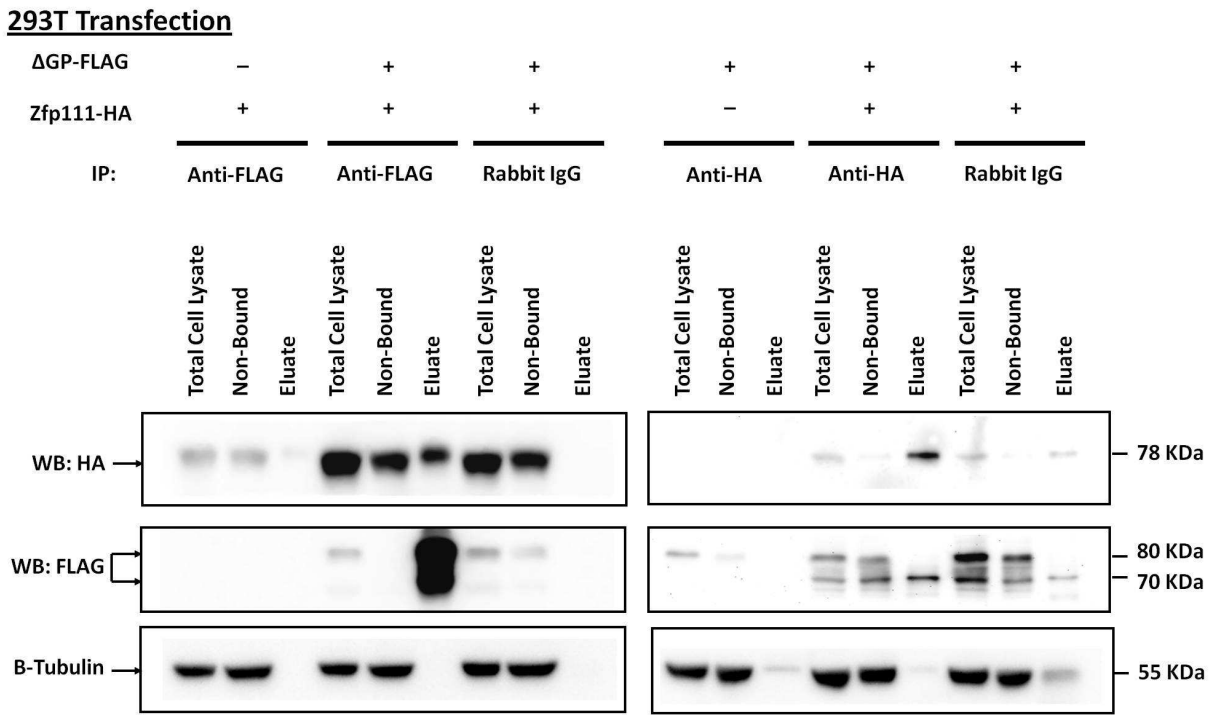

Fig 2.1: Co-immunoprecipitation of JSRV Env and Zfp111. HEK 293T cells were transfected with ΔGP-FLAG (JSRV Env expression vector with C-terminal FLAG tag), Zfp111-HA, or both. Total cell lysates were incubated with either anti-HA antibody followed by protein A sepharose beads, or anti-FLAG affinity gel (purified monoclonal antibody attached to agarose) as described in Materials and Methods. For each lane, equal fractions of total cell lysate and non-binding fraction, and twenty times more eluate were loaded into 10% acrylamide gel and analyzed by Western blotting with either anti-FLAG or anti-HA antibody. Afterwards the blots were stripped and re-probed with the alternate antibody.

LVTHm-Scrambled) and the shRNA knockdown lentiviral vectors (r27-1 and r36-2) were used to infect rat 208F fibroblasts. The endogenous zfp111 RNA expression levels were analyzed by quantitative RT-PCR and normalized expression levels relative to infection with LVTHm are shown in Fig. 2.2A. The most effective zfp111 shRNA vector, r36-2, showed a decrease in zfp111 expression level of 60% while the r27-1 shRNA vector was less effective. Two more shRNA vectors were tested for zfp111 knockdown efficiency, but were not effective in decreasing zfp111 expression levels (data not shown).

Subsequently, 208F cells stably transduced with the vectors in Fig. 2.2A were transfected with JSRV Env expression vector ΔGP and incubated in focus formation assays (8); the levels of cell transformation were quantified by counting the number of resulting transformed foci for each cell line. For each experiment, the transfections were performed in triplicate, and the experiments were repeated three times. For cells transduced with r36-2, there was a statistically significant 40% decrease in JSRV Env transformation levels compared to cells transduced with control LVTHm and LVTHm-Scrambled (Fig. 2.2B). Cells transduced with r27-1, which showed less knockdown of zfp111 expression, did not show a significant decrease in JSRV Env transformation. Thus knockdown of zfp111 resulted in dose-dependent reduction in JSRV Env transformation, consistent with a role of this protein in transformation.

To test if the reduction in JSRV Env transformation by zfp111 knockdown was specific, the transduced cell lines were also tested in transformation assays with *v-mos*, an oncogene that does not activate the same signaling pathways as for JSRV Env [Ras-Raf-MEK and PI3K-Akt-mTOR (14)]. As also shown in Fig. 2.2B, zfp111 knockdown had no effect on *v-mos* transformation, particularly in r36-2 transduced cells, where the levels of transformation were similar to those for the LVTHm transduced cells.

To test if the reduction in JSRV transformation in r36-2 transduced 208F cells was due to knockdown of zfp111 as opposed to an off-target effect, we tested if restoration of zfp111 expression in these cells increased JSRV transformation. 208F cells transduced with r36-2 were co-transfected with a rat zfp111 expression vector containing silent mutations in the r36-2 shRNA recognition site along with JSRV Env expression vector ΔGP, and incubated in focus formation assays. Quantitative PCR results showed an increase in zfp111 expression levels

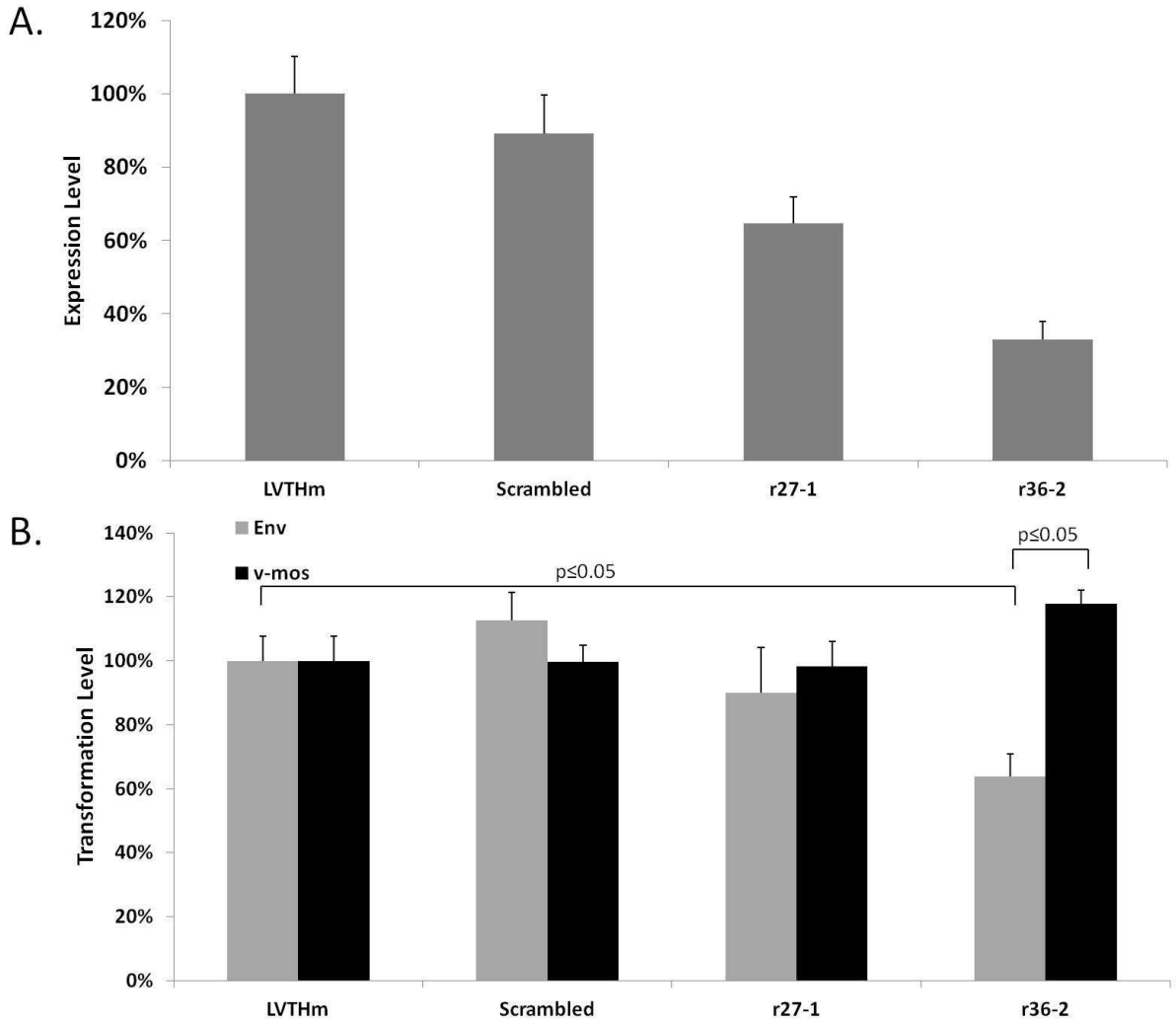

Fig 2.2: Effects of zfp111 knockdown on JSRV Env transformation. 208F cells were transduced with control shRNA vector LVTHm (empty vector) and LVTHm containing a scrambled shRNA (Scrambled-LVTHm) or with r27-1 and r36-2 (shRNAs targeting Zfp111). (A) zfp111 expression levels in transduced cells were determined by quantitative RT-PCR analysis 4-5 weeks post-transduction. (B) Mass cultures of 208F cells transduced by each of the vectors were transfected in triplicate with ΔGP DNA, incubated in transformation assays, and the transformation levels were determined by counting the number of transformed foci 4-5 weeks post-transfection. (Mass cultures were used to minimize effects of clonal cell variation in response to ΔGP transformation.) The levels of transformation for each shRNA vector were normalized to that of control LVTHm transduced cells (light bars). The means and standard deviations were determined from at least three independent assays; reduction of JSRV Env transformation in the r36-2 transduced cells was statistically significant. The same transduced cell cultures were transformed with *v-mos* oncogene, and transformation assays were performed under the same conditions (black bars).

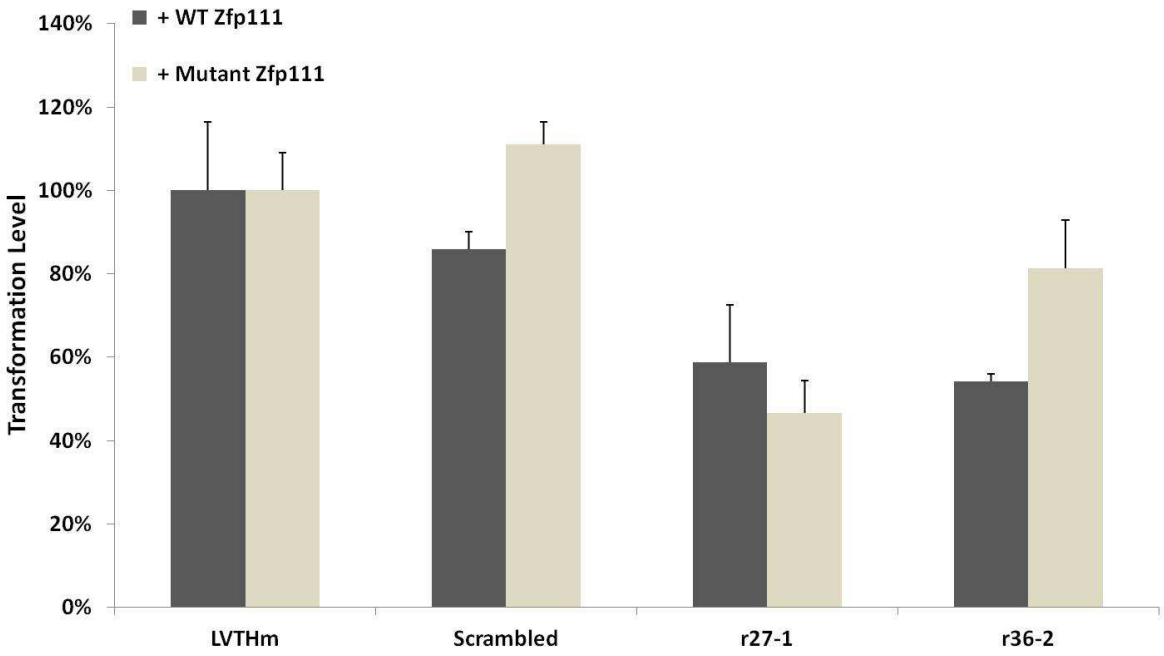

Fig 2.3: Rescue of transformation by shRNA-resistant Zfp111. Similar transduced cell cultures as in Fig. 2.2 were transfected with ΔGP DNA and plasmids expressing either wild-type (WT) rat Zfp111 or an r36-2 shRNA-resistant (Mutant) rat Zfp111 cDNA. Transformation assays were performed and analyzed as in Fig. 2.2.

compared to r36-2 transduced 208F cells (data not shown). As a control, Wild-Type (WT) rat zfp111 expression vector was co-transfected with JSRV Env into the transduced cells. As shown in Fig. 2.3, r36-2 transduced cells co-transfected with WT zfp111 showed similar levels of Env transformation as previously observed in Fig. 2.2B, with 50% decrease in transformation compared to control LVTHm transduced cells. When the same cells were co-transfected with the mutant zfp111 plasmid and ΔGP, there was a statistically significant 30% increase in transformation. In fact the level of transformation (80%), while lower was not statistically different from that observed for cells transduced with the control LVTHm vector (no zfp111 knockdown). In cells transduced with the r27-1 knockdown vector, co-transfection with the mutant zfp111 vector did not enhance JSRV Env transformation (Fig. 2.3). This was consistent

with the fact that the mutant zfp111 expression plasmid was mutant for the seed sequence for the 36-2 but not the 27-1 shRNA. This indicated specificity of the restoration of transformation for the 36-2 knockdown cells, and further supported the role of Zfp111 in JSRV transformation.

In summary, knockdown of endogenous zfp111 in rat fibroblast 208F cells specifically reduced transformation levels by JSRV Env, but not for a different oncogene *v-mos*. Partial restoration of JSRV Env transformation in zfp111 knockdown cells was observed by transfecting a shRNA resistant zfp111 expression vector, which also supported the specificity of the effects on zfp111 knockdown.

Effects of zfp111 over-expression on JSRV Env transformation. In light of the reduction in JSRV Env transformation after zfp111 knockdown, the effect of zfp111 over-expression in JSRV Env transformation was also analyzed. 208F cells were co-transfected with different amounts of zfp111 expression vector and constant amounts of JSRV Env expression vector ΔGP. The transfected cells were tested for the levels of zfp111 RNA expression by qRT-PCR at 4-5 weeks post-transfection, at the time focus formation assays were scored. In Fig. 2.4A, increasing amounts of zfp111 expression vector showed corresponding increases in zfp111 expression. The level of zfp111 expression in the 5µg zfp111 only cells as compared with 5µg zfp111 plus 5µg Env cells was similar, indicating that Env expression does not increase zfp111 RNA expression. The transfected cells were plated in transformation assays and the results are shown in Fig. 2.4B. Zfp111 alone was not sufficient to induce cell transformation. However, when zfp111 was co-transfected with JSRV Env the overall cell transformation levels were higher than with JSRV Env alone. Furthermore, increasing amounts of zfp111 showed a dose-dependent increase in transformation levels, with the greatest effect (ca. two-fold enhancement) for the highest level of Zfp111 (5µg). To test if this increase in transformation was specific to

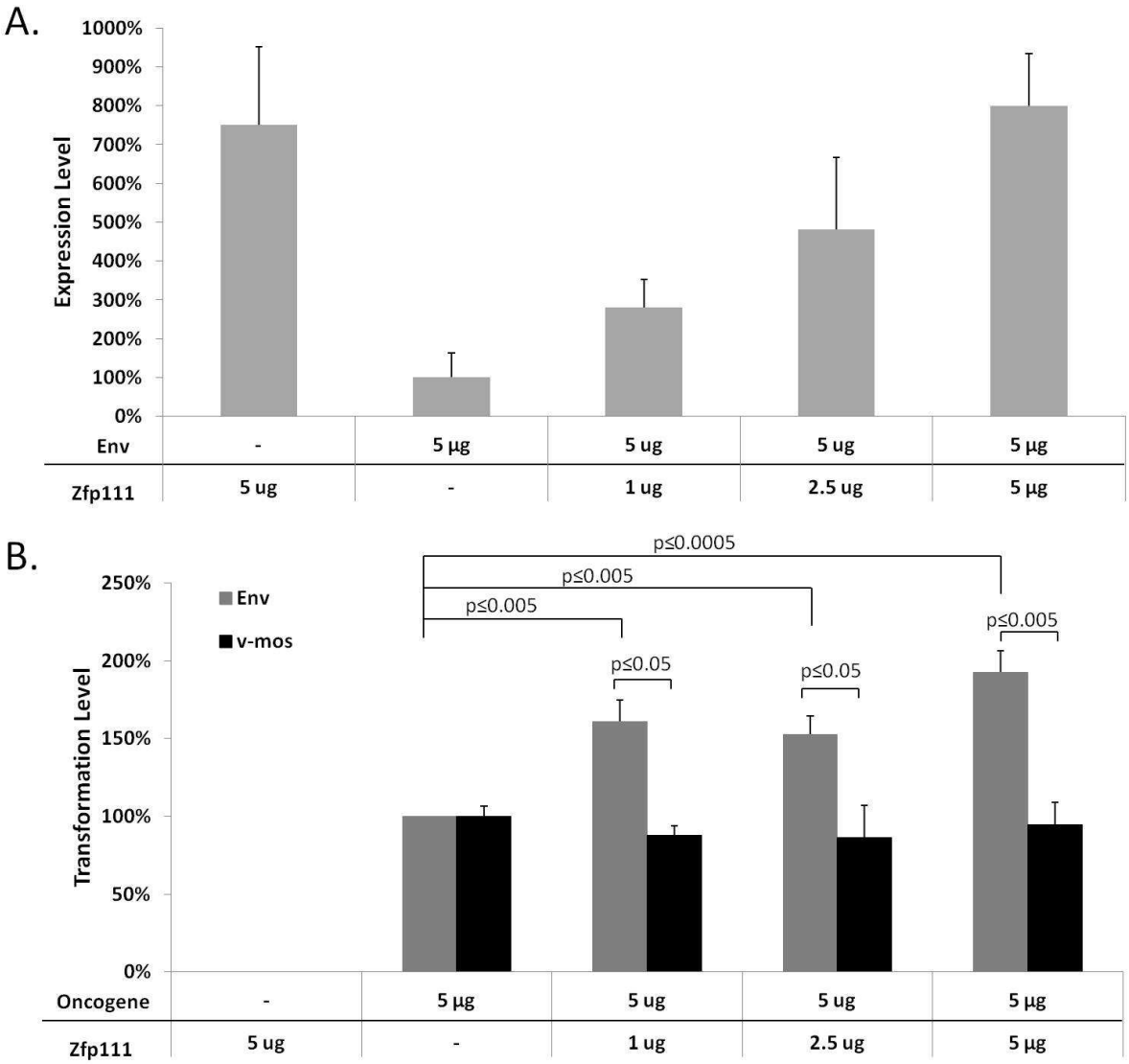

Fig 2.4: Effects of zfp111 overexpression on JSRV Env transformation. Rat 208F cells were transfected with either ΔGP and/or the WT zfp111 expression vector, as indicated. A total of 10ug of plasmid was transfected into each culture, with pCDNA making up the remainder where applicable. (A) Zfp111 expression levels in the transfected cells were determined by quantitative RT-PCR analysis. Levels were normalized to Env (5ug) alone. (B) The transfected cultures were incubated in transformation assays and transformation levels were determined by counting the numbers of foci (shaded bars). The means and standard deviations were determined from at least two independent assays done in triplicate, and levels were normalized to Env (5µg) alone. Equivalent cultures were co-transfected with *v-mos* expression vector and different levels of zfp111 expression vector, and the results are shown (black bars).

JSRV Env, these cells were also co-transfected with *v-mos* and zfp111. As also shown in Fig. 2.4B, overexpression of zfp111 had no effect on *v-mos* transformation levels, indicating that the Zfp111-mediated increase in transformation was specific to JSRV Env.

Effects of zfp111 knockdown on cell proliferation. To test if knockdown of zfp111 affected cell proliferation rates (which could influence focus formation assays), growth rates of three cell lines were measured: untransformed parental 208F, 208F transduced with the scrambled shRNA vector, and 208F transduced with the r36-2 zfp111 shRNA vector. In Fig. 2.5A, the proliferation rates for these three cell lines were compared over four days, and their growth rates were comparable, as evident from the similar slopes in the semi-log plot. This suggested that knockdown of zfp111 does not affect growth rates of 208F cells. In Fig. 2.5B, JSRV Env transformed 208F cells were transduced with the same two vectors and the proliferation rates of the resulting cell lines were also measured. Transformed 208F cells and those transduced with the control vector (208F Env and Scrambled Env) showed similar proliferation rates, while transformed cells transduced with the zfp111 shRNA (r36-2 Env) showed decreased proliferation. Thus in JSRV Env-transformed cells, knockdown of zfp111 results in a decreased growth rate, suggesting that JSRV-transformed cells became more dependent on Zfp111 for growth.

Discussion

In this study we sought to identify cellular proteins involved in oncogenic transformation by JSRV Env. JSRV Env transformation involves the activation of signaling pathways such as PI3K-Akt and Ras-MEK-ERK, but JSRV Env has not been shown to directly interact with proteins/enzymes of these pathways (11, 14, 21, 34). Through yeast 2-hybrid screening, we

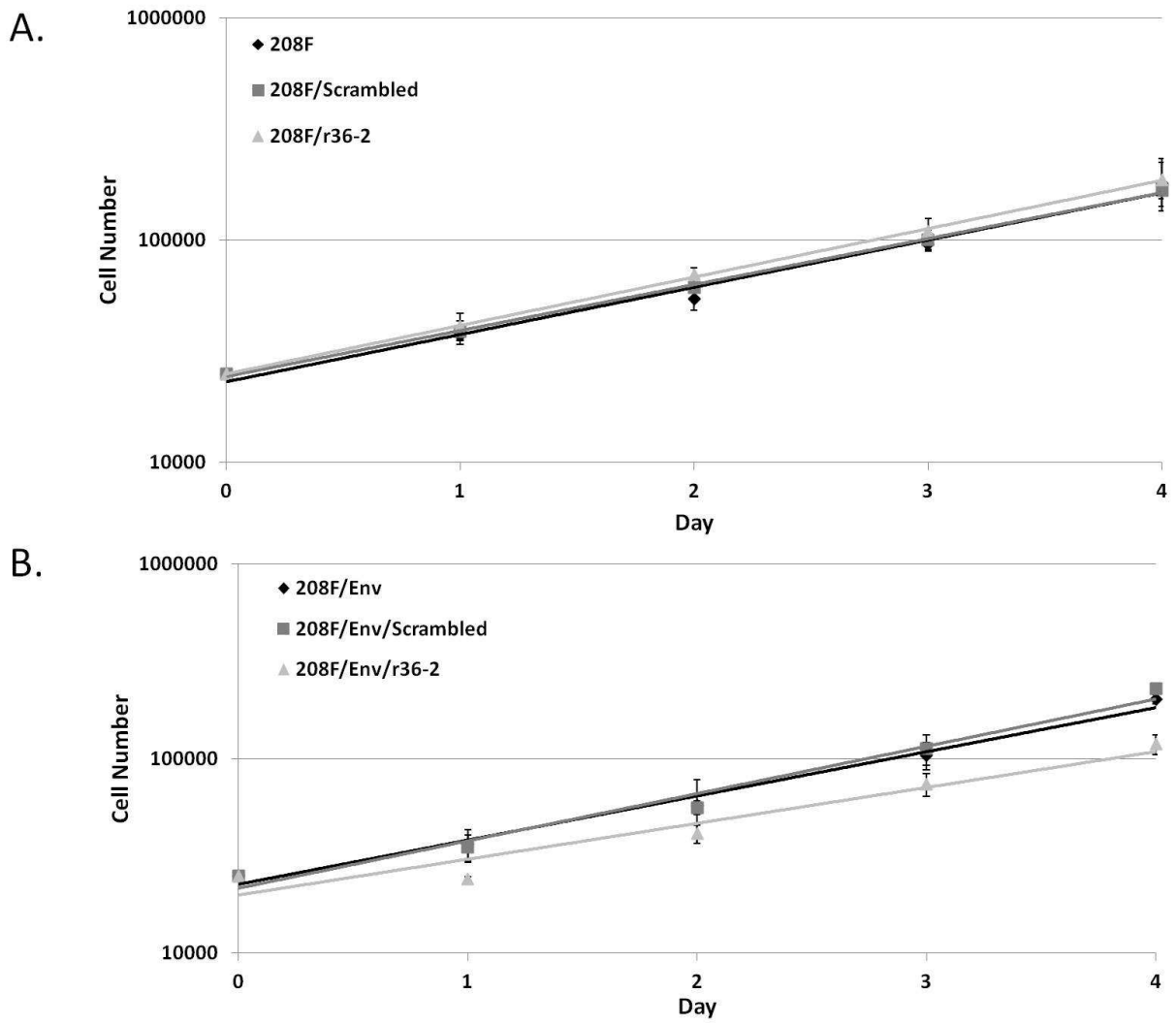

Fig 2.5: Effects of zfp111 knockdown on cell proliferation. Untransformed or Env transformed 208F cells were transduced with scrambled shRNA or zfp111 targeting shRNA vectors (Scrambled and r36-2, respectively) to generate additional cell lines. A total of 2.5 X 10^4 cells were seeded in all wells of 6-well plates and the number of viable cells was determined by trypsinization and counting viable cells as measured by trypan blue exclusion over a period of 4 days. The results (semi-log plots) from three independent experiments, each performed in duplicate, are shown. (A) Growth rates of parental 208F cells and 208F cells transduced with Scrambled and r36-2. (B) Growth rates for JSRV Env transformed 208F cells and Env transformed 208F cells transduced with Scrambled and r36-2.

identified candidate proteins that interact with either the JSRV Env cytoplasmic tail or with the whole Env protein, and Zfp111 was studied here. Pull-down experiments confirmed that Zfp111 interacts with JSRV Env in cells, and knockdown of Zfp111 corresponded to a reduced

efficiency of JSRV transformation in rat 208F cells. Conversely, over-expression of zfp111 corresponed with an enhanced efficiency of JSRV Env transformation. The role of Zfp111 appeared to be specific for JSRV Env transformation since transformation by the *v-mos* oncogene was not affected by alterations in Zfp111 levels. While knockdown of zfp111 did not affect the growth rate of normal 208F cells, knockdown in JSRV Env-transformed cells resulted in a reduction of growth rate, suggesting that JSRV Env-transformed cells have become dependent on Zfp111 for growth. Together these results indicate that Zfp111 plays a role in transformation by JSRV Env.

Zfp111, or also known as rKr2, was previously identified as a Cys2/His2 zinc finger protein with 19 zinc fingers in the C-terminal domain (13). It is a member of the Krüppel family of zinc finger proteins, which are largely transcriptional repressors due to their Krüppel-associated box (KRAB) domains (29). Like other KRAB-containing zinc finger proteins, Zfp111 contains an amino terminal KRAB domain that for other KRAB proteins has been found to have transcriptional repression activity (29), and it is localized in the nucleus in oligodendrocytes (13). Northern blot analysis of zfp111 mRNA expression in adult rats has shown that zfp111 mRNA is expressed at the highest levels in oligodendrocytes of the cerebellum/spinal cord and in testis, but it is also found at lower levels in liver, spleen, and lungs (13, 24). Not much is currently known about the target genes for Zfp111, although it has been suggested that Zfp111 plays a role in oligodendrocyte differentiation from neuronal stem cells (13); in general Krüppel family zinc finger proteins have roles in cell differentiation, proliferation, and tumorigenesis (1).

Two additional observations were made during co-immunoprecipitation of JSRV Env and Zfp111. First, we found an increase in Zfp111-HA signal in western blots upon co-transfection

with JSRV Env compared to transfection of Zfp111-HA alone (Fig. 2.1). This might result from stabilization of Zfp111-HA protein by JSRV Env-FLAG binding, and vice versa, as we also observed stronger JSRV Env-FLAG signals upon co-transfection with Zfp111-HA. Co-transfection of JSRV Env with Zfp111 did not significantly enhance zfp111 RNA expression levels (Fig. 2.4A), which was consistent with stabilization of Zfp111 protein. Stabilization of Zfp111 by JSRV Env is currently being investigated by pulse-chase experiments. Second, co-transfection with Zfp111 resulted in the appearance of a faster migrating Env band (70 Kda) compared to the major Env polyprotein (80 Kda) found when Env was transfected alone (Fig. 2.1). In Chapter 3 of this thesis, we found the faster migrating Env band in the nuclear fraction ("nuclear Env" or $P70^{env}$) as opposed to the standard Env polypeptide which was cytoplasmic. Details on the characterization of $P70^{env}$ will be covered in Chapter 3 of this thesis. Digestion with endoglycosidase F indicated that both cytoplasmic and nuclear Env are N-glycosylated, but they have the same sized polypeptide backbone. The co-immunoprecipitation experiment of Fig. 2.1 also indicated that Zfp111 binds the nuclear but not cytoplasmic Env. These results suggest that binding of Zfp111 to Env results in diversion of a fraction of Env to the nucleus, and during this process there is differential glycosylation of the Env polypeptide.

Several lines of evidence supported a role for Zfp111 in JSRV Env transformation. First, knockdown of endogenous zfp111 expression by transduction with a lentiviral shRNA significantly reduced JSRV Env transformation in rat 208F cells. Moreover, co-transfection of a shRNA-resistant zfp111 expression plasmid partially restored JSRV Env transformation in the zfp111 knockdown cells (Fig. 2.3). While statistically significant, the reduction in transformation by Zfp111 knockdown was modest (ca. 50%), reflecting the partial zfp111 knockdown by the most efficient lentiviral plasmid r36-2 (ca. 50-65%). Alternatively, many

viral oncogenes transform cells by interacting with multiple cellular proteins, and interruption of individual interactions could reduce transformation without abolishing it (2, 6, 17). Second, over-expression of zfp111 by co-transfection enhanced JSRV Env transformation. Third, while knockdown of zfp111 did not affect the growth rate of parental rat 208F fibroblasts, knockdown in JSRV-transformed cells reduced the growth rate. This indicated that JSRV-transformed cells have become dependent on Zfp111. Moreover, the role of Zfp111 in transformation was specific for JSRV Env, since transformation by the viral oncogene *v-mos* [which does not activate signaling through PI3K-Akt and Ras-Raf-MEK (14, 15, 18, 23)] was not affected by either knockdown or over-expression of zfp111. The fact that *v-mos* transformation was not affected in cells transduced with the r36-2 knockdown vector also indicated that the reduction in JSRV Env transformation was not due to general or off-target effects.

Determining the mechanism by which Zfp111 participates in JSRV Env transformation will be of considerable interest in future studies. When Zfp111 was first identified as a candidate interacter with JSRV Env, a role in transformation was challenging to conceive, since Zfp111 is a nuclear protein and Env was considered to be cytoplasmic. The findings of the stabilization of Zfp111 by Env binding, and of the appearance of nuclear Env after Zfp111 binding raise several possible mechanisms. First, a role of Zfp111 could be to chaperone Env to the nucleus, where Env could cause transformation in conjunction with other proteins. Second, nuclear Env could modify the activity of Zfp111 so that the latter protein induces transformation. A third possibility is that cytoplasmic Env re-localizes a portion of Zfp111 to the cytoplasm where it is involved in transformation; however, we have not detected cytoplasmic relocalization of Zfp111 by either immunofluorescence or cell fractionation (T. Hsu and H. Fan, unpublished). It should be noted that over-expression of zfp111 in the absence of JSRV Env does not result in

transformation (Fig. 2.4), so JSRV is not transforming cells simply by enhancing levels of Zfp111.

We are also currently determining the region and sequences of JSRV Env involved in interaction with Zfp111. The initial 2-hybrid screening indicated that Zfp111 binds to the cytoplasmic tail of Env, and we have previously shown that the CT is crucial for Env transformation (21). We previously carried out alanine scanning mutagenesis of the Env CT and assessed the transformation potentials of the different mutants (9). Chapter 3 of this thesis will present experiments that show a general correlation between the ability of different Env mutants to bind Zfp111 and their transforming potentials, consistent with a role for Zfp111 in JSRV transformation. Analysis of the mutants may identify specific Env residues important for Zfp111 binding.

Ideally these experiments would be performed in sheep lung cells, since JSRV induces OPA in sheep. However an in vitro transformation system for JSRV in sheep cells is not yet available and identification of a sheep homolog for Zfp111 has not yet been reported. Once mechanisms of Zfp111 action in JSRV transformation of rodent cells are elucidated, then it will be interesting to see if they are also applicable to ovine or human lung cancers.

References

1. **Bieker, J. J.** 2001. Kruppel-like factors: three fingers in many pies. J Biol Chem **276:**34355-8.
2. **Cheng, A. M., T. M. Saxton, R. Sakai, S. Kulkarni, G. Mbamalu, W. Vogel, C. G. Tortorice, R. D. Cardiff, J. C. Cross, W. J. Muller, and T. Pawson.** 1998. Mammalian Grb2 regulates multiple steps in embryonic development and malignant transformation. Cell **95:**793-803.
3. **Cousens, C., N. Maeda, C. Murgia, M. P. Dagleish, M. Palmarini, and H. Fan.** 2007. In vivo tumorigenesis by Jaagsiekte sheep retrovirus (JSRV) requires Y590 in Env TM, but not full-length orfX open reading frame. Virology **367:**413-21.
4. **De las Heras, M., A. Ortin, C. Cousens, E. Minguijon, and J. M. Sharp.** 2003. Enzootic nasal adenocarcinoma of sheep and goats. Curr Top Microbiol Immunol **275:**201-23.

5. **DeMartini, J. C., J. V. Bishop, T. E. Allen, F. A. Jassim, J. M. Sharp, M. de las Heras, D. R. Voelker, and J. O. Carlson.** 2001. Jaagsiekte sheep retrovirus proviral clone JSRV(JS7), derived from the JS7 lung tumor cell line, induces ovine pulmonary carcinoma and is integrated into the surfactant protein A gene. J Virol **75:**4239-46.
6. **Fluck, M. M., and B. S. Schaffhausen.** 2009. Lessons in signaling and tumorigenesis from polyomavirus middle T antigen. Microbiol Mol Biol Rev **73:**542-63, Table of Contents.
7. **Gyuris, J., E. Golemis, H. Chertkov, and R. Brent.** 1993. Cdi1, a human G1 and S phase protein phosphatase that associates with Cdk2. Cell **75:**791-803.
8. **Hofacre, A., and H. Fan.** 2004. Multiple domains of the Jaagsiekte sheep retrovirus envelope protein are required for transformation of rodent fibroblasts. J Virol **78:**10479-89.
9. **Hull, S., and H. Fan.** 2006. Mutational analysis of the cytoplasmic tail of jaagsiekte sheep retrovirus envelope protein. Journal of virology **80:**8069-8080.
10. **Linnerth-Petrik, N. M., L. A. Santry, D. L. Yu, and S. K. Wootton.** 2012. Adeno-associated virus vector mediated expression of an oncogenic retroviral envelope protein induces lung adenocarcinomas in immunocompetent mice. PLoS One **7:**e51400.
11. **Liu, S. L., M. I. Lerman, and A. D. Miller.** 2003. Putative phosphatidylinositol 3-kinase (PI3K) binding motifs in ovine betaretrovirus Env proteins are not essential for rodent fibroblast transformation and PI3K/Akt activation. J Virol **77:**7924-35.
12. **Liu, S. L., and A. D. Miller.** 2007. Oncogenic transformation by the jaagsiekte sheep retrovirus envelope protein. Oncogene **26:**789-801.
13. **Lovas, G., W. Li, U. Pott, T. Verga, and L. D. Hudson.** 2001. Expression of the Kruppel-type zinc finger protein rKr2 in the developing nervous system. Glia **34:**110-120.
14. **Maeda, N., W. Fu, A. Ortin, M. de las Heras, and H. Fan.** 2005. Roles of the Ras-MEK-mitogen-activated protein kinase and phosphatidylinositol 3-kinase-Akt-mTOR pathways in Jaagsiekte sheep retrovirus-induced transformation of rodent fibroblast and epithelial cell lines. J Virol **79:**4440-50.
15. **Maeda, N., Y. Inoshima, D. A. Fruman, S. M. Brachmann, and H. Fan.** 2003. Transformation of mouse fibroblasts by Jaagsiekte sheep retrovirus envelope does not require phosphatidylinositol 3-kinase. J Virol **77:**9951-9.
16. **Maeda, N., M. Palmarini, C. Murgia, and H. Fan.** 2001. Direct transformation of rodent fibroblasts by jaagsiekte sheep retrovirus DNA. Proc Natl Acad Sci U S A **98:**4449-54.
17. **Maroulakou, I. G., W. Oemler, S. P. Naber, and P. N. Tsichlis.** 2007. Akt1 ablation inhibits, whereas Akt2 ablation accelerates, the development of mammary adenocarcinomas in mouse mammary tumor virus (MMTV)-ErbB2/neu and MMTV-polyoma middle T transgenic mice. Cancer Res **67:**167-77.
18. **Nebreda, A. R., C. Hill, N. Gomez, P. Cohen, and T. Hunt.** 1993. The protein kinase mos activates MAP kinase kinase in vitro and stimulates the MAP kinase pathway in mammalian somatic cells in vivo. FEBS Lett **333:**183-7.
19. **Palmarini, M., and H. Fan.** 2001. Retrovirus-induced ovine pulmonary adenocarcinoma, an animal model for lung cancer. J Natl Cancer Inst **93:**1603-14.
20. **Palmarini, M., H. Fan, and J. M. Sharp.** 1997. Sheep pulmonary adenomatosis: a unique model of retrovirus-associated lung cancer. Trends in microbiology **5:**478-483.
21. **Palmarini, M., N. Maeda, C. Murgia, C. De-Fraja, A. Hofacre, and H. Fan.** 2001. A phosphatidylinositol 3-kinase docking site in the cytoplasmic tail of the Jaagsiekte sheep retrovirus transmembrane protein is essential for envelope-induced transformation of NIH 3T3 cells. J Virol **75:**11002-9.
22. **Palmarini, M., J. M. Sharp, M. de las Heras, and H. Fan.** 1999. Jaagsiekte sheep retrovirus is necessary and sufficient to induce a contagious lung cancer in sheep. J Virol **73:**6964-72.

23. **Posada, J., N. Yew, N. G. Ahn, G. F. Vande Woude, and J. A. Cooper.** 1993. Mos stimulates MAP kinase in Xenopus oocytes and activates a MAP kinase kinase in vitro. Mol Cell Biol **13:**2546-53.
24. **Pott, U., H. J. Thiesen, R. J. Colello, and M. E. Schwab.** 1995. A new Cys2/His2 zinc finger gene, rKr2, is expressed in differentiated rat oligodendrocytes and encodes a protein with a functional repressor domain. Journal of neurochemistry **65:**1955-1966.
25. **Sharp, J. M., K. W. Angus, E. W. Gray, and F. M. Scott.** 1983. Rapid transmission of sheep pulmonary adenomatosis (jaagsiekte) in young lambs. Brief report. Arch Virol **78:**89-95.
26. **Songyang, Z., S. E. Shoelson, M. Chaudhuri, G. Gish, T. Pawson, W. G. Haser, F. King, T. Roberts, S. Ratnofsky, R. J. Lechleider, and et al.** 1993. SH2 domains recognize specific phosphopeptide sequences. Cell **72:**767-78.
27. **Suau, F., V. Cottin, F. Archer, S. Croze, J. Chastang, G. Cordier, F. Thivolet-Bejui, J. F. Mornex, and C. Leroux.** 2006. Telomerase activation in a model of lung adenocarcinoma. Eur Respir J **27:**1175-82.
28. **Travis, W. D., E. Brambilla, M. Noguchi, A. G. Nicholson, K. R. Geisinger, Y. Yatabe, D. G. Beer, C. A. Powell, G. J. Riely, P. E. Van Schil, K. Garg, J. H. Austin, H. Asamura, V. W. Rusch, F. R. Hirsch, G. Scagliotti, T. Mitsudomi, R. M. Huber, Y. Ishikawa, J. Jett, M. Sanchez-Cespedes, J. P. Sculier, T. Takahashi, M. Tsuboi, J. Vansteenkiste, I. Wistuba, P. C. Yang, D. Aberle, C. Brambilla, D. Flieder, W. Franklin, A. Gazdar, M. Gould, P. Hasleton, D. Henderson, B. Johnson, D. Johnson, K. Kerr, K. Kuriyama, J. S. Lee, V. A. Miller, I. Petersen, V. Roggli, R. Rosell, N. Saijo, E. Thunnissen, M. Tsao, and D. Yankelewitz.** 2011. International association for the study of lung cancer/american thoracic society/european respiratory society international multidisciplinary classification of lung adenocarcinoma. J Thorac Oncol **6:**244-85.
29. **Urrutia, R.** 2003. KRAB-containing zinc-finger repressor proteins. Genome Biol **4:**231.
30. **Verwoerd, D. W., A. L. Williamson, and E. M. De Villiers.** 1980. Aetiology of jaagsiekte: transmission by means of subcellular fractions and evidence for the involvement of a retrovirus. Onderstepoort J Vet Res **47:**275-80.
31. **Wiznerowicz, M., and D. Trono.** 2003. Conditional suppression of cellular genes: lentivirus vector-mediated drug-inducible RNA interference. J Virol **77:**8957-61.
32. **Wootton, S. K., C. L. Halbert, and A. D. Miller.** 2005. Sheep retrovirus structural protein induces lung tumours. Nature **434:**904-907.
33. **York, D. F., R. Vigne, D. W. Verwoerd, and G. Querat.** 1992. Nucleotide sequence of the jaagsiekte retrovirus, an exogenous and endogenous type D and B retrovirus of sheep and goats. J Virol **66:**4930-9.
34. **Zavala, G., C. Pretto, Y. H. Chow, L. Jones, A. Alberti, E. Grego, M. De las Heras, and M. Palmarini.** 2003. Relevance of Akt phosphorylation in cell transformation induced by Jaagsiekte sheep retrovirus. Virology **312:**95-105.

CHAPTER 3: CHARACTERIZATION OF A NUCLEAR FORM OF JAAGSIEKTE SHEEP RETROVIRUS ENVELOPE PROTEIN

Abstract

Jaagsiekte sheep retrovirus (JSRV) is a betaretrovirus that causes ovine pulmonary adenocarcinoma, a transmissible lung cancer in sheep. Oncogenic transformation is caused by the JSRV envelope protein, Env, through the activation of signaling pathways such as Akt and MAPK pathways. Current understanding of the mechanism of JSRV Env transformation has been enhanced with the identification of Zfp111 as an Env-interacting protein involved in transformation as described in Chapter 2. Interestingly, co-immunoprecipitations revealed that Zfp111 preferentially binds to a higher mobility form of JSRV Env that has not been identified previously. In this chapter, the faster migrating form of Env was found to be 70 kDa in apparent molecular weight ($P70^{env}$) compared to the standard Env polyprotein precursor of 80 kDa ($Pr80^{env}$). $P70^{env}$ was found exclusively in the nuclear fraction, and its peptide backbone was the same size as $Pr80^{env}$ backbone, differing only in glycosylation levels. Locations of glycosylation sites for $Pr80^{env}$ and $P70^{env}$ were investigated by partial proteolytic cleavage with and without digestion with endoglycosidase F. To further investigate the interaction of Zfp111 and JSRV Env, co-immunoprecipitations with alanine scanning mutants of JSRV Env cytoplasmic tail were performed. For different Env mutants the signal intensities of both Zfp111 and $P70^{env}$ varied coordinately, and those Env mutants that showed apparent abundance similar to those of wild-type Env were previously shown to have the highest levels of cell transformation. These results indicated that mechanism of JSRV Env transformation may not be limited to activation of

signaling pathways in the cytoplasm but also to changes in the nucleus mediated by $P70^{env}$ and Zfp111.

Introduction

Jaagsiekte sheep retrovirus (JSRV) is a betaretrovirus that causes ovine pulmonary adenocarcinoma (OPA), a contagious lung cancer in sheep characterized by the transformation of lung secretory epithelial cells (38). Morphologically, OPA resembles human adenocarcinoma in situ (AIS), formerly known as bronchiole-alveolar carcinoma (46), a type of lung cancer that is less associated with tobacco smoking (41). Thus OPA is an appropriate animal model for the study of AIS.

JSRV is a simple retrovirus that contains only the basic retroviral genes *gag*, *pro*, *pol*, and *env* (51). Although JSRV does not carry a classical oncogene, in experimental inoculation of lambs JSRV is able to induce tumors as early as in 10 days (43, 48). An unusual characteristic of JSRV is that its native envelope protein Env also functions as an oncogene that can induce cell transformation in culture (31) and lung tumors in mice (24, 50). This rare feature is shared by only a small number of retroviruses including enzootic nasal tumor virus, avian hemangioma retrovirus, and the replication-defective Friend spleen focus forming virus of mice (1, 2, 13, 42).

JSRV Env is initially translated from spliced viral mRNA into a precursor polyprotein $Pr80^{env}$. This polyprotein is subsequently cleaved at the cell surface by furin protease to the surface (SU) and transmembrane (TM) domains; these proteins are bound by disulfide bonds and incorporated into the JSRV envelope. SU is responsible for virion binding to cell receptors during infection while TM is responsible for embedding SU in the viral envelope lipid bilayer. TM contains a cytoplasmic tail (CT) that has been found to be necessary for Env transformation

(3, 20, 26, 28, 39). The CT of JSRV Env contains a YXXM motif, which is a putative binding site for the regulatory subunit p85 of phosphatidyl inositol 3-kinase (PI3K) if the tyrosine residue is phosphorylated (44). The importance of this YXXM motif in JSRV is still unclear, as there are various reports of either this motif's significance or irrelevance in JSRV Env (3, 16, 26-28, 39). Nevertheless JSRV transformation has been shown to utilize three main signaling pathways: the PI3K/Akt/mTOR pathway (1, 3, 7, 22, 28-30, 37, 45), Ras/Raf/MEK/MAPK pathway (12, 20, 29), and the Hyal2-RON pathway (11, 25, 28, 35) as reviewed in Chapter 1.

Chapter 2 described yeast two-hybrid screens using JSRV CT and full-length Env to identify candidate interacting proteins of JSRV Env. One of the candidates was zinc finger protein 111 (Zfp111), a member of the Krüppel-like transcription factor family whose family members have been shown to be involved in transcriptional repression, and cellular processes such as proliferation, differentiation, and tumorigenesis (10). In Chapter 2 a co-immunoprecipitation assays revealed that Zfp111 does interact with JSRV Env *in vivo*, though Zfp111 interacted with a distinct form of JSRV Env. This form of JSRV Env migrated faster than the $Pr80^{env}$ polyprotein, with an apparent molecular weight of 70 kDa ($P70^{env}$). It was also a bit surprising to find Zfp111, which is a nuclear protein, as a candidate Env-interacting protein; retroviral envelope proteins are generally considered to be cytoplasmic. Interestingly $P70^{env}$ but not $Pr80^{env}$ bound to Zfp111. Oncogenic retroviral proteins that undergo deletion modification have been shown to be able to re-localize to other subcellular compartment (47), such as from nucleus to the cytoplasm. In this chapter, we identified the location of $P70^{env}$ as nuclear. The size differences between $P70^{env}$ and $Pr80^{env}$ were attributed to glycosylation, and sites of glycosylation were investigated. In addition, binding between Zfp111 and alanine scanning mutants in the CT of JSRV Env was explored to 1) identify the portions of cytoplasmic tail

important for Zfp111 interaction and 2) to see if changes in Env transformation level due to alanine mutations were reflected in Zfp111 levels as well.

Material and Methods

Plasmid constructs. The JSRV Env expression vector ΔGP and the Flag-tagged version have been described (30, 31). The mouse Zfp111-HA expression vector was described in chapter 2. The alanine scanning mutants for JSRV Env cytoplasmic tail were described previously (19).

Cell lines and transfections. Human embryonic kidney cells 293T were grown in Dulbecco's modified Eagle's medium supplemented with 10% fetal bovine serum, penicillin (100 U/mL) and streptomycin (100 µg/mL). For subcellular fractionations, 293T cells were plated at 2 X 10^6 cells in a 10 cm dish. The cells were then transfected with 28 µg of DNA using CalPhos Mammalian Transfection Kit (Clontech) as per manufacturer's instructions. Cells were incubated for 48 hours prior to cell lysis. Cells were collected by directly washing the cells off the plate using cold 1X PBS solution. For co-immunoprecipitation of alanine scanning mutants with Zfp111, 293T cells were plated at 3 X 10^5 cells per well in 6 well plates. The cells were then transfected with 4.8 µg of DNA using CalPhos Mammalian Transfection Kit as per manufacturer's instructions. Cells were incubated for 48 hours prior to cell lysis. Cells were collected by directly washing the cells off the plate using cold 1X PBS solution.

Subcellular fractionation. One half of the Env-transfected cells were lysed directly with RIPA–SDS Lysis Buffer (50mM Tris-HCl, 150mM NaCl, 1% NP-40, 0.5% sodium deoxycholate with 1 tablet of Complete Mini EDTA Free protease inhibitor tablet (Roche)) to be used as the total cell lysate fraction. The other half was harvested by centrifugation at 300 x g or

5 mins in a 15 mL conical tube, and the cells in the pellet were swelled by incubation in 215 µL hypotonic buffer (10mM HEPES, pH 7.9 at 4°C, 1.5mM $MgCl_2$, 10mM NaCl) for 10 mins at 4°C. The cells were lysed by ~50 strokes in a glass Dounce homogenizer with a Type B pestle; lysis was monitored by phase contrast microscopy. The lysate was centrifuged in a 15 mL conical tube at 300 x *g* for 5 min at 4°C, and the supernatant was taken as the cytoplasmic fraction. The remaining pellet was washed by resuspension in hypotonic buffer then centrifuged as above; the supernatant was removed, and the pellet was designated the nuclear fraction. The nuclear pellet was resuspended in ionic and non-ionic detergent buffer Solution A (Mixture of 1 part 10% sodium deoxycholate with 2 part 10% Tween 40. Solution A was mixed 3:17 with hypotonic buffer). After brief mixing by vortex, nuclei were re-pelleted by centrifugation at 300 x *g* for 5 min at 4°C and the supernatant was collected and designated the peri-nuclear fraction. 215 µL RIPA –SDS Lysis Buffer was added to the remaining pellet, which was then sonicated using Sonifier 200W (Branson) at 25% power for 5 seconds. One volume of 2X Laemmelli Buffer was added to all fractions prior to heating (100°C for 5 mins). 10% of the total volume from each of the fractions were loaded onto a 10% SDS-polacrylamide slab gel for electrophoresis; after wet transfer to PVDF membranes (Bio-Rad), blots were probed or re-probed with primary antibodies mouse anti-HA, rabbit anti-FLAG, rabbit anti-β Tubulin, or rabbit anti-Lamin A/C antibodies (Cell Signaling Technologies), followed by probing with secondary antibodies [goat anti-mouse HRP and goat anti-rabbit HRP (Pierce)], respectively. The blot was visualized by chemiluminescence (SuperSignal West Femto Maximum Sensitivity Substrate, Pierce).

Endoglycosidase F and chymotrypsin treatment. Total cell lysates in RIPA –SDS Lysis Buffer were prepared from one half of the transfected 293T cells as described above. The

remaining half was incubated with 200 µl 0.5% NP-40 lysis buffer and then centrifuged at 300 x *g* at 4°C for 5 mins in Allegra 6R Centrifuge (Beckman Coulter), and the supernatant was collected as the cytoplasmic fraction. 200µl RIPA –SDS Lysis Buffer was added to the remaining nuclear pellet, followed by sonication as above to give the nuclear fraction. Protein concentrations of each sample were determined by Bradford assay (Bio-Rad), and up to 20 µg of protein from each fraction was digested with Endoglycosidase F (Endo F) as per manufacturer's directions (New England Biolabs). For chymotrypsin digestion, the native or deglycosylated proteins were digested with 0.2-0.5 µg of chymotrypsin (Promega) in 20 µl total volume for 1 hour at room temperature. The entire digests were loaded onto 10% or 15% SDS-polyacrylamide gels followed by western blotting and probing with primary antibody (rabbit anti-FLAG) followed by goat anti-Rabbit HRP secondary antibody and visualization by chemiluminescence as above. Colored molecular weight protein markers PageRuler Prestained Protein Ladder (Fermentas) were run in parallel on the same gels. Western blots were deprobed by incubating the membrane in deprobe buffer (62.5 mM Tris-HCl, pH 6.7, 2% SDS, 0.7% β-Mercaptoethanol) for 30 mins at 55°C, replaced with fresh deprobe buffer, then incubated for another 30 min. Afterward, the membrane was washed 4x with 1X TBST and blocked in 5% non-fat skim milk in TBST.

Characterization of JSRV Env glycosylation. Samples from cells transfected with ΔGP-FLAG (or co-transfected with Zfp111-HA) were subjected to partial chymotryptic cleavage then SDS-PAGE and western blotting for FLAG as described above. Chymotryptic fragment sizes were determined by first measuring migration distance for each of the molecular weight markers on each gel which was then used to generate a semi-log graph for that blot. This semi-log graph was then used to estimate the sizes of the chymotryptic fragment based on their

migration. Since the FLAG epitope was at the C-terminus of the Env protein, the sizes of the chymotryptic fragments could be used to estimate the sites of chymotryptic cleavage relative to the C-terminus. The size differences between each fragment were deduced and normalized to the known sizes for JSRV Env, SU and TM regions. To measure the amount of glycosylation in between each chymotryptic site, P70env or Pr80env was first treated with Endo F for de-glycosylation then undergo partial chymotryptic cleavage to generate de-glycosylated chymotryptic fragments. The estimated size of the de-glycosylated chymotryptic fragment was subtracted from the estimated size of its corresponding glycosylated chymotryptic fragment. The values shown were the means of 4 independent experiments. The N-glycosylation sites on JSRV Env were predicted using the NetNGlyc 1.0 Server prediction program.

Co-immunoprecipitation of alanine scanning JSRV Env mutants with Zfp111. 293T cells were co-transfected with different FLAG-tagged alanine scanning mutants of JSRV Env (in the ΔGP expression plasmid) (30) along with the HA-tagged mouse Zfp111 cDNA plasmid described above. Transfected cells were harvested and lysed in 500 μl 1% NP-40 Lysis Buffer (50mM Tris-HCl, 150mM NaCl, 1% NP-40 substitute, and 1 tablet of Complete Mini EDTA Free protease inhibitor tablet [Roche]) then sonicated as previously described to obtain total cell lysates. Sonicated total cell lysates were pre-cleared by adding 25 μl Protein A-Agarose beads (Roche) followed by incubation at 4°C for 1 hour with rocking. After removal of the beads by centrifugation at 14,000 RPM for 5 mins at 4°C, pre-cleared lysate were subsequently incubated with 25 μl Anti-FLAG M2 Affinity Gel (Sigma) overnight at 4°C with rocking. Next day, cell lysates were briefly centrifuged at 14,000 RPM to pellet the affinity gel. The supernatant was removed and the gel was washed 3 times with 1% NP-40 Lysis Buffer, then heated in 2X Laemmli buffer at 100°C for 5 mins. 15% of each sample was loaded on 10% SDS

polyacrylamide gels followed by electrophoresis and western blotting with primary antibodies (mouse anti-HA or rabbit anti-FLAG antibody) followed by secondary antibodies (goat anti-mouse HRP or goat anti-rabbit HRP). Blots were visualized by chemiluminescence as above.

Results

A faster migrating form of JSRV Env is observed in 293T cells co-transfected with JSRV Env and Zfp111. In Chapter 2 (Fig. 2.1) co-tranfection of JSRV Env ΔGP and Zfp111 expression vector s into human embryonic kidney cells 293T led to the appearance of a faster migrating form of Env. Based on its electrophoretic mobility, this form of JSRV Env (designated $P70^{env}$) was estimated to be around ~70 kDa in molecular weight, slightly smaller than the standard $Pr80^{env}$ polyprotein (~80 kDa). In addition, $P70^{env}$ was preferentially co-immunoprecipitated with Zfp111, suggesting that it is this form of JSRV Env that interacts with Zfp111. To characterize this form of JSRV Env, 293T cells were transfected with epitope tagged Zfp111-HA alone, epitope tagged JSRV Env alone (ΔGP-FLAG), or with both. The transfected cells were lysed and also subjected to cell fractionation to determine the intracellular localization of $P70^{env}$. Since $P70^{env}$ was able to bind Zfp111, which is a nuclear protein, it seemed possible that this form of Env may be localized in the nucleus. Western blot of fractionated cell lysates from cells co-transfected with ΔGP-FLAG and Zfp111-HA showed that $P70^{env}$ was found in the total cell lysate at lower levels than $Pr80^{env}$, and it was enriched in the nuclear fraction (Fig. 3.1A). Moreover $P70^{env}$ was not detected in the cytoplasmic fraction at all, indicating that it is a found exclusively in the nucleus.

JSRV Env, like other envelope proteins, is generally considered a cytoplasmic (plasma membrane) protein; this localization is necessary for its incorporation into the viral envelope

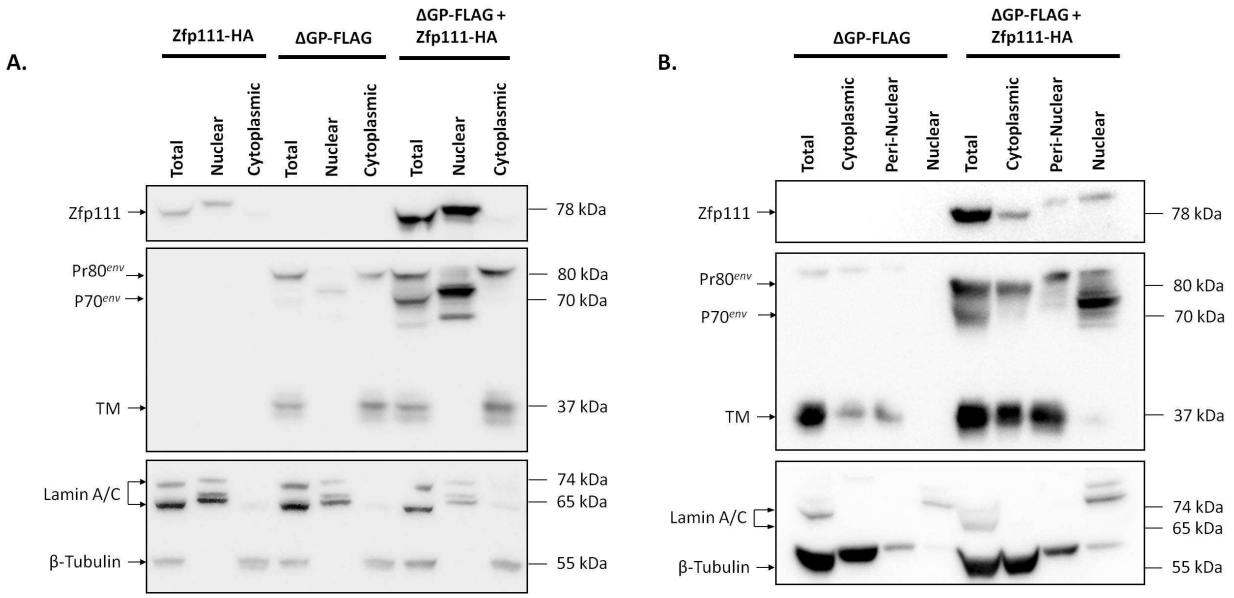

Fig. 3.1: P70^{env} is found exclusively in the nuclear fraction. 293T cells were transfected with ΔGP-FLAG, Zfp111-HA, or both, as indicated. (A) Transfected cells were fractionated into nuclear "Nuclear" and cytoplasmic "Cytoplasmic" fractions. Total cell lysates (Total) without fractionation were also collected. Fractions were analyzed by western blot, and the blot was probed and reprobed with either anti-HA, FLAG, Lamin A/C, or β-Tubulin antibodies. Names and sizes of the observed proteins are indicated to the sides of the blot. (B) P70^{env} is not found in the peri-nuclear fraction. Transfected cells were subjected to cell fractionation, generating cytoplasmic, peri-nuclear (Peri-Nuclear), and nuclear fractions. Total cell lysates without fractionation were also collected. The cell fractions were analyzed by western blot. The blot was probed with anti-HA, FLAG, Lamin A/C, and β-tubulin antibodies. Names and sizes of the observed proteins are indicated on the sides of the blot.

as particles bud from the cell. Thus it was somewhat surprising to find P70^{env} in the nuclear fraction. One possible explanation is that P70^{env} is found in the peri-nuclear region of the cytoplasm, which still may allow for interaction between the nuclear Zfp111 and P70^{env}. A second cell fractionation procedure included washing of the nuclei with an ionic/nonionic detergent mixture, to give a peri-nuclear fraction separate from the rest of the cytoplasm. Western blot analysis revealed that P70^{env} was found exclusively in the nuclear fraction along with Zfp111 and not in the peri-nuclear fraction (Fig. 3.1B). Low levels of Zfp111 were observed in the cytoplasmic and peri-nuclear fractions, but this did not likely reflect re-

localization of Zfp111 into the cytoplasm by JSRV Env since the co-immunoprecipitations shown in Chapter 2 (Fig 2.1) indicated that Zfp111 binds $P70^{env}$ (which is in the nucleus) and not $Pr80^{env}$ (which is cytoplasmic).

It was noteworthy that only the cells transfected with both ΔGP-FLAG and Zfp111-HA showed readily detectable $P70^{env}$. [In some but not all experiments, low levels $P70^{env}$ along with high levels of $Pr80^{env}$ were detected in cells transfected with ΔGP-FLAG alone (Fig. 3.1A)] At the same time in cells transfected with Zfp111 only, the Zfp111 signal was much weaker than the signal in ΔGP-FLAG and Zfp111 co-transfected cells (Fig. 3.1A). This suggested that JSRV Env-HA ($P70^{env}$) in co-transfected cells may result in stabilization.

$Pr80^{env}$ and $P70^{env}$ differ in glycosylation levels. We next investigated the molecular basis for the differences between $Pr80^{env}$ and $P70^{env}$. Like many plasma membrane proteins, JSRV Env is modified by glycosylation (8). The size difference between $Pr80^{env}$ and $P70^{env}$ could be due to differences in their glycosylation levels, the polypeptide backbones or both. To characterize the difference between $Pr80^{env}$ and $P70^{env}$, both proteins were de-glycosylated by *in vitro* endoglycosidase F (Endo F) digestion that will remove all N-linked glycosylation from asparagines, the predominant glycosylation in retroviral Env proteins (40). 293T cells were co-transfected with ΔGP-FLAG and Zfp111-HA and fractionated into cytoplasmic and nuclear fractions. The cytoplasmic fraction contained exclusively $Pr80^{env}$ while nuclei contained $P70^{env}$ as described above. Cytoplasmic and nuclear samples (as well as total cell extract) were incubated with and without Endo F and then analyzed by SDS-PAGE and western blotting for FLAG epitope (Fig. 3.2). Endo F digestion of $Pr80^{env}$ (Total or cytoplasmic fractions) resulted in its conversion to a protein of 60 kDa, which represented the de-glycosylated polypeptide core of $Pr80^{env}$. Endo F digestion of $P70^{env}$ resulted in comparable band of 60 kDa (nuclear fraction,

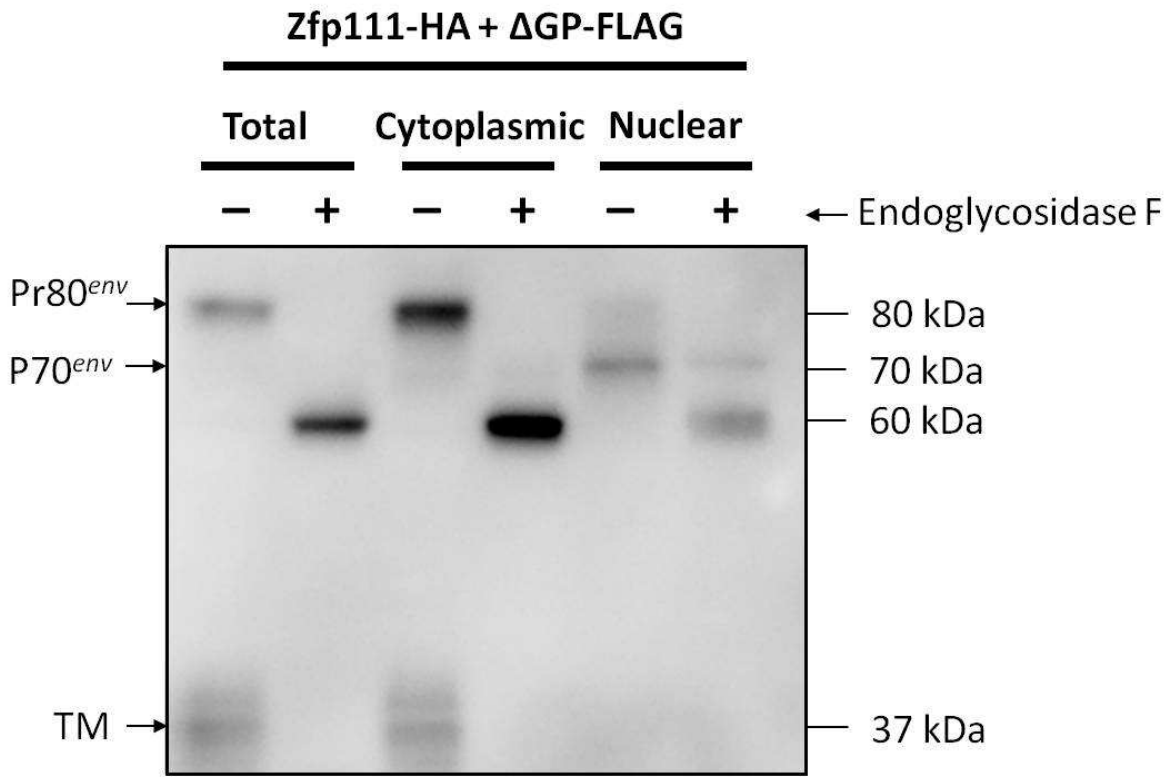

Fig. 3.2: De-glycosylation of Pr80^{env} and P70^{env}. Total, cytoplasmic, and nuclear fractions from Zfp111-HA and ΔGP-FLAG transfected 293T cells were treated with Endoglycosidase F to remove N-linked glycosylation. The treated and untreated fractions were analyzed by western blot and probed with anti-FLAG. Names and sizes of the observed proteins are indicated on the sides of the blot.

Fig 3.2). This result indicated that Pr80^{env} and P70^{env} share the same polypeptide backbone, but differ in their glycosylation levels.

To determine the differences in glycosylation between Pr80^{env} and P70^{env} we first characterized the regions of Pr80^{env} that were glycosylated. This was accomplished by partial proteolytic cleavage with chymotrypsin combined with de-glycosylation by Endo F, followed by size analysis on SDS-PAGE and western blotting. Zfp111-HA and ΔGP-FLAG were co-transfected into 293T cells, and a portion of the cytoplasmic extracts (that contained Pr80^{env} as well as cleaved SU and TM) was partially digested with limiting amounts of chymotrypsin.

Some extracts were treated with Endo F first to de-glycosylate the proteins, then digested with chymotrypsin. The digests were then analyzed by SDS-PAGE and western blotting with anti-FLAG antibody. A typical analysis is shown in Fig 3.3A. A series of partial proteolytic products for Pr80^{env} (P1, P2 and P3) were evident in the samples treated with chymotrypsin only, as well as the cleaved TM protein. Since the FLAG epitope was at the C-terminus of Pr80^{env}, only cleavage products containing the C-terminus were visualized. As a result, the locations of the chymotryptic cleavage sites along Pr80^{env} could be calculated from the sizes of the products in the chymotrypsin digests. As also shown in Fig 3.3A, a corresponding ladder of partial chymotryptic cleavage products was observed for the samples treated with Endo F first. Comparison between sizes of the cleavage products before and after Endo F treatment could be used to calculate the amount of carbohydrate on each product. Moreover, comparison of the amounts of carbohydrate on successively smaller partial chymotrypic products could be used to infer the amount of glycosylation within regions between two chymotryptic cleavage sites. Table 3.1 shows size analysis of the partial chymotrypic cleavage products (with and without Endo F treatment) for Pr80^{env}. Overall, there was an average of 23 kDa of glycosylation on Pr80^{env} polypeptide based on the size difference between glycosylated and de-glycosylated Pr80^{env}. Each subsequent fragment showed a decrease in glycosylation levels until T1, which had no glycosylation. Predicted N-linked glycosylation sites and the major chymotryptic cleavage sites are indicated in Fig. 3.3B. The estimated glycosylation levels between each chymotryptic cleavage site of Pr80^{env} are also shown in Fig. 3.3B, with the amount of glycosylation between each chymotryptic site shown Table 3.2. Comparisons of the sizes of the partial chymotryptic products with and without Endo F indicated that there were glycosylation sites in the regions between residues 84-133, 134-224, and 225-253 (Fig. 3.3B). The amount of

glycosylation between residues 84-133 was estimated to be around 6 kDa, between residues 134-224 was around 3 kDa, and between residues 225-253 was around 3 kDa (Table 3.2). Between residues 225-253 there were no predicted glycosylation sites, although there is an asparagine residue at 248 (N248). This asparagine was not predicted to be glycosylated because it is not positioned in a known N-linked glycosylation motif [N-X-S/T, where X is any amino acid (33)]. In remaining parts of Pr80^{env}, glycosylation was found between 254-412 and had a total of 11 kDa of glycosylation; the C-terminal cleavage product T1, which extends from 413 to 615 and is estimated to be around 23 kDa in size without Endo F treatment, retained the same mobility after Endo F treatment (Table 3.1). This suggested that there was no glycosylation in this last part of Env. However, at the same time it is unclear whether the T1 fragment belongs to Pr80^{env} or the cleaved TM peptide. If T1 belongs to TM, then the only area for the 11 kDa glycosylation is between residues 378-412, which actually has no asparagine residues in that region. If T1 belongs to Pr80^{env}, then the remaining 11 kDa glycosylation should be between residues 254-412, which do have asparagine residues and also a high probability N-linked glycosylation site within that region (N275). The more logical conclusion would be that T1 belongs to Pr80^{env}, and

Fig. 3.3: Current model of the glycosylation levels and sites on Pr80^{env}. (A) A representative western blot of the cytoplasmic fraction from 293T cells co-transfected with ΔGP-FLAG and Zfp111-HA. The fraction was treated with Endoglycosidase F (Endo F) or Chymotrypsin as indicated. Glycosylation levels for each fragment were calculated by measuring the size differences between the glycosylated fragments and their respective deglycosylated counterparts. (right 2 lanes). The estimated band mobility from 4 independent experiments shown in Table 3.1. (B) Diagram of Pr80^{env} glycosylation, with Env divided into SU and TM regions. Estimated chymotrypsin cleavage sites are indicted by dotted black lines along with their residue location. Since the FLAG epitope was at the C-terminus of the Env protein, the sizes of the chymotryptic fragments could be used to estimate the sites of chymotryptic cleavage relative to the C-terminus. Predicted glycosylation sites from prediction program are shown as black diamonds. Glycosylations are shown by the red "lollipops" on the polypeptide, with the sizes proportional to the amount of glycosylation in that chymotryptic fragment. The size differences with and without Endo F treatment were then used to calculate the amount of glycosylation in the protein between the two adjoining chymotryptic cleavage sites, with the numerical values in Table 3.2.

A.

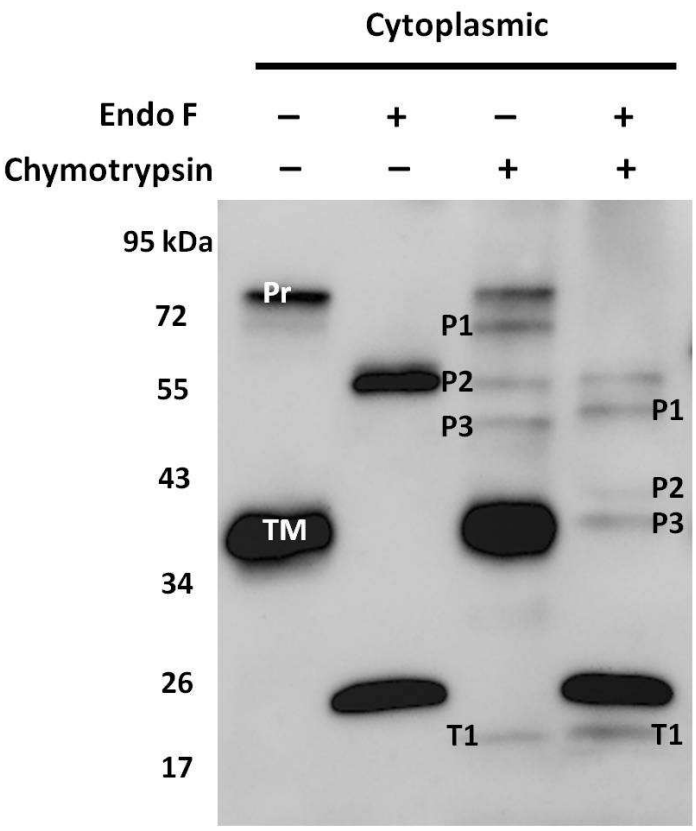
Cytoplasmic
Endo F
Chymotrypsin
95 kDa
72
55
43
34
26
17
Pr
TM
P1
P2
P3
T1
P1
P2
P3
T1

B.

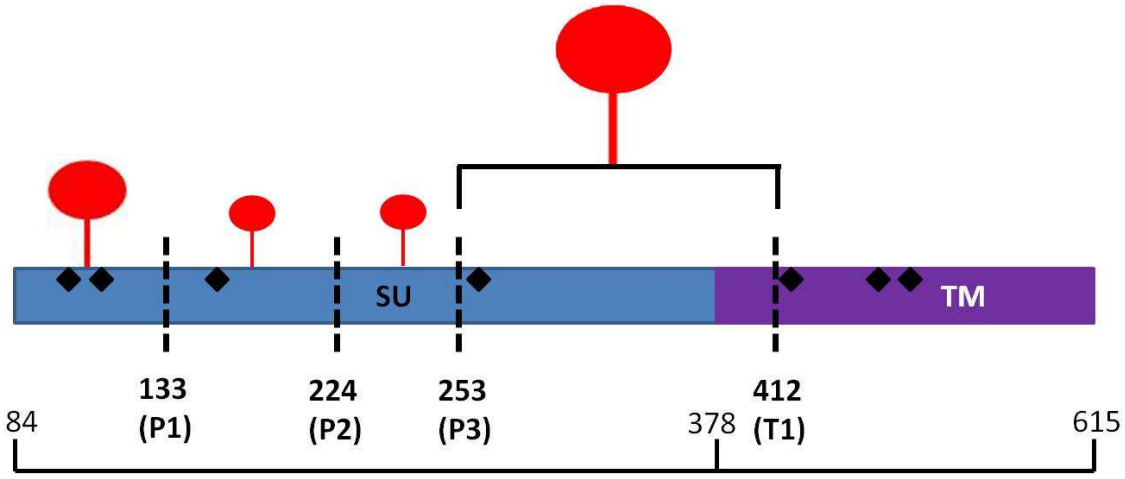
SU
TM
133
(P1)
224
(P2)
253
(P3)
412
(T1)
84
378
615

Table 3.1: Level of glycosylation on Pr80^{env}.

	Pr80^{env} (cytoplasmic)		
	+ Chymo	+Chymo +Endo F	Estimated Glyco Levels (kDa)
Full length Polypeptide (Pr)	79 ± 4	56 ± 2	23 ± 3
Polypeptide Fragment 1 (P1)	69 ± 3	51 ± 2	18 ± 1
Polypeptide Fragment 2 (P2)	57 ± 2	41 ± 1	15 ± 1
Polypeptide Fragment 3 (P3)	50 ± 2	38 ± 1	11 ± 0
Transmembrane (TM)	37 ± 3	26 ± 2	11 ± 3
Transmembrane Fragment 1 (T1)	23 ± 9	23 ± 5	0

293T cells co-transfected with ΔGP-FLAG and Zfp111 were lysed, and the cell lysate fraction containing Pr80^{env} (cytoplasmic) were treated under the conditions of Chymotrypsin (Chymo) only or Chymotrypsin with Endoglycosidase F (Endo F). Treatment with Chymotrypsin generates peptide fragments. The fragments generated under both conditions were analyzed on a western blot as shown in Fig. 3.3A. Glycosylation levels "Glyco Levels" for each fragment were calculated by measuring the size difference between the glycosylated fragments and their respective deglycosylated counterparts. The numbers shown are the mean molecular weight and standard deviation from 4 independent experiments. All values are rounded to the nearest whole number, and given in kDa.

the resulting model of Pr80^{env} glycosylation that reflects this conclusion is shown in Fig. 3.2B. A more definitive conclusion can be drawn when TM is removed completely (e.g. size exclusion chromatography to remove the smaller TM protein and leave the larger Pr80^{env}).

The identification of glycosylation sites and levels of P70^{env} was conducted similarly and is shown in Fig 3.4 and Table 3.3 and 3.4. P70^{env} was found to have 5 chymotrypsin partial

Table 3.2: Estimated amount of glycosylation between chymotrypsin sites in Pr80^{env}.

Residue ranges	Estimated amount of Glycosylation Pr80^{env}
84-133 (Pr-P1)	6
134-224 (P1-P2)	3
225-253 (P2-P3)	3
254-412 (P3-T1)	11
413-615 (T1-End)	0

The residue ranges between each chymotryptic cleavage site are based on Fig. 3.3B. Amount of glycosylation in each chymotryptic fragment was estimated by subtracting the glycosylation levels (calculated in Table 3.1) of the smaller fragment from the immediately larger fragment, here shown in parenthesis next to the residue ranges. All values are rounded to the nearest whole number, and given in kDa.

cleavage sites, NP1 to NP5, based on the chymotrypsin digestion of P70^{env} (Fig. 3.4A). However, NP1 and NP2 fragments were not readily resolved by SDS-PAGE after P70^{env} had undergone deglycosylation and chymotrypsin digestion, and therefore NP1 and NP2 cleavage sites are currently undetermined in P70^{env}. On the other hand, NP3 to NP5 resolved discernibly, and were found to be the same size before and after Endo F treatment, suggesting that from NP3 to the C-terminus of P70^{env} there were no glycosylation on the polypeptide. Based on Endo F treatment, P70^{env} had a total of 10 kDa of glycosylation. Since from NP3 (at residue 215) to the C-terminus there was no more glycosylation, the 10 kDa of glycosylation must be found between residues 84-215 (Table 3.4). Fig. 3.4B is the current model for P70^{env} glycosylation levels and location. Compared with Pr80^{env}, P70^{env} appears to be glycosylated only at the N-terminus of the polypeptide, while Pr80^{env} has glycosylation spread across the polypeptide.

Mapping sites of interaction between Zfp111 and P70^{env}. We next investigated the sites of interaction between Zfp111 and P70^{env}. As described in Chapter 2, the cytoplasmic tail of TM contains the region of Zfp111 binding, since a yeast two-hybrid bait plasmid containing only the CT of JSRV TM is sufficient to show the interaction. As shown in Figure 3.1, visualization of both Env (Pr80^{env} and P70^{env}) and Zfp111 was greatly enhanced when cells were co-transfected with expression plasmids for both of these proteins. Previously we generated alanine scanning mutants of the JSRV Env cytoplasmic tail (CT) to test the importance of individual CT residues in JSRV Env transformation (19). We used some of these mutants to investigate regions of the CT that are involved in Zfp111 binding. Our previous studies indicated that the amino-terminal 14 residues of the CT are in an amphipathic helix, while the last ten residues are not required for JSRV transformation (19). Therefore we focused on the internal residues (580 – 604), some of which are important for transformation (see below). 293T cells were transfected with Zfp111-HA only, ΔGP-FLAG only, or they were co-transfected with Zfp111-HA and ΔGP-FLAG or FLAG-tagged alanine mutants. The Env proteins in the cell

Fig. 3.4: Current model of the glycosylation levels and sites on P70^{env}. (A) A representative western blot of the cytoplasmic fraction from 293T cells co-transfected with ΔGP-FLAG and Zfp111-HA. The fraction was treated with Endoglycosidase F (Endo F) or Chymotrypsin as indicated. Glycosylation levels for each fragment were calculated by measuring the size differences between the glycosylated fragments and their respective deglycosylated counterparts. (2nd and 4th lanes from the left). The estimated band mobilities from from two independent treatments shown in Table 3.3. (B) Diagram of P70^{env} glycosylation, with Env divided into SU and TM regions. Estimated chymotrypsin cleavage sites are indicted by dotted black lines along with their residue location. Since the FLAG epitope was at the C-terminus of the Env protein, the sizes of the chymotryptic fragments could be used to estimate the sites of chymotryptic cleavage relative to the C-terminus. Predicted glycosylation sites from prediction program are shown as black diamonds. Glycosylations are shown by the red "lollipops" on the polypeptide, with the sizes proportional to the amount of glycosylation in that chymotryptic fragment. The size differences with and without Endo F treatment were then used to calculate the amount of glycosylation in the protein between the two adjoining chymotryptic cleavage sites, with the numerical values in Table 3.4.

A.

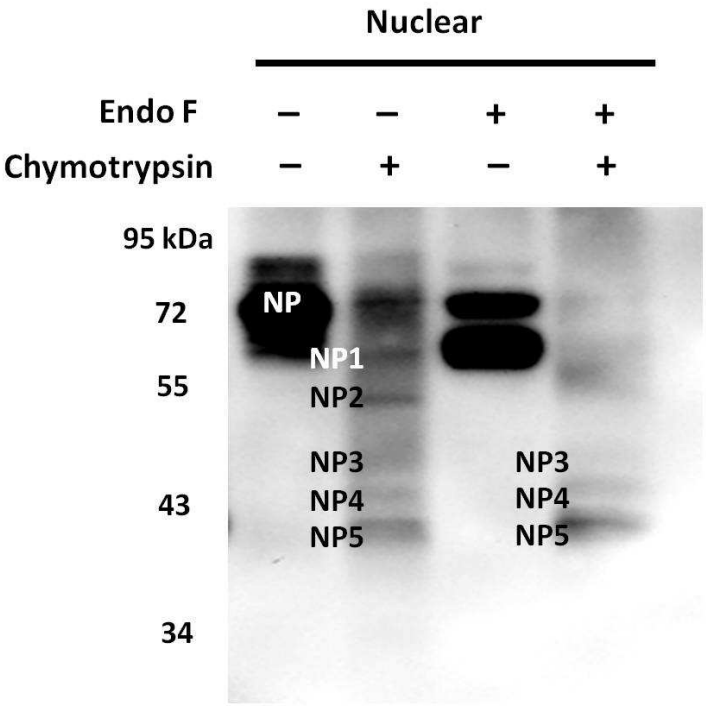
Nuclear
Endo F – – + +
Chymotrypsin – + – +
95 kDa
72
55
43
34
NP
NP1
NP2
NP3
NP4
NP5
NP3
NP4
NP5

B.

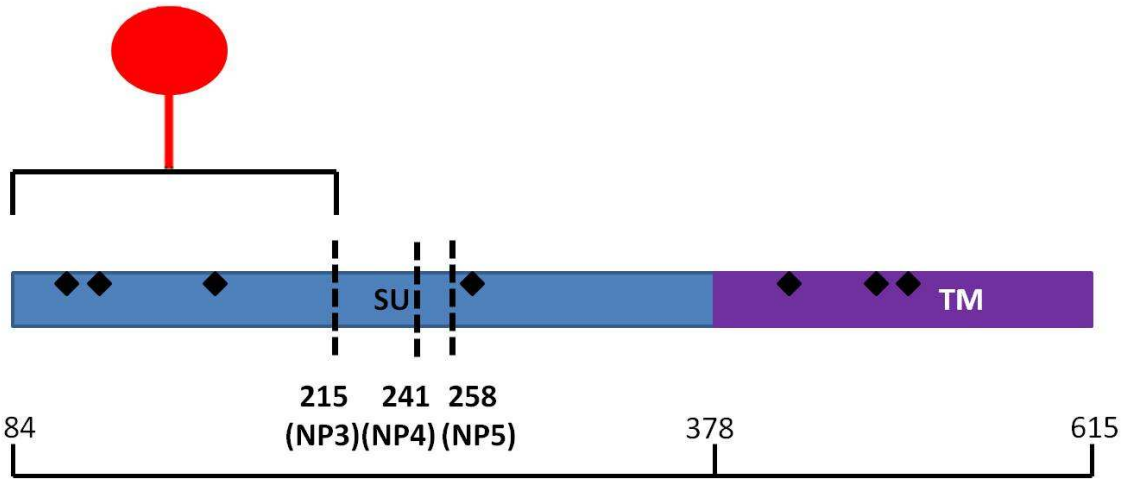
SU
TM
215 (NP3)
241 (NP4)
258 (NP5)
84
378
615

Table 3.3: Level of glycosylation on P70^{env}.

	P70^{env} (Nuclear)		
	+ Chymo	+Chymo +Endo F	Estimated Glyco Levels (kDa)
Full length Polypeptide (NP)	72	62	10
Polypeptide Fragment 1 (NP1)	62	Undetermined	Undetermined
Polypeptide Fragment 2 (NP2)	55	Undetermined	Undetermined
Polypeptide Fragment 3 (NP3)	50	50	0
Polypeptide Fragment 4 (NP4)	46	46	0
Polypeptide Fragment 5 (NP5)	41	41	0

293T cells co-transfected with ΔGP-FLAG and Zfp111 were lysed, and the cell lysate fraction containing and P70^{env} (nuclear) were treated under the conditions of Chymotrypsin (Chymo) only or Chymotrypsin with Endoglycosidase F (Endo F). Treatment with Chymotrypsin generates peptide fragments. The fragments generated under both conditions were analyzed on a western blot as shown in Fig. 3.4A. Glycosylation levels "Glyco Levels" for each fragment were calculated by measuring the size difference between the glycosylated fragments and their respective deglycosylated counterparts. The numbers shown are the mean molecular weight from two independent treatments. All values are rounded to the nearest whole number, and given in kDa.

lysates were immunoprecipitated with anti-FLAG and the immunoprecipitates were analyzed by SDS-PAGE and western blotting for Env (anti-FLAG, Fig 3.5 top panels) or Zfp111 (anti-HA, Fig. 3.5 bottom panels). With the exception of mutant H587A, the Env mutations between residues 583 and 596 resulted in lower or abolition of co-immunoprecipitated Zfp111 compared to co-immunoprecipitation with WT Env levels. This suggested that the region encompassed by

Table 3.4: Estimated amount of glycosylation between chymotrypsin sites in P70^{env}.

Residue ranges	Estimated amount of Glycosylation P70^{env}
84-215 (NP-NP3)	10
216-241 (NP3-NP4)	0
242-258 (NP4-NP5)	0
259-615 (NP5-End)	0

The residue ranges between each chymotryptic cleavage site are based on Fig. 3.4B. Amount of glycosylation in each chymotryptic fragment was estimated by subtracting the glycosylation levels (calculated in Table 3.3) of the smaller fragment from the immediately larger fragment, here shown in parenthesis next to the residue ranges. All values are rounded to the nearest whole number, and given in kDa.

CT residues 583 to 596 is important for Zfp111 binding although within this region the histidine at 587 is not. In contrast Env mutations between residues 597 and 604 showed less loss of co-immunoprocipitation of Zfp111, with levels similar to WT Env for some. This suggested that this region of Env was probably not involved in binding of Zfp111. As previously shown in Fig 3.1A, co-transfection with Zfp111 had a reciprocal effect in enhancing levels of Env as well. In Fig 3.5 those Env mutants that showed levels of co-immunoprecipitated Zfp111 equivalent to WT Env, also generally showed higher levels of Env (Pr80^{env} and P70^{env}) compared to cells transfected with ΔGP (WT Env) alone. This was consistent with the idea that binding of Zfp111 and Env results in stabilization of both proteins.

We previously characterized the Env CT alanine scanning mutants for their effects on JSRV Env transformation (19). The mutants showed differences in their transformation efficiencies based on the mutated residue. The mutants could be organized into four categories:

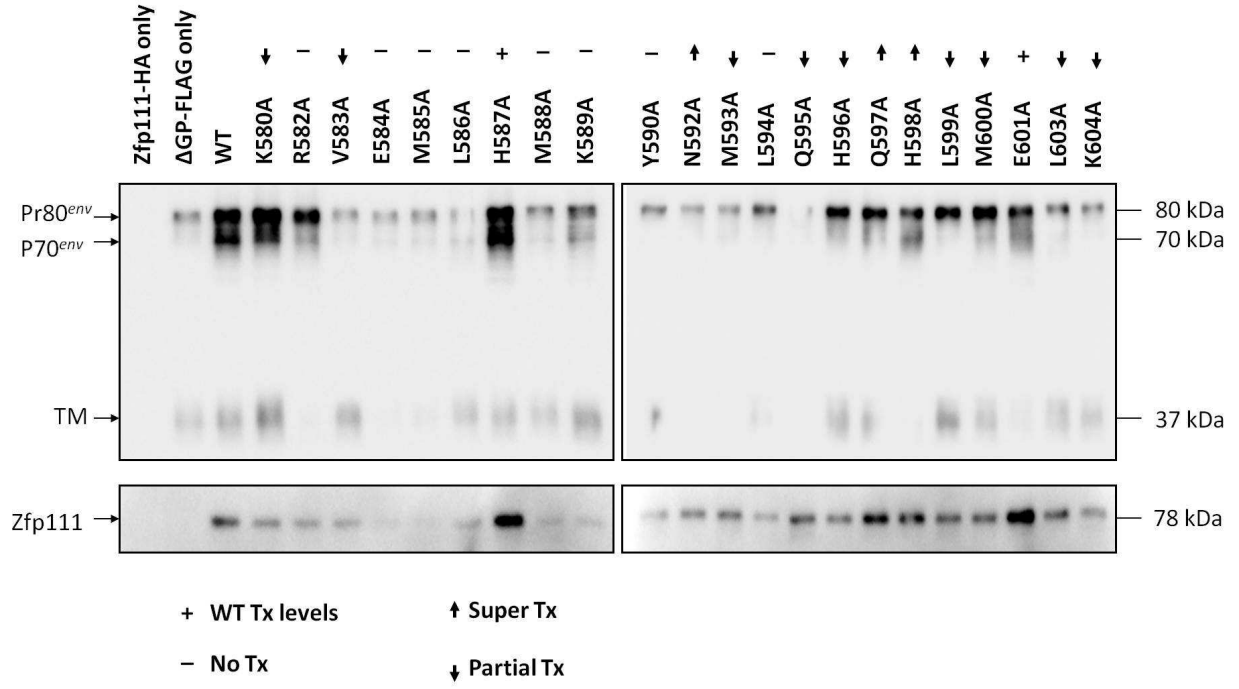

Fig. 3.5: Expression of JSRV Env cytoplasmic tail mutants and Zfp111. 293T cells were transfected with FLAG-tagged alanine scanning mutants along the cytoplasmic tail of JSRV Env, and Zfp111-HA. The cell lysates were immunoprecipitated with anti-FLAG agarose beads, then analyzed by western blot. The blot was probed with anti-HA and FLAG antibodies. Names and sizes of the observed proteins are indicated to the sides of the blot. WT is the FLAG-tagged wild-type JSRV Env, and the alanine mutants used here are shown here. Each mutant's transformation efficiency was determined by foci counting, as reported in (19), and their transformation efficiency is labeled for each alanine mutant. Tx is transformation.

super-transformers (Super Tx) that displayed transformation levels 2-3 fold higher than WT Env, mutants that showed transformation equivalent to WT Env (WT Tx), mutants that showed reduced transformation (Partial Tx), and mutants for which transformation was abolished (No Tx). The relative transformation efficiencies of the different alanine scanning mutants are also shown in Fig. 3.5. In the region implicated in Zfp111 binding (583-596) reduced or absent binding was generally associated with no or reduced transformation, with the lowest levels of Zfp111 binding correlated with no transformation. This supported the conclusion of Chapter 2 that Zfp111 plays a role in JSRV Env transformation. It was noteworthy that the one mutant in

this region (H587A) that showed high level Zfp111 binding also showed WT level transformation. The one super-transformer in this region (N592A) did not show super-elevated levels of Zfp111 binding (see Discussion). For Env mutants in the region that does not appear to be directly involved in Zfp111 binding (597-604), all of the mutants showed transformation at some level, and there was a general correlation between the level of Zfp111 binding and efficiency of transformation. Interestingly, the two super-transformers (Q597A, H598A) did not show enhanced levels of Zfp111 binding (see Discussion).

Discussion

This report identifies a previously uncharacterized form of JSRV Env that may be involved in JSRV transformation. The faster migrating form of JSRV Env is found in the nucleus of the cell. This form of Env, which we referred to as $P70^{env}$ based on its apparent molecular weight, appeared different in the level of glycosylation compared with the uncleaved cytoplasmic Env protein $Pr80^{env}$. The estimated areas of glycosylation in the $Pr80^{env}$ are shown, as well as the approximate level of glycosylation in each area. $P70^{env}$ appears to be highly associated with the zinc finger protein Zfp111, as previous co-immunoprecipitation results showed that only the $P70^{env}$ version of Env is associated with Zfp111. Co-transfection of ΔGP-FLAG with Zfp111-HA showed increase in signal detectability for both $P70^{env}$ and Zfp111. This is emphasized in the co-transfection of Zfp111 with the various alanine scanning mutants for the cytoplasmic tail of JSRV Env. Previous reports showed that different alanine scanning mutations on the cytoplasmic tail of Env exhibited different transformation efficiencies (19). In 293T cells co-transfected with the JSRV CT alanine scanning mutants and Zfp111, there was a correlation between Zfp111 and $P70^{env}$ levels and the transformation efficiency of an alanine mutant. An interesting result from this experiment was that for the Super Tx mutants that have

high transformation efficiencies, Zfp111 and P70^{env} did not show higher signal strength. Co-immunoprecipitation of the alanine scanning mutants and Zfp111 also helped to reveal the sites on JSRV CT that are important for Zfp111 binding. Given that JSRV Env transformation utilizes multiple signaling pathways, it could be that these Super-Tx mutants do not only rely on Zfp111 or P70^{env} to reach higher transformation efficiency. Although its function in the nucleus is still unknown, P70^{env} still may be involved in JSRV Env transformation given its close association with Zfp111.

One question is how P70^{env} enters the nucleus while Pr80^{env} does not. The facts that both of these proteins are glycosylated and that they share polypeptide backbones indicate that they both are initially translocated into the ER during translation. One possibility is that a portion of the Env polyprotein destined to become P70^{env} associates with a cellular protein(s) that directs it to the nucleus. Zfp111 would be a prime candidate for such a protein since it binds and appear to stabilize P70^{env} in co-transfections, and it is a nuclear protein. However it is currently unclear if or how Zfp111 can enter the ER, which would be required for it to conduct P70^{env} to the nucleus; nevertheless the co-immunoprecipitation and stabilization experiments clearly indicate that these two proteins interact in some compartment within the cell. Alternatively it is possible that some other cellular protein directs P70^{env} to the nucleus, where the observed binding with Zfp111 (and stabilization) takes place. Another possibility could be that the Env polyprotein contains a nuclear localization signal (NLS) that directs a portion of it to the nucleus (P70^{env}), with the remainder continuing through the ER to the plasma membrane (Pr80^{env}). It is noteworthy that the JSRV Env coding sequences also specify a regulatory protein Rej in the signal peptide (6, 17, 36). Rej functions in regulation of unspliced viral RNA translation and nuclear export, analogous to the murine mammary tumor virus (MMTV) Rem protein and the HIV-1 Rev

protein (9, 21, 32, 34). Indeed Rej carries an NLS; however as a signal peptide it is cleaved from the Env polyprotein precursor during translation so its NLS is not likely to be present in $P70^{env}$ or $Pr80^{env}$. While scanning the $P70^{env}$ protein sequence did not reveal an obvious NLS [T.H. unpublished data; scans performed with NucPred (4) and RNABindR v2.0 (49)], it is possible that there is a cryptic NLS. Perhaps differential (lower) glycosylation of $P70^{env}$ exposes a cryptic NLS in those molecules, resulting in nuclear import while it is shielded in fully glycosylated $Pr80^{env}$ which is transported to the plasma membrane for incorporation into viral envelopes. A related question is how $P70^{env}$ gains access from the ER (where it is glycosylated) to the cytosol, from where it presumably imported into the nucleus. In the case of MMTV Rem protein, the ER-associated protein degradation (ERAD) pathway is responsible for retro-translocation of this protein (the signal peptide of MMTV Env polyprotein) from the ER back to the cytosol (5). The normal function of ERAD is to transport misfolded proteins (marked by ubiquitination) from the ER back to the cytosol for proteosomal degradation; it seems possible that like MMTV Rem, JSRV $P70^{env}$ could be transported back to the cytoplasm by this mechanism without degradation. In mammalian cells misfolded proteins are targeted to the ERAD pathway following the removal of 3-4 mannose residues by ER processing alpha1,2-mannosidase (ER ManI) (14, 15, 18, 23). $P70^{env}$ could be a misfolded version of Env (or at least appear to be misfolded by the ERAD machinery) that becomes more abundant in cells that were co-transfected with Zfp111. After partial mannose removal, misfolded Env ($P70^{env}$) would enter the ERAD pathway to escape to the cytoplasm, where it would be transported back into the nucleus by a currently unknown chaperone protein.

Some of the questions that were brought up from these results were that the exact location of the glycosylation sites on $Pr80^{env}$ and $P70^{env}$ was not specified. Also, the types of

glycosylation on $Pr80^{env}$ and $P70^{env}$ were not determined in this report. To address the first question, mutations on the putative glycosylation sites on JSRV Env could be made by running the JSRV Env peptide sequence with a glycosylation prediction program, then mutate the putative glycosylation residues on JSRV Env and check for Env glycosylation levels. An early attempt has been made to find the putative glycosylation sites on JSRV Env. Ultimately other techniques such as mass spectrometry in conjunction with digestions with proteases and glycosidases could be used to further characterize the nature of glycosylation on $Pr80^{env}$ and $P70^{env}$ but they are beyond the scope of this thesis. In addition, there are currently no clues as to $P70^{env}$'s function in the nucleus. A good place to start is to look at the cellular interactors of $P70^{env}$. A high stringency protein purification method is detailed in Chapter 5 of this dissertation, which could be applied to $P70^{env}$ to find cellular proteins that interacts with it.

$P70^{env}$ is novel in the sense that a viral envelope protein is found in the nucleus of a cell, rather than the cytoplasm. As a cytoplasmic protein, JSRV Env was always thought to induce cell transformation via activation of growth signaling pathways starting in the cytoplasm. The characterization of $P70^{env}$ shows that the mechanism of JSRV Env transformation may extend beyond the cytoplasmic signaling pathways and into the nucleus. Its existence brings exciting possibilities in the area of JSRV Env transformation mechanism.

References

1. **Alberti, A., C. Murgia, S. L. Liu, M. Mura, C. Cousens, M. Sharp, A. D. Miller, and M. Palmarini.** 2002. Envelope-induced cell transformation by ovine betaretroviruses. J Virol **76:**5387-94.
2. **Alian, A., D. Sela-Donenfeld, A. Panet, and A. Eldor.** 2000. Avian hemangioma retrovirus induces cell proliferation via the envelope (env) gene. Virology **276:**161-8.
3. **Allen, T. E., K. J. Sherrill, S. M. Crispell, M. R. Perrott, J. O. Carlson, and J. C. DeMartini.** 2002. The jaagsiekte sheep retrovirus envelope gene induces transformation of the avian fibroblast cell line DF-1 but does not require a conserved SH2 binding domain. J Gen Virol **83:**2733-42.
4. **Brameier, M., A. Krings, and R. M. MacCallum.** 2007. NucPred--predicting nuclear localization of proteins. Bioinformatics **23:**1159-60.

5. **Byun, H., N. Halani, J. A. Mertz, A. F. Ali, M. M. Lozano, and J. P. Dudley.** 2010. Retroviral Rem protein requires processing by signal peptidase and retrotranslocation for nuclear function. Proc Natl Acad Sci U S A **107:**12287-92.
6. **Caporale, M., F. Arnaud, M. Mura, M. Golder, C. Murgia, and M. Palmarini.** 2009. The signal peptide of a simple retrovirus envelope functions as a posttranscriptional regulator of viral gene expression. J Virol **83:**4591-604.
7. **Chow, Y. H., A. Alberti, M. Mura, C. Pretto, P. Murcia, L. M. Albritton, and M. Palmarini.** 2003. Transformation of rodent fibroblasts by the jaagsiekte sheep retrovirus envelope is receptor independent and does not require the surface domain. J Virol **77:**6341-50.
8. **Coffin, J. M., Hughes, S.H., Varmus, H.E., editors.** 1997. Synthesis and Organization of Env Glycoproteins. Retroviruses. Cold Spring Harbor (NY): Cold Spring Harbor Laboratory Press.
9. **D'Agostino, D. M., B. K. Felber, J. E. Harrison, and G. N. Pavlakis.** 1992. The Rev protein of human immunodeficiency virus type 1 promotes polysomal association and translation of gag/pol and vpu/env mRNAs. Mol Cell Biol **12:**1375-86.
10. **Dang, D. T., J. Pevsner, and V. W. Yang.** 2000. The biology of the mammalian Kruppel-like family of transcription factors. Int J Biochem Cell Biol **32:**1103-21.
11. **Danilkovitch-Miagkova, A., F. M. Duh, I. Kuzmin, D. Angeloni, S. L. Liu, A. D. Miller, and M. I. Lerman.** 2003. Hyaluronidase 2 negatively regulates RON receptor tyrosine kinase and mediates transformation of epithelial cells by jaagsiekte sheep retrovirus. Proceedings of the National Academy of Sciences of the United States of America **100:**4580-4585.
12. **De Las Heras, M., A. Ortin, A. Benito, C. Summers, L. M. Ferrer, and J. M. Sharp.** 2006. In-situ demonstration of mitogen-activated protein kinase Erk 1/2 signalling pathway in contagious respiratory tumours of sheep and goats. J Comp Pathol **135:**1-10.
13. **Dirks, C., F. M. Duh, S. K. Rai, M. I. Lerman, and A. D. Miller.** 2002. Mechanism of cell entry and transformation by enzootic nasal tumor virus. J Virol **76:**2141-9.
14. **Ermonval, M., C. Kitzmuller, A. M. Mir, R. Cacan, and N. E. Ivessa.** 2001. N-glycan structure of a short-lived variant of ribophorin I expressed in the MadIA214 glycosylation-defective cell line reveals the role of a mannosidase that is not ER mannosidase I in the process of glycoprotein degradation. Glycobiology **11:**565-76.
15. **Frenkel, Z., W. Gregory, S. Kornfeld, and G. Z. Lederkremer.** 2003. Endoplasmic reticulum-associated degradation of mammalian glycoproteins involves sugar chain trimming to Man6-5GlcNAc2. J Biol Chem **278:**34119-24.
16. **Hofacre, A., and H. Fan.** 2004. Multiple domains of the Jaagsiekte sheep retrovirus envelope protein are required for transformation of rodent fibroblasts. J Virol **78:**10479-89.
17. **Hofacre, A., T. Nitta, and H. Fan.** 2009. Jaagsiekte sheep retrovirus encodes a regulatory factor, Rej, required for synthesis of Gag protein. J Virol **83:**12483-98.
18. **Hosokawa, N., L. O. Tremblay, Z. You, A. Herscovics, I. Wada, and K. Nagata.** 2003. Enhancement of endoplasmic reticulum (ER) degradation of misfolded Null Hong Kong alpha1-antitrypsin by human ER mannosidase I. J Biol Chem **278:**26287-94.
19. **Hull, S., and H. Fan.** 2006. Mutational analysis of the cytoplasmic tail of jaagsiekte sheep retrovirus envelope protein. Journal of virology **80:**8069-8080.
20. **Hull, S., J. Lim, A. Hamil, T. Nitta, and H. Fan.** 2012. Analysis of jaagsiekte sheep retrovirus (JSRV) envelope protein domains in transformation. Virus Genes.
21. **Indik, S., W. H. Gunzburg, B. Salmons, and F. Rouault.** 2005. A novel, mouse mammary tumor virus encoded protein with Rev-like properties. Virology **337:**1-6.
22. **Johnson, C., K. Sanders, and H. Fan.** 2010. Jaagsiekte sheep retrovirus transformation in Madin-Darby canine kidney epithelial cell three-dimensional culture. J Virol **84:**5379-90.

23. **Kitzmuller, C., A. Caprini, S. E. Moore, J. P. Frenoy, E. Schwaiger, O. Kellermann, N. E. Ivessa, and M. Ermonval.** 2003. Processing of N-linked glycans during endoplasmic-reticulum-associated degradation of a short-lived variant of ribophorin I. Biochem J **376:**687-96.
24. **Linnerth-Petrik, N. M., L. A. Santry, D. L. Yu, and S. K. Wootton.** 2012. Adeno-associated virus vector mediated expression of an oncogenic retroviral envelope protein induces lung adenocarcinomas in immunocompetent mice. PLoS One **7:**e51400.
25. **Liu, S. L., F. M. Duh, M. I. Lerman, and A. D. Miller.** 2003. Role of virus receptor Hyal2 in oncogenic transformation of rodent fibroblasts by sheep betaretrovirus env proteins. J Virol **77:**2850-8.
26. **Liu, S. L., M. I. Lerman, and A. D. Miller.** 2003. Putative phosphatidylinositol 3-kinase (PI3K) binding motifs in ovine betaretrovirus Env proteins are not essential for rodent fibroblast transformation and PI3K/Akt activation. J Virol **77:**7924-35.
27. **Liu, S. L., and A. D. Miller.** 2007. Oncogenic transformation by the jaagsiekte sheep retrovirus envelope protein. Oncogene **26:**789-801.
28. **Liu, S. L., and A. D. Miller.** 2005. Transformation of madin-darby canine kidney epithelial cells by sheep retrovirus envelope proteins. J Virol **79:**927-33.
29. **Maeda, N., W. Fu, A. Ortin, M. de las Heras, and H. Fan.** 2005. Roles of the Ras-MEK-mitogen-activated protein kinase and phosphatidylinositol 3-kinase-Akt-mTOR pathways in Jaagsiekte sheep retrovirus-induced transformation of rodent fibroblast and epithelial cell lines. J Virol **79:**4440-50.
30. **Maeda, N., Y. Inoshima, D. A. Fruman, S. M. Brachmann, and H. Fan.** 2003. Transformation of mouse fibroblasts by Jaagsiekte sheep retrovirus envelope does not require phosphatidylinositol 3-kinase. J Virol **77:**9951-9.
31. **Maeda, N., M. Palmarini, C. Murgia, and H. Fan.** 2001. Direct transformation of rodent fibroblasts by jaagsiekte sheep retrovirus DNA. Proc Natl Acad Sci U S A **98:**4449-54.
32. **Malim, M. H., J. Hauber, S. Y. Le, J. V. Maizel, and B. R. Cullen.** 1989. The HIV-1 rev trans-activator acts through a structured target sequence to activate nuclear export of unspliced viral mRNA. Nature **338:**254-7.
33. **Medzihradszky, K. F.** 2005. Characterization of protein N-glycosylation. Methods Enzymol **405:**116-38.
34. **Mertz, J. A., M. S. Simper, M. M. Lozano, S. M. Payne, and J. P. Dudley.** 2005. Mouse mammary tumor virus encodes a self-regulatory RNA export protein and is a complex retrovirus. J Virol **79:**14737-47.
35. **Miller, A. D.** 2008. Hyaluronidase 2 and its intriguing role as a cell-entry receptor for oncogenic sheep retroviruses. Semin Cancer Biol **18:**296-301.
36. **Nitta, T., A. Hofacre, S. Hull, and H. Fan.** 2009. Identification and mutational analysis of a Rej response element in Jaagsiekte sheep retrovirus RNA. J Virol **83:**12499-511.
37. **Palmarini, M., and H. Fan.** 2001. Retrovirus-induced ovine pulmonary adenocarcinoma, an animal model for lung cancer. J Natl Cancer Inst **93:**1603-14.
38. **Palmarini, M., H. Fan, and J. M. Sharp.** 1997. Sheep pulmonary adenomatosis: a unique model of retrovirus-associated lung cancer. Trends in microbiology **5:**478-483.
39. **Palmarini, M., N. Maeda, C. Murgia, C. De-Fraja, A. Hofacre, and H. Fan.** 2001. A phosphatidylinositol 3-kinase docking site in the cytoplasmic tail of the Jaagsiekte sheep retrovirus transmembrane protein is essential for envelope-induced transformation of NIH 3T3 cells. J Virol **75:**11002-9.
40. **Petropoulos, C.** 1997. Retroviral Taxonomy, Protein Structures, Sequences, and Genetic Maps. In: Coffin JM, Hughes SH, Varmus HE, editors. Retroviruses. Cold Spring Harbor (NY): Cold Spring Harbor Laboratory Press; 1997.

41. **Raz, D. J., B. He, R. Rosell, and D. M. Jablons.** 2006. Bronchioloalveolar carcinoma: a review. Clin Lung Cancer **7:**313-22.
42. **Ruscetti, S. K.** 1999. Deregulation of erythropoiesis by the Friend spleen focus-forming virus. Int J Biochem Cell Biol **31:**1089-109.
43. **Sharp, J. M., K. W. Angus, E. W. Gray, and F. M. Scott.** 1983. Rapid transmission of sheep pulmonary adenomatosis (jaagsiekte) in young lambs. Brief report. Arch Virol **78:**89-95.
44. **Songyang, Z., S. E. Shoelson, M. Chaudhuri, G. Gish, T. Pawson, W. G. Haser, F. King, T. Roberts, S. Ratnofsky, R. J. Lechleider, and et al.** 1993. SH2 domains recognize specific phosphopeptide sequences. Cell **72:**767-78.
45. **Suau, F., V. Cottin, F. Archer, S. Croze, J. Chastang, G. Cordier, F. Thivolet-Bejui, J. F. Mornex, and C. Leroux.** 2006. Telomerase activation in a model of lung adenocarcinoma. Eur Respir J **27:**1175-82.
46. **Travis, W. D., E. Brambilla, M. Noguchi, A. G. Nicholson, K. R. Geisinger, Y. Yatabe, D. G. Beer, C. A. Powell, G. J. Riely, P. E. Van Schil, K. Garg, J. H. Austin, H. Asamura, V. W. Rusch, F. R. Hirsch, G. Scagliotti, T. Mitsudomi, R. M. Huber, Y. Ishikawa, J. Jett, M. Sanchez-Cespedes, J. P. Sculier, T. Takahashi, M. Tsuboi, J. Vansteenkiste, I. Wistuba, P. C. Yang, D. Aberle, C. Brambilla, D. Flieder, W. Franklin, A. Gazdar, M. Gould, P. Hasleton, D. Henderson, B. Johnson, D. Johnson, K. Kerr, K. Kuriyama, J. S. Lee, V. A. Miller, I. Petersen, V. Roggli, R. Rosell, N. Saijo, E. Thunnissen, M. Tsao, and D. Yankelewitz.** 2011. International association for the study of lung cancer/american thoracic society/european respiratory society international multidisciplinary classification of lung adenocarcinoma. J Thorac Oncol **6:**244-85.
47. **Van Etten, R. A., P. Jackson, and D. Baltimore.** 1989. The mouse type IV c-abl gene product is a nuclear protein, and activation of transforming ability is associated with cytoplasmic localization. Cell **58:**669-78.
48. **Verwoerd, D. W., A. L. Williamson, and E. M. De Villiers.** 1980. Aetiology of jaagsiekte: transmission by means of subcellular fractions and evidence for the involvement of a retrovirus. Onderstepoort J Vet Res **47:**275-80.
49. **Walia, R. R., C. Caragea, B. A. Lewis, F. Towfic, M. Terribilini, Y. El-Manzalawy, D. Dobbs, and V. Honavar.** 2012. Protein-RNA interface residue prediction using machine learning: an assessment of the state of the art. BMC Bioinformatics **13:**89.
50. **Wootton, S. K., C. L. Halbert, and A. D. Miller.** 2005. Sheep retrovirus structural protein induces lung tumours. Nature **434:**904-907.
51. **York, D. F., R. Vigne, D. W. Verwoerd, and G. Querat.** 1992. Nucleotide sequence of the jaagsiekte retrovirus, an exogenous and endogenous type D and B retrovirus of sheep and goats. J Virol **66:**4930-9.

CHAPTER 4: ANALYSIS OF THE ROLE OF RIBONUCLEOTIDE REDUCTASE SUBUNIT 2 (RRM2) IN JAAGSIEKTE SHEEP RETROVIRUS ENVELOPE MEDIATED CELL TRANSFORMATION

Abstract

Jaagsiekte sheep retrovirus (JSRV) is the etiologic agent of a contagious lung cancer in sheep, ovine pulmonary adenocarcinoma. The immigrant envelope gene (*env*) acts as the oncogene in JSRV transformation. To understand the mechanism of JSRV transformation, we previously performed yeast two-hybrid screening for candidate proteins that interact with Env. We identified Ribonucleotide Reductase Subunit 2 (RRM2), a subunit of ribonucleotide reductase that functions in generating deoxyribonucleoside triphosphates, as a candidate. The interaction between RRM2 and JSRV Env was confirmed *in vitro* with pull-down assays and *in vivo* with immunofluorescence assays in NIH 3T3 cells. Knockdown of endogenous RRM2 in rat 208F fibroblasts caused a decrease in cell transformation efficiency by JSRV Env. Reduction in transformation also was observed in RRM2 knockdown cells transformed with a different oncogene, *v-mos*. A potential explanation for the general reduction in cell transformation was that knockdown of RRM2 may have inhibitory effects on cell growth, which was verified in cell proliferation assays of RRM2 knockdown cells. Nevertheless RRM2 knockdown had a significantly larger effect on JSRV Env transformation than *v-mos* transformation, suggesting that RRM2 may have a specific role in JSRV transformation.

Introduction

Jaagsiekte sheep retrovirus (JSRV) is a betaretrovirus that causes ovine pulmonary adenocarcinoma (OPA), a contagious lung cancer in sheep characterized by the transformation of

lung secretory epithelial cells (25). JSRV infected sheep display severe respiratory distress, due to the accumulation of fluid in the lungs in addition to tumor formation. This lung fluid contains large amounts of JSRV, which can be easily spread to other sheep after expulsion of the fluid through the mouth or nose of the sheep (10). OPA morphologically resembles human adenocarcinoma in situ (AIS), formerly known as bronchiole-alveolar carcinoma (34), a type of lung cancer that is less associated with tobacco smoking (29). This allows OPA to function well as a potential animal model for the study of AIS.

A unique feature of JSRV is that its envelope protein Env also functions as an oncogene (22). JSRV Env can transform cells in culture (22) and induce lung tumors in mice (16, 37). This rare feature is shared only by a small group of viruses that includes enzootic nasal tumor virus of sheep and goats, avian hemangioma retrovirus, and the replication-defective Friend spleen focus forming virus of mice (1, 2, 7, 30). Much work has been done to understand how JSRV Env can induce cell transformation, with an emphasis on the mechanism of Env transformation.

JSRV Env is initially translated from spliced viral mRNA into a polyprotein of approximately 615 amino acids (6, 26, 40). This polyprotein is then cleaved by cellular furin protease into the surface (SU) and transmembrane (TM) subunits. The SU protein is responsible for receptor recognition and virus entry, while TM is responsible for the fusion of viral and cellular membranes upon infection. TM contains a 45 amino acid cytoplasmic tail (CT) that extends into the cytoplasm of the cell and has been found to be important for JSRV Env transformation in a variety of cell lines (3, 17, 19, 24). The CT of Env contains a YXXM sequence, a putative binding site for the regulatory subunit (p85) of phosphatidyl inositol 3-kinase (PI3K) if the tyrosine residue is phosphorylated (32). Although PI3K was found not to

bind to CT of Env (18), the downstream signaling pathway that PI3K is associated with is found to be constitutively activated (17, 41). This signaling pathway is the Akt-mTOR signaling pathway, and inhibitors of this pathway have been shown to reduce Env transformation in various cell lines (20). Another important signaling pathway for JSRV transformation is the Ras-Raf-MEK-MAPK pathway; inhibitors of this pathway also reduce Env transformation in different cell lines (5, 13, 14, 20). Despite their importance in JSRV Env transformation, none of the proteins in these two pathways seem to directly interact with JSRV Env. To activate these signaling pathways, there are presumably cellular proteins that JSRV Env interacts with directly that will lead to the activation of these downstream pathways.

In a previous study, we performed a yeast two-hybrid screen using full-length JSRV Env or only the CT portion as bait proteins to identify interacting proteins, as described in Chapters 1 and 2. One of the candidates was ribonucleotide reductase subunit 2 (RRM2). RRM2 is an important subunit of the ribonucleotide reductase enzyme, which functions to synthesize deoxyribonucleoside triphosphates (dNTPs) needed for DNA synthesis and repair (23). The RRM2 subunit contains a tyrosine whose free radical is necessary for enzyme activity (23). Its role in oncogenesis has also been the focus of various studies, where in inhibitors of RRM2 have been effective in reducing cell transformation both *in vitro* and *in vivo* (4, 11, 15). In particular, RRM2 overexpression from the human cytomegalovirus immediate early promoter in transgenic mice induces tumors but only in the lung (39). Moreover the tumor cells in the lungs of these mice were derived from type II pneumocytes, which are also the main target cells of JSRV infection and tumorigenesis in sheep (27, 28, 31, 38). In another report, overexpression of RRM2 led to an increase in focus formation in NIH 3T3 cells transfected by an *Hras* expression plasmid (9), suggesting that RRM2 is important for Ras transformation. Given that the Ras

pathway is also activated in JSRV transformation, RRM2 may be playing a role in the activation of the Ras pathway by JSRV Env.

In this study, we confirmed the interaction between JSRV Env and RRM2 *in vitro* and *in vivo* in mouse cell line, and we investigated the importance of RRM2 in JSRV Env transformation via knockdown of endogenous RRM2 in JSRV Env transformation assays. We also tested whether RRM2's role in JSRV transformation is specific to JSRV Env by studying the effects of down RRM2 knockdown on transformation by another viral oncogene, *v-mos*. The results of *v-mos* transformation led to the hypothesis that knockdown of RRM2 may have inhibitory effects on cell growth that are oncogene independent. This hypothesis was verified in cell proliferation assays in which RRM2 knockdown cells exhibited slower growth rates as compared with parental non-knockdown cells. Nevertheless, RRM2 knockdown showed a significantly stronger effect on JSRV Env transformation than *v-mos* transformation, suggesting that RRM2 may also be involved specifically in JSRV transformation.

Material and methods

Cell lines. Human embryonic kidney cells 293T, rat fibroblast 208F, rat epithelial RK3E cells were grown in Dulbecco's modified Eagle's medium supplemented with 10% fetal bovine serum, penicillin (100 U/mL) and streptomycin (100 µg/mL). Mouse NIH 3T3 fibroblasts were grown in Dulbecco's modified Eagle's medium supplemented with 10% calf serum, penicillin (100 U/mL) and streptomycin (100 µg/mL).

Plasmid constructs. The JSRV Env expression plasmid (ΔGP) and the HA-tagged version have been previously been described (21, 22). FLAG-tagged mouse RRM2 expression vector was generated by PCR amplifying mouse cDNA from Open Biosystems. Mouse primers

are as follows: 5' – TCCCCGGGATCCATGCTCTCCGTCCGCAC and 5' – TCCCCGCTCGA GTTATTTATCATCATCATCTTTATAATCGAAGTCAGCATCCAAGGT. All PCR products were gel purified and then digested with BamHI and XhoI (New England Biolabs), then cloned in pcDNA3.1 (Invitrogen Life Sciences) using the BamHI and XhoI cloning sites.

Pull-down of RRM2. Bacterial colonies containing a glutathione S-transferase (GST) expression plasmid pGEX-2T or a plasmid expressing a GST fusion with the cytoplasmic tail of JSRV Env (GST-CT) were amplified overnight in 5 mL of LB Broth. Next day, the 5 mL of overnight culture was used to inoculate 1 L of LB and grown at 37°C to an O.D. of 0.5-1.0. Protein expression was induced by addition of IPTG (final concentration 0.1 mM) and grown for an additional 3 hrs at 37°C. The bacteria were collected by centrifugation (3,500 x g for 20 min at 4°C) and the supernatants removed. Cultures were lysed by adding 20 mL of PBS lysis buffer (PBS with 1% Triton X-100, and 2 µg/mL aprotinin, 1 µg/mL leupeptin, and 25µg/mL PMSF) and sonicated on ice using three cycles of 10 second bursts with the Sonifier 200W (Branson). Lysates were centrifuged at 12,000 x g for 15 mins at 4°C, and the supernatants were transferred to tubes containing 5 mL of a 50:50 slurry of glutathione-Sepharose beads (GE Healthcare) in PBS lysis buffer. Lysates were mixed with beads for 30 mins at 4°C in an end-to-end rotator. Beads were collected by centrifugation (750 x g for 1 min at 4°C) and washed twice with cold PBS with protease inhibitors. Beads with GST or GST-CT were stored at 4°C until use.

NIH 3T3 cells were plated at 1 X 10^5 in 6 cm plates. The next day, cells were transfected with 5 µg of expression plasmids for FLAG tagged RRM2 (RRM2-FLAG) or GFP tagged NM23-H1 (GFP-NM23-H1, negative control) with Fugene 6 Transfection Reagent (Promega) as per the manufacturer's instructions. 48 hours post-transfection, cells were lysed with 1% NP-40 lysis buffer [50mM Tris-HCl, pH 8, 150 mM NaCl, 1% NP-40 Substitute, and 1 tablet of

Complete Mini EDTA Free (Roche)] and total cell lysates were incubated with 25 µL of GST bead slurry or GST-CT bead slurry, overnight at 4°C in the end-over-end rotator. Next day the beads were collected by centrifugation (10,000 RPM for 1 min at 4°C), washed three times with 1% NP-40 lysis buffer and eluted by boiling in 2X Laemmli buffer. Proteins were resolved on 10% SDS-polyacrylamide gels, transferred to PVDF membranes (Bio-Rad) and probed with primary antibody rabbit anti-FLAG antibody (Cell Signaling) and secondary antibody goat anti-rabbit HRP (Pierce). Blots were visualized by chemiluminescence using SuperSignal Femto Maximum Sensitivity Subtrate (Pierce).

Immunofluorescence. NIH 3T3 cells were plated at 1 X 10^5 cells per well on top of Poly-L-Lysine (Sigma) coated glass cover slips placed in wells of a 6 well plate. Cells were transfected the next day with 5 µg of pcDNA or ΔGP-HA using Fugene 6 Transfection Reagent (Promega). 48 hours post-transfection, cells on the cover slips were fixed with 100% methanol for 15 mins at 4°C and permeabilized with 0.2% Triton X-100 for 5 mins at room temperature. Cells were probed with goat anti-RRM2 (Santa Cruz) and rabbit anti-HA overnight. The next day, cells were washed 3 times with 1X PBS then probed with donkey anti-goat 488 and donkey anti-rabbit 546 for 1 hour, then mounted on cover slides with Vectashield with DAPI (Vector Labs). Samples were analyzed on a Zeiss LSM 510 Meta Confocal Microscope.

RRM2 knockdown and transformation. Construction of the lentiviral shRNA vectors were based the LVTHm vectors developed by Wiznerowicz & Trono (36). The sense sequences for the shRNA used here were: m653, 5' –GCTATTGAAACTATCGCTTGT; r492, 5' –GGAGCGATTTAGCCAA GAAGT; r1104, 5' –GGAGAATATTTCACTAGAAGG; and Scrambled control, 5' –CCTAA GGTTAAGTCGCCCT. Vector stocks were generated by co-transfecting the shRNA-containing LVTHm plasmids along with the helper plasmids

pCMVdR8.74 (HIV gag-pol) and pMD2G (VSV G protein) into 293T cells, followed by harvest of the supernatants after 48 hrs. Stocks were titered by infecting dilutions onto 208F cells and counting foci of EGFP fluorescence (present in the LVTHM vector) after 4 days. For transduction with the lentiviral vectors, cells were seeded in 6-well plates at a multiplicity of infection of 10 or greater with polybrene (final concentration of polybrene: 8 µg/mL), and then incubated for 24 hours with the lentiviral vectors. At 24 hours post-transduction, transduced cells were harvested by trypsinization and seeded for transformation assays. Transformation assays with the transduced cells were as follows: cells were seeded at 3 X 10^5 cells in 6-cm dishes and transfected with 5 µg of ΔGP using Fugene 6 Transfection Reagent (Promega). Cells were examined by phase-contrast microscopy at 4 to 5 weeks and the number of transformed foci were counted. The number of foci relative to those in LVTHm (empty vector)-transduced cells in the same experiment was calculated, and mean results from at least three independent experiments was calculated. Statistical significance was determined by Student's t-test.

Analysis of knockdown levels using quantitative RT-PCR and western blot. For quantitative RT-PCR, total RNA was isolated from cells using Trizol Reagent (Life Technologies) and 2 µg of RNA was digested with DNase I and converted to cDNA using qScript cDNA Synthesis Kit (Quantas) as per manufacturer's instructions. Resulting cDNAs were diluted to a final concentration of 20 ng/µL. Primers for amplification of target genes were as follows: mouse RRM2, 5' –CCTACTAACCCCAGCGTTGA and 5' –GTTTCAGAGC TTCCCAGTGC; mouse β-actin, 5' –TGGATCGGTGGCTCCATCCTGG and 5' –GCAGTTC AGTAACAGTCCGCCTAGA; rat RRM2, 5' –GACAGGCTTATGCTGGAGCTGG and 5' – GCAAA GAGCACACGGATCGGTTG; rat β-actin, 5' –CACCAGTTCGCCATGGATGAC GAT and 5' –TCTCTTGCTCTGGGCCTCG TCG. Quantitative real-time PCR reactions were

performed using Power SYBR Green PCR Master Mix in the 7900HT Fast Real-Time PCR System (Applied Biosystems) as per manufacturer's instructions. All qPCR reactions were run in triplicate. The RNA expression levels were determined by both absolute standard curve and relative comparative C_t methods. For western blots, transduced cells were lysed with RIPA lysis buffer [50mM Tris-HCl, 150mM NaCl, 1% NP-40, 0.5% sodium deoxycholate, 0.1% SDS with 1 tablet of Complete Mini EDTA Free protease inhibitor tablet (Roche)], then cell debris was removed by centrifugation at 10,000 RPM for 20 min at 4°C. 2X Laemmli buffer was added to the supernatant followed by heating for 5 min, and one-tenth of the samples were loaded in a 10% SDS-polyacrylamide gel for resolution followed by western blot transfer to PVDF membranes. Blots were probed with primary antibodies goat anti-RRM2 (Santa Cruz) then re-probed with rabbit anti-β-Tubulin antibody (Cell signaling), and with secondary antibodies bovine anti-goat HRP (Santa Cruz) and goat anti-rabbit-HRP (Pierce), respectively. Blots were visualized by chemiluminescence with SuperSignal Femto Maximum Sensitivity Substrate (Pierce).

Cell Proliferation Assays. 208F cells transduced with control or RRM2 shRNA knockdown vectors were seeded at 3 X 10^4 cells in 6-cm dishes. The cells were removed from replicate dishes daily by trypsinization and the number of cells was determined by counting in a hemacytometer, using trypan blue exclusion to score only live cells.

Results

***In vitro* and *in vivo* interaction between RRM2 and JSRV Env.** As previously reported, RRM2 was found to be a JSRV Env interacting protein through yeast two-hybrid screens. To determine if JSRV Env and RRM2 interact outside of yeast, NIH 3T3 cells were

transfected with a FLAG tagged RRM2 expression vector and cell lysate was collected 48 hours later. The cell lysate was then incubated with glutathione beads containing GST-JSRV Env cytoplasmic tail (CT) fusion or GST tag alone. As shown in Fig. 4.1, RRM2 was successfully pulled down with JSRV CT. Pull-down was also performed on a lysate of cells transfected with a plasmid expressing a GFP fusion of NM23-H2, an enzyme that catalyzes the phosphorylation of nucleoside diphosphates to their corresponding nucleoside triphosphates (33); while this protein was also identified in the yeast 2-hybrid screen as a CT-interacter, this construct did not contain a FLAG epitope, but did have GFP fused to NM23-H2 for visualization of transfection efficiency. RRM2 was not pulled down by GST tag alone. This demonstrated an *in vitro* interaction between CT of JSRV Env and RRM2.

To determine if there is also an *in vivo* interaction between JSRV Env and RRM2, mouse fibroblast NIH 3T3 cells were transfected with HA-tagged JSRV Env (ΔGP-HA) or pcDNA, and the transfected cells were subjected to 2-color confocal immunofluorescence analysis for HA and RRM2 staining. In 3T3 cells transfected with pcDNA, staining of endogenous RRM2 showed a diffuse, punctate staining pattern with a cytoplasmic localization (Fig. 4.2, left column, middle row). In 3T3 cells transfected with ΔGP-HA, endogenous RRM2 showed re-localization towards the plasma membrane, where JSRV Env is located (right column, middle row). When the RRM2 and Env fluorescence was overlaid, there was evidence of co-localization in the area around the plasma membrane (yellow color, right column, bottom row).

Effects of RRM2 knockdown on JSRV transformation. To investigate the role of RRM2 in JSRV Env transformation, lentiviral shRNA vectors containing shRNA sequences targeting different areas of rat RRM2 mRNA were constructed. The lentiviral vectors were chosen since long-term knockdown of RRM2 was needed for the course of in vitro

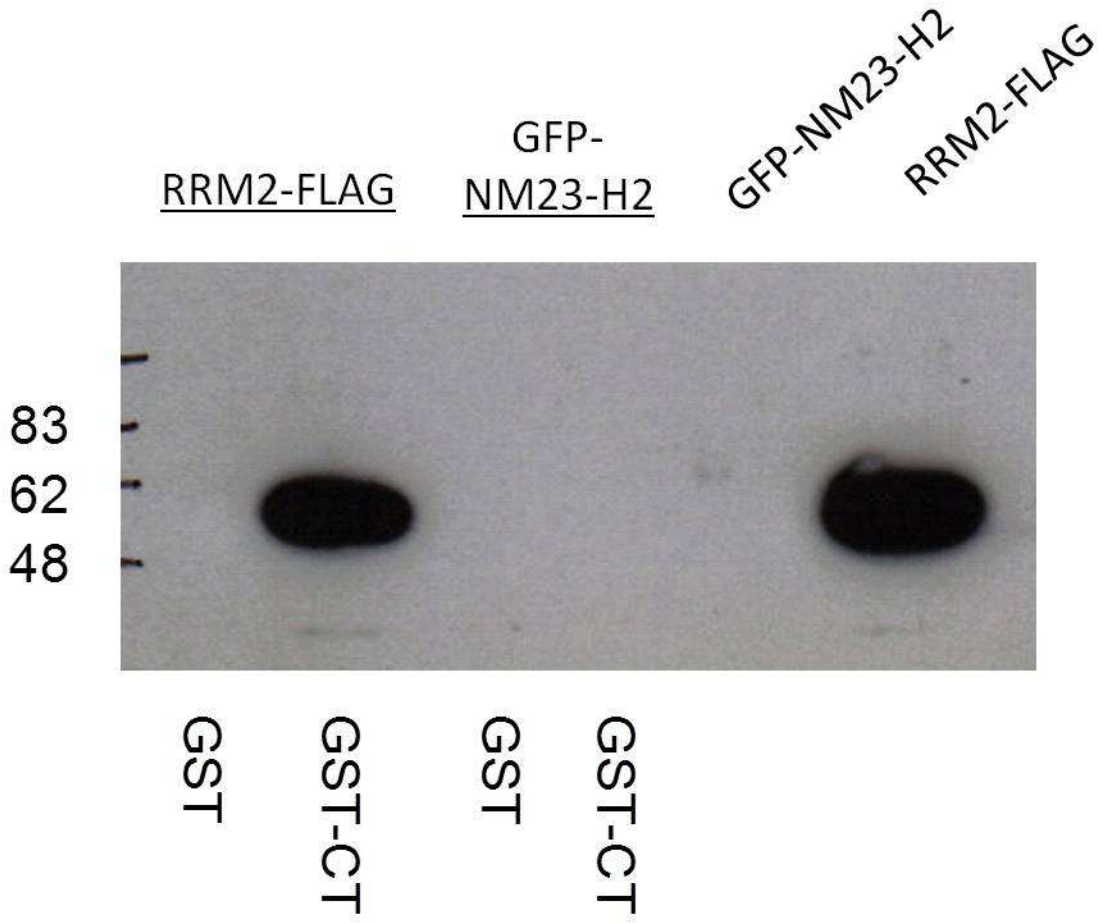

Fig. 4.1: Pull-down of RRM2 by JSRV CT. NIH 3T3 cells were transfected with RRM2-FLAG or GPF-NM23-H2, and the cell lysates were incubated with beads containing GST alone or GST-CT fusion protein. The bound proteins were eluted and analyzed by western blot with anti FLAG antibody. Total lysates before pull-down are shown on the right. Sizes of the observed proteins are indicated on the sides of the blot. The GFP-NM23-H2 plasmid lacks a FLAG epitope and instead had GFP for visualization of transfection efficiency.

transformation assays (4-5 weeks). The control lentiviral vectors LVTHm, LVTHm with scrambled shRNA (Scrambled), and the shRNA knockdown vectors m653 (targeting murine RRM2 mRNA) was used for transduction of mouse NIH 3T3 cells; r492 and r1104 (targeting rat RRM2 mRNA) were used to transduce rat RK3E and 208F cells. One week post-transduction, RNAs and whole cell lysates were collected; endogenous RRM2 mRNA levels analyzed by

quantitative RT-PCR and RRM2 protein levels analyzed by western blot. In NIH 3T3 cells, m653 showed a 50% reduction in RRM2 RNA levels, and a modest decrease in protein levels (Fig. 4.3A). Three additional shRNA vectors were tested that did not show any knockdown (not shown). In rat RK3E and 208F cells, r492 did not knockdown RRM2 very efficiently, as shown by qRT-PCR and western blotting although minor reductions (not statistically significant) may have occurred. On the other hand, the r1104 shRNA vector showed a 50% decrease in RRM2 RNA expression levels in RK3E cells and a 70% decrease in 208F cells, as well as a noticeable decrease in RRM2 protein levels in the transduced cells (Fig. 4.3B and C).

To check if RRM2 knockdown affects JSRV Env transformation, cells displaying potent knockdown of RRM2 was desired. The effect of RRM2 knockdown on JSRV Env transformation was tested in 208F cells because they showed the greatest level of RRM2 knockdown with shRNA r1104. 208F cells transduced with the different shRNA or control vectors were transfected with the JSRV Env expression vector ΔGP and cultured in standard conditions for focus formation (monolayer culture without transfer). Transformation efficiencies were determined from the numbers of transformed foci counted at 4-5 weeks post-transfection. For each experiment, the numbers of foci for each of the shRNA-transduced 208F cells were expressed as the percentage of transformed foci compared to cells transduced by the backbone

Fig. 4.2: Co-localization of RRM2 and JSRV Env. NIH 3T3 cells were plated on poly-L-lysine coated glass cover slips in a 6 well dish, then transfected with ΔGP-HA or pcDNA. After 48 hours, the samples were fixed with methanol and stained with goat anti-RRM2 and rabbit anti-HA antibodies then visualized with Alexafluor donkey anti-goat 488 or Alexafluor donkey anti-rabbit 546. The nuclei were counter-stained with DAPI, and the cover slips were mounted with Vectashield, then examined with confocal immunofluorescence microscopy. Left panels: cells transfected with pcDNA3.1; right panels, cells transfected with ΔGP-HA. Top row, fluorescence observed through a red filter (for HA staining); second row, the same image observed through a green filter (for RRM2 staining); bottom row, overlay of images through both red and green filters as well as for DAPI.

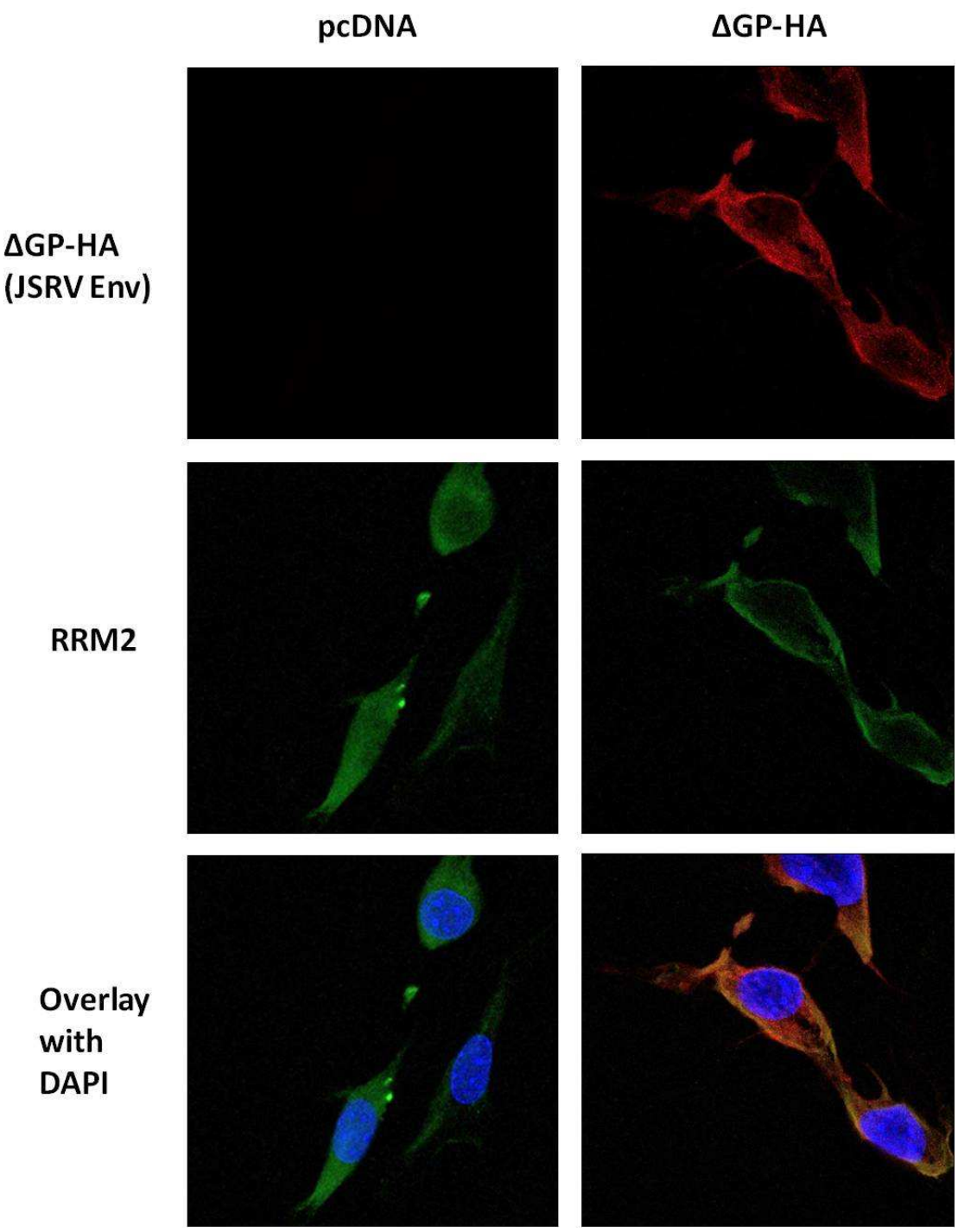
pcDNA
ΔGP-HA
ΔGP-HA
(JSRV Env)
RRM2
Overlay
with
DAPI

vector LVTHm. The numbers of foci after ΔGP transfection in LVTHm-transduced 208F cells ranged from 40 to 80 in three independent experiments. There was a significant decrease in transformation levels in the r1104-transduced cells, which showed a 50% decrease in JSRV Env transformation levels due to RRM2 knockdown (Fig. 4.4, gray bars). On the other hand, r492-transduced cells did not show significant changes in JSRV Env transformation levels as compared with 208F cells transduced with LVTHm or Scrambled RRM2 shRNA vector. Thus reduction in JSRV Env transformation was correlated with the degree of RRM2 knockdown, which supported the hypothesis that RRM2 plays a role in JSRV transformation.

To test if the decrease in JSRV Env transformation levels by RRM2 knockdown was specific to JSRV Env, the RRM2 knockdown cells were also tested for transformation level changes with a different oncogene, *v-mos*. *V-mos* was chosen because it does not activate the same signaling pathways as JSRV Env transformation (20). As seen in r1104 cells, knockdown of RRM2 did decrease *v-mos* transformation levels by 30%, albeit not as much as JSRV Env transformation levels (Fig 4.4, black bars). This difference in transformation inhibition between JSRV Env and *v-mos* (which was statistically significant) suggested that RRM2 may play a specific role in JSRV Env transformation, but there may also be a general effect of RRM2 knockdown on transformation by other oncogenes.

Fig. 4.3: Knockdown of endogenous RRM2 in rodent cells. NIH 3T3, RK3E, and 208F cells were transduced with control shRNA vector LVTHm (empty vector) and LVTHm containing a scrambled shRNA (Scrambled-LVTHm) or with m653, r492, or r1104 (shRNAs targeting mouse and rat RRM2 respectively). Top panels show RRM2 mRNA levels in transduced cells, which were determined by quantitative RT-PCR analysis one week post-transduction. All values were normalized to LVTHm levels. Bottom panels shows RRM2 protein levels in the transduced cells. Total cell lysates were collected one week post-transduction, along with total cell lysates from untransduced parental cell lines. Equal amounts of samples were loaded onto 10% SDS-polyacrylamide gels followed by western blot analysis. Blots were first probed with anti-RRM2 then re-probed with anti-β-Tubulin antibodies. Blots were visualized via chemiluminescence. (A) NIH 3T3 cells. (B) RK3E cells. (C) 208F cells.

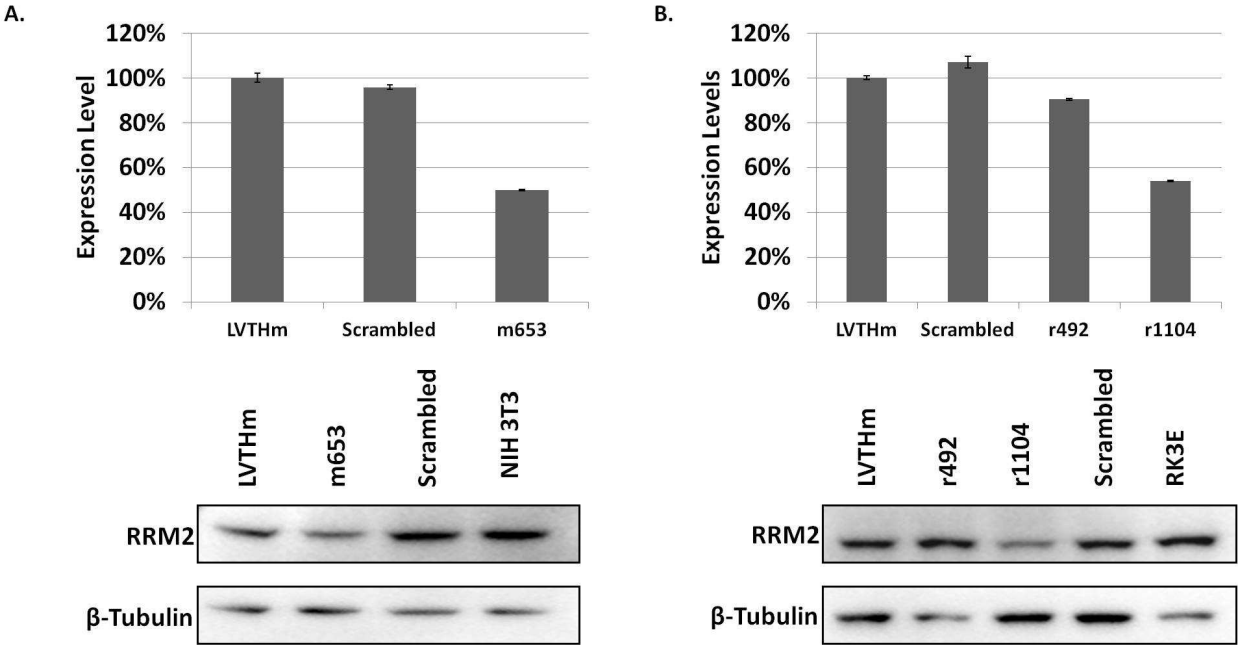
A.
120%
100%
80%
60%
40%
20%
0%
Expression Level
LVTHm
Scrambled
m653
LVTHm
m653
Scrambled
NIH 3T3
RRM2
β-Tubulin
B.
120%
100%
80%
60%
40%
20%
0%
Expression Levels
LVTHm
Scrambled
r492
r1104
LVTHm
r492
r1104
Scrambled
RK3E
RRM2
β-Tubulin

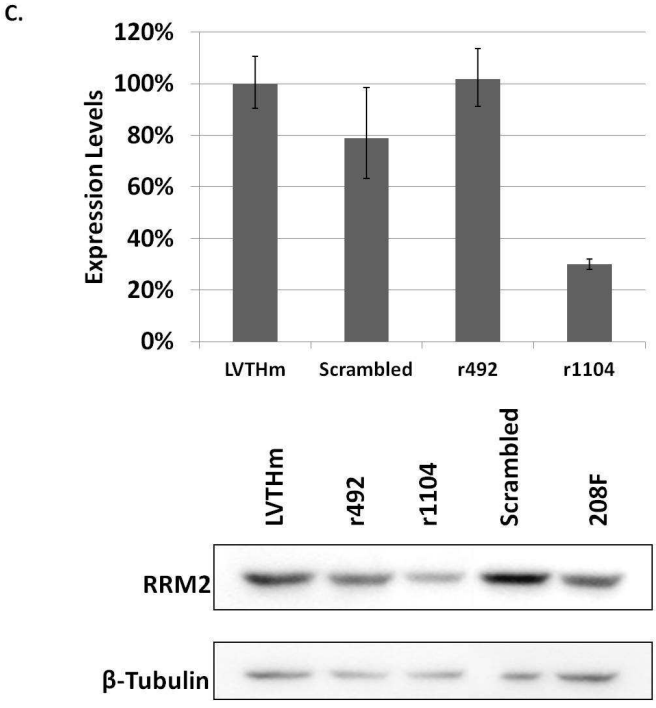
C.
120%
100%
80%
60%
40%
20%
0%
Expression Levels
LVTHm
Scrambled
r492
r1104
LVTHm
r492
r1104
Scrambled
208F
RRM2
β-Tubulin

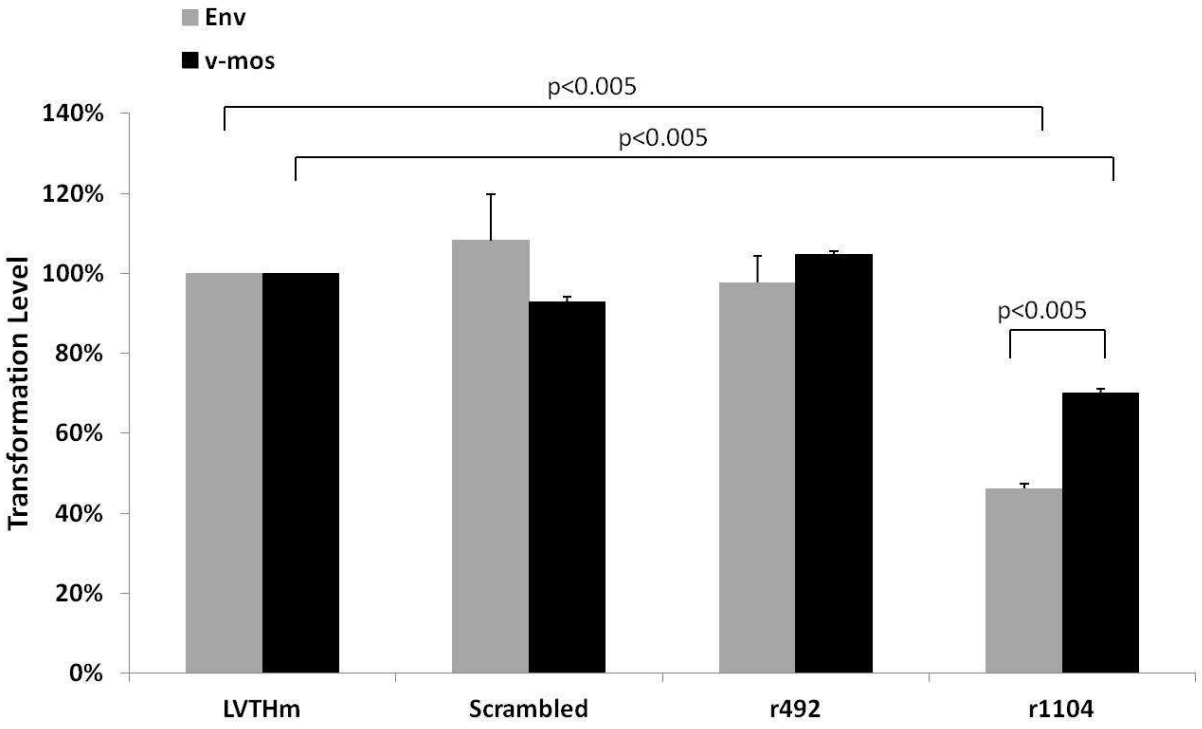

Fig. 4.4: Effects of RRM2 knockdown on JSRV Env and *v-mos* transformation. 208F cells with RRM2 knockdown were transfected with JSRV Env expression plasmid ΔGP to induce focus formation. Transformation levels were determined by counting the number of transformed foci 4-5 weeks post-transfection. (Mass cultures were used to minimize effects of clonal cell variation in response to ΔGP transformation, as in Chapter 2). The levels of Env transformation for cells transduced with each vector were normalized to that of control LVTHm transduced cells (light bars). The means and standard deviations were determined from at least three independent assays; reduction of JSRV Env transformation in the r1104 transduced cells compared to LVTHm-transduced cells was statistically significant. The same transduced cell cultures were transformed with *v-mos* oncogene, and transformation assays were performed under the same conditions (black bars). The difference in transformation reduction in r1104-transduced cells for Env and *v-mos* was statistically significant.

RRM2 knockdown can decrease cell proliferation rates. One possible explanation for the decrease in *v-mos* transformation levels in r1104-transduced 208F cells could be due to a decrease in cell proliferation rate. RRM2 is important for DNA synthesis in the cell cycle, and inhibition of RRM2 can cause cell arrest (23, 42). Thus knockdown of RRM2 might inhibit cell proliferation rates, leading to a general decrease in growth of foci of transformed cells independent of the oncogene. Therefore parental 208F and 208F cells transduced with LVTHm,

Scrambled, r492, and r1104 vectors were tested for their cell proliferation rates as shown in Fig. 4.5. The cell proliferation rates (doubling times) for each cell line can be calculated from the slopes of their growth curves on semi-log plots. The results showed that parental 208F cells, LVTHm, Scrambled, and r492 cells had comparable proliferation rates while r1104 cells had significantly lower proliferation rates. Parental 208F, and cells transduced with LVTHm, Scrambled, and r492 had doubling times of 20-22 hrs. On the other hand r1104 transduced cells had a doubling time of 33 hrs. Thus the degree of RRM2 knockdown was correlated with slower proliferation rates, as measured by a longer doubling time. This was consistent with hypothesis that the cause of *v-mos* transformation reduction in r1104-transduced 208F cells was a reduction in proliferation resulting from RRM2 knockdown.

Discussion

In this chapter, RRM2 was evaluated as a candidate interacter with JSRV Env protein, and it was tested for a role in JSRV Env transformation. RRM2 had been identified originally in a yeast 2-hybrid screen with the CT of Env. RRM2 was able to interact with JSRV Env in vitro and in vivo, and knockdown of endogenous RRM2 reduced the efficiency of JSRV Env transformation in rat 208F fibroblasts. However knockdown of RRM2 also reduced efficiency of *v-mos* transformation in the same cells, although there was less of a reduction compared to the effect on JSRV Env transformation. One possibility was that knockdown of RRM2 reduced the cell proliferation rate, which could lower the efficiency of transformed focus formation regardless of the oncogene used. Cell proliferation rates were indeed decreased in cells that were transduced with the r1104 RRM2 knockdown vector as determined through cell doubling times. The fact that RRM2 knockdown had a larger reduction in transformation by JSRV Env than for

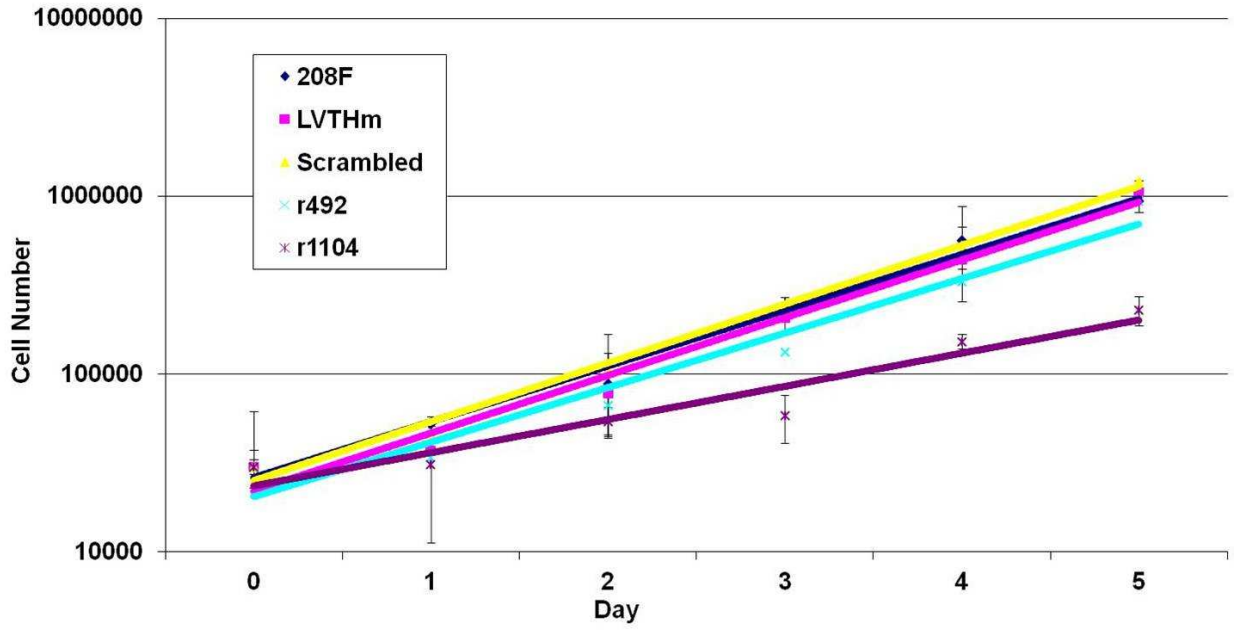

Fig. 4.5: Effects of RRM2 knockdown on cell proliferation rates. Transduced 208F cells were seeded at 3 X 10^4 cells in 6-well plates and the number of viable cells was determined daily by trypsinization and counting viable cells over a period of 5 days. The results (semi-log plots) show results from three independent experiments, each performed in duplicate.

v-mos suggested that RRM2 may play a specific role in JSRV transformation, in addition to having a more general negative effect on cell proliferation. Interaction between RRM2 and JSRV Env was demonstrated by both pull-down and immunofluorescence assays.

The mechanism of JSRV Env transformation currently is not well defined. Although JSRV Env mainly activates important signal transduction pathways involved in cell growth such as the PI3K-Akt-mTORand Ras-Raf-MAPK pathways and these pathways are important for JSRV transformation, it has not been shown that JSRV Env physically interacts with any proteins in these two pathways. The findings in this chapter may provide insights into the mechanism(s) of JSRV transformation, and in particular RRM2's role in the process. Although RRM2 knockdown also decreased transformation by *v-mos*, we hypothesize that this resulted

from a decrease in cell proliferation which could reduce transformation by any oncogene. Evidence for a specific role of RRM2 in JSRV Env transformation was suggested by the greater inhibition of JSRV vs. *v-mos* transformation after RRM2 knockdown. One possible way to further determine the role of RRM2 in JSRV Env transformation would be to restore the proliferation rate in RRM2 knockdown cells. It has been reported that exogenous addition of deoxyadenosine (dA) and deoxyguanosine (dG) can enhance the growth rate of RAW 264.7 mouse macrophage cells, whose growth is limited by low levels of dNTPs from hydroxyurea inhibition of ribonucleotide reductase (15). Thus it would be interesting to restore the growth rate of r1104-transduced 208F cells by addition of dA and dG to the culture medium, then test the efficiency of transformation by JSRV Env and *v-mos.* If restoration of the growth rate of r1104-transduced cells is accompanied by restoration of *v-mos* transformation efficiency, this would confirm our hypothesis. If under these conditions, the r1104-transduced cells still show reduced transformation efficiency for JSRV Env, this would definitively demonstrate a role for RRM2 in JSRV Env transformation independent of dNTP-regulated proliferation rates. We have attempted to perform these experiments, but toxicities of exogenous dA and dG have been a problem and will need to be resolved first.

Several investigations have explored the roles of ribonucleotide reductase and/or RRM2 in cancer. Many studies have explored targeting ribonucleotide reductase as an anti-cancer target since inhibiting DNA synthesis will preferentially target rapidly dividing cancer cells (4, 11, 15, 42). As described in the Introduction (Chapter 1), a more specific role for RRM2 over-expression (perhaps independent of its involvement in ribonucleotide reductase activity) has also been suggested -- for instance the fact that transgenic mice over-expressing RRM2 developed lung tumors (39). Our findings here support the potential role of RRM2 role in lung cancer,

including JSRV-induced lung adenocarcinoma. Although RRM2 knockdown did not completely abolish JSRV Env transformation, this was not necessarily surprising since JSRV Env activates multiple signaling pathways during transformation (e.g. PI3K-Akt-mTOR and Ras-Raf-MEK-MAPK) and RRM2 may only be involved in a subset of the JSRV Env-induced signaling changes. Indeed over-expression of RRM2 enhances *Ras* transformation of NIH-3T3 cells, and in this system RRM2 over-expression leads to an increase in Raf activity at the plasma membrane (9). In addition, RRM2 appears to be synergistic with other oncogenes in enhancing their transformation levels (8). One of the oncogenes reported was *v-src*; signaling through *c-src* is important in JSRV Env transformation as well (35). The combination of the findings in this report with the other reports on RRM2 provides support for RRM2's role in JSRV transformation.

In this study, we only studied transformation in one cell line, 208F. Given that JSRV Env utilizes different signaling pathways in different cell lines (20), it would be interesting to see if knockdown of endogenous RRM2 in other cell lines would affect JSRV Env transformation similarly to 208F cells. It would also be interesting to see if RRM2 over-expression can enhance JSRV Env's transformation efficiency, similar to the enhancement of *Ras* transformation (9). Ultimately, the role of RRM2 in transformation/tumorigenesis of ovine lung epithelial cells would be of greatest interest, since these cells are the in vivo targets of JSRV. However in vitro transformation systems for these cells have not yet been developed.

From the yeast two-hybrid screen, the JSRV Env CT was able to interact with RRM2 (Table 2.1). However, it is not known exactly where the RRM2 interaction area is within the JSRV CT. As discussed in Chapter 3, alanine scanning mutations along the cytoplasmic tail of JSRV Env had different effects on JSRV Env transformation (12). Studies analogous to those in

Chapter 3 should allow elucidation of the region of the CT involved in RRM2 binding, and the relationship to transformation. It will also be interesting to consider if binding of RRM2 and Zfp111 is at the same region of the CT. If so, questions would arise as to whether these two proteins bind simultaneously to the Env CT, although RRM2 binding appears to be cytoplasmic while Zfp111 is nuclear. Overall, identification of RRM2 in JSRV transformation contributes to our understanding of the mechanisms of JSRV Env transformation in mammalian cells.

References

1. **Alberti, A., C. Murgia, S. L. Liu, M. Mura, C. Cousens, M. Sharp, A. D. Miller, and M. Palmarini.** 2002. Envelope-induced cell transformation by ovine betaretroviruses. J Virol **76:**5387-94.
2. **Alian, A., D. Sela-Donenfeld, A. Panet, and A. Eldor.** 2000. Avian hemangioma retrovirus induces cell proliferation via the envelope (env) gene. Virology **276:**161-8.
3. **Allen, T. E., K. J. Sherrill, S. M. Crispell, M. R. Perrott, J. O. Carlson, and J. C. DeMartini.** 2002. The jaagsiekte sheep retrovirus envelope gene induces transformation of the avian fibroblast cell line DF-1 but does not require a conserved SH2 binding domain. J Gen Virol **83:**2733-42.
4. **Cerqueira, N. M., S. Pereira, P. A. Fernandes, and M. J. Ramos.** 2005. Overview of ribonucleotide reductase inhibitors: an appealing target in anti-tumour therapy. Curr Med Chem **12:**1283-94.
5. **De Las Heras, M., A. Ortin, A. Benito, C. Summers, L. M. Ferrer, and J. M. Sharp.** 2006. In-situ demonstration of mitogen-activated protein kinase Erk 1/2 signalling pathway in contagious respiratory tumours of sheep and goats. J Comp Pathol **135:**1-10.
6. **DeMartini, J. C., J. V. Bishop, T. E. Allen, F. A. Jassim, J. M. Sharp, M. de las Heras, D. R. Voelker, and J. O. Carlson.** 2001. Jaagsiekte sheep retrovirus proviral clone JSRV(JS7), derived from the JS7 lung tumor cell line, induces ovine pulmonary carcinoma and is integrated into the surfactant protein A gene. J Virol **75:**4239-46.
7. **Dirks, C., F. M. Duh, S. K. Rai, M. I. Lerman, and A. D. Miller.** 2002. Mechanism of cell entry and transformation by enzootic nasal tumor virus. J Virol **76:**2141-9.
8. **Fan, H., C. Villegas, A. Huang, and J. A. Wright.** 1998. The mammalian ribonucleotide reductase R2 component cooperates with a variety of oncogenes in mechanisms of cellular transformation. Cancer Res **58:**1650-3.
9. **Fan, H., C. Villegas, and J. A. Wright.** 1996. Ribonucleotide reductase R2 component is a novel malignancy determinant that cooperates with activated oncogenes to determine transformation and malignant potential. Proc Natl Acad Sci U S A **93:**14036-40.
10. **Griffiths, D. J., H. M. Martineau, and C. Cousens.** 2010. Pathology and pathogenesis of ovine pulmonary adenocarcinoma. J Comp Pathol **142:**260-83.
11. **Heidel, J. D., J. Y. Liu, Y. Yen, B. Zhou, B. S. Heale, J. J. Rossi, D. W. Bartlett, and M. E. Davis.** 2007. Potent siRNA inhibitors of ribonucleotide reductase subunit RRM2 reduce cell proliferation in vitro and in vivo. Clin Cancer Res **13:**2207-15.
12. **Hull, S., and H. Fan.** 2006. Mutational analysis of the cytoplasmic tail of jaagsiekte sheep retrovirus envelope protein. Journal of virology **80:**8069-8080.

13. **Hull, S., J. Lim, A. Hamil, T. Nitta, and H. Fan.** 2012. Analysis of jaagsiekte sheep retrovirus (JSRV) envelope protein domains in transformation. Virus Genes.
14. **Johnson, C., K. Sanders, and H. Fan.** 2010. Jaagsiekte sheep retrovirus transformation in Madin-Darby canine kidney epithelial cell three-dimensional culture. J Virol **84:**5379-90.
15. **Kwon, N. S., D. J. Stuehr, and C. F. Nathan.** 1991. Inhibition of tumor cell ribonucleotide reductase by macrophage-derived nitric oxide. J Exp Med **174:**761-7.
16. **Linnerth-Petrik, N. M., L. A. Santry, D. L. Yu, and S. K. Wootton.** 2012. Adeno-associated virus vector mediated expression of an oncogenic retroviral envelope protein induces lung adenocarcinomas in immunocompetent mice. PLoS One **7:**e51400.
17. **Liu, S. L., M. I. Lerman, and A. D. Miller.** 2003. Putative phosphatidylinositol 3-kinase (PI3K) binding motifs in ovine betaretrovirus Env proteins are not essential for rodent fibroblast transformation and PI3K/Akt activation. J Virol **77:**7924-35.
18. **Liu, S. L., and A. D. Miller.** 2007. Oncogenic transformation by the jaagsiekte sheep retrovirus envelope protein. Oncogene **26:**789-801.
19. **Liu, S. L., and A. D. Miller.** 2005. Transformation of madin-darby canine kidney epithelial cells by sheep retrovirus envelope proteins. J Virol **79:**927-33.
20. **Maeda, N., W. Fu, A. Ortin, M. de las Heras, and H. Fan.** 2005. Roles of the Ras-MEK-mitogen-activated protein kinase and phosphatidylinositol 3-kinase-Akt-mTOR pathways in Jaagsiekte sheep retrovirus-induced transformation of rodent fibroblast and epithelial cell lines. J Virol **79:**4440-50.
21. **Maeda, N., Y. Inoshima, D. A. Fruman, S. M. Brachmann, and H. Fan.** 2003. Transformation of mouse fibroblasts by Jaagsiekte sheep retrovirus envelope does not require phosphatidylinositol 3-kinase. J Virol **77:**9951-9.
22. **Maeda, N., M. Palmarini, C. Murgia, and H. Fan.** 2001. Direct transformation of rodent fibroblasts by jaagsiekte sheep retrovirus DNA. Proc Natl Acad Sci U S A **98:**4449-54.
23. **Nordlund, P., and P. Reichard.** 2006. Ribonucleotide reductases. Annu Rev Biochem **75:**681-706.
24. **Palmarini, M., and H. Fan.** 2001. Retrovirus-induced ovine pulmonary adenocarcinoma, an animal model for lung cancer. J Natl Cancer Inst **93:**1603-14.
25. **Palmarini, M., H. Fan, and J. M. Sharp.** 1997. Sheep pulmonary adenomatosis: a unique model of retrovirus-associated lung cancer. Trends in microbiology **5:**478-483.
26. **Palmarini, M., J. M. Sharp, M. de las Heras, and H. Fan.** 1999. Jaagsiekte sheep retrovirus is necessary and sufficient to induce a contagious lung cancer in sheep. J Virol **73:**6964-72.
27. **Perk, K., I. Hod, and T. A. Nobel.** 1971. Pulmonary adenomatosis of sheep (jaagsiekte). I. Ultrastructure of the tumor. J Natl Cancer Inst **46:**525-37.
28. **Platt, J. A., N. Kraipowich, F. Villafane, and J. C. DeMartini.** 2002. Alveolar type II cells expressing jaagsiekte sheep retrovirus capsid protein and surfactant proteins are the predominant neoplastic cell type in ovine pulmonary adenocarcinoma. Vet Pathol **39:**341-52.
29. **Raz, D. J., B. He, R. Rosell, and D. M. Jablons.** 2006. Bronchioloalveolar carcinoma: a review. Clin Lung Cancer **7:**313-22.
30. **Ruscetti, S. K.** 1999. Deregulation of erythropoiesis by the Friend spleen focus-forming virus. Int J Biochem Cell Biol **31:**1089-109.
31. **Sharp, J. M.** 1987. Sheep pulmonary adenomatosis: a contagious tumour and its cause. Cancer Surv **6:**73-83.
32. **Songyang, Z., S. E. Shoelson, M. Chaudhuri, G. Gish, T. Pawson, W. G. Haser, F. King, T. Roberts, S. Ratnofsky, R. J. Lechleider, and et al.** 1993. SH2 domains recognize specific phosphopeptide sequences. Cell **72:**767-78.
33. **Tee, Y. T., G. D. Chen, L. Y. Lin, J. L. Ko, and P. H. Wang.** 2006. Nm23-H1: a metastasis-associated gene. Taiwan J Obstet Gynecol **45:**107-13.

34. **Travis, W. D., E. Brambilla, M. Noguchi, A. G. Nicholson, K. R. Geisinger, Y. Yatabe, D. G. Beer, C. A. Powell, G. J. Riely, P. E. Van Schil, K. Garg, J. H. Austin, H. Asamura, V. W. Rusch, F. R. Hirsch, G. Scagliotti, T. Mitsudomi, R. M. Huber, Y. Ishikawa, J. Jett, M. Sanchez-Cespedes, J. P. Sculier, T. Takahashi, M. Tsuboi, J. Vansteenkiste, I. Wistuba, P. C. Yang, D. Aberle, C. Brambilla, D. Flieder, W. Franklin, A. Gazdar, M. Gould, P. Hasleton, D. Henderson, B. Johnson, D. Johnson, K. Kerr, K. Kuriyama, J. S. Lee, V. A. Miller, I. Petersen, V. Roggli, R. Rosell, N. Saijo, E. Thunnissen, M. Tsao, and D. Yankelewitz.** 2011. International association for the study of lung cancer/american thoracic society/european respiratory society international multidisciplinary classification of lung adenocarcinoma. J Thorac Oncol **6:**244-85.
35. **Varela, M., M. Golder, F. Archer, M. de las Heras, C. Leroux, and M. Palmarini.** 2008. A large animal model to evaluate the effects of Hsp90 inhibitors for the treatment of lung adenocarcinoma. Virology **371:**206-15.
36. **Wiznerowicz, M., and D. Trono.** 2003. Conditional suppression of cellular genes: lentivirus vector-mediated drug-inducible RNA interference. J Virol **77:**8957-61.
37. **Wootton, S. K., C. L. Halbert, and A. D. Miller.** 2005. Sheep retrovirus structural protein induces lung tumours. Nature **434:**904-907.
38. **Wootton, S. K., M. J. Metzger, K. L. Hudkins, C. E. Alpers, D. York, J. C. DeMartini, and A. D. Miller.** 2006. Lung cancer induced in mice by the envelope protein of jaagsiekte sheep retrovirus (JSRV) closely resembles lung cancer in sheep infected with JSRV. Retrovirology **3:**94.
39. **Xu, X., J. L. Page, J. A. Surtees, H. Liu, S. Lagedrost, Y. Lu, R. Bronson, E. Alani, A. Y. Nikitin, and R. S. Weiss.** 2008. Broad overexpression of ribonucleotide reductase genes in mice specifically induces lung neoplasms. Cancer Res **68:**2652-60.
40. **York, D. F., R. Vigne, D. W. Verwoerd, and G. Querat.** 1992. Nucleotide sequence of the jaagsiekte retrovirus, an exogenous and endogenous type D and B retrovirus of sheep and goats. J Virol **66:**4930-9.
41. **Zavala, G., C. Pretto, Y. H. Chow, L. Jones, A. Alberti, E. Grego, M. De las Heras, and M. Palmarini.** 2003. Relevance of Akt phosphorylation in cell transformation induced by Jaagsiekte sheep retrovirus. Virology **312:**95-105.
42. **Zuckerman, J. E., T. Hsueh, R. C. Koya, M. E. Davis, and A. Ribas.** 2011. siRNA knockdown of ribonucleotide reductase inhibits melanoma cell line proliferation alone or synergistically with temozolomide. J Invest Dermatol **131:**453-60.

CHAPTER 5: CONSTRUCTION AND PURIFICATION OF HISTIDINE-BIOTIN-HISTIDINE (HBH) TAGGED JSRV ENV

Abstract

Jaagsiekte sheep retrovirus can cause a contagious form of lung cancer in sheep called ovine pulmonary adenocarcinoma, a type of lung cancer that is histologically similar to human lung adenocarcinoma in situ, formerly known as bronchiolo-alveolar carcinoma. JSRV envelope protein is the oncoprotein that causes lung tumor formation in sheep, and it induces cell transformation in cultured cells. JSRV Env transformation activates important cell signaling pathways such as Akt/mTORand Ras/Raf/MAPK, but Env proteins have not yet been shown to interact directly with components of these two pathways. This suggests that Env interacts indirectly, perhaps by interacting with other cellular proteins that subsequently activate these pathways. A previous attempt to identify Env-interacting proteins was performed by a genetic approach, namely yeast two-hybrid screening using the cytoplasmic tail of JSRV Env, or the entire Env protein, as baits. Two candidate interactors were evaluated for roles in JSRV transformation as described in previous chapters of this thesis. An alternative approach to identifying Env-interacting proteins is a biochemical one, namely to employ proteomics, specifically affinity purification of Env protein (and associated cellular proteins) from cells expressing JSRV Env, followed by proteolysis and mass spectrometry to identify proteins based on the masses of peptides. Here we report generation of JSRV Env with a C-terminal tandem affinity purification tag (HBH) consisting of a biotinylation site flanked by two histidine-rich sequences; this tag has been used to identify interacting cellular proteins under both native and denaturing conditions. The HBH-tagged JSRV Env (encoded by the ΔGP-HBH plasmid)

retained the ability to transform rat fibroblast 208F cells, albeit at lower efficiency than untagged JSRV Env. Single-cell clones from ΔGP-HBH transformed cells were verified for the presence of ΔGP-HBH via RT-PCR and western blot. Tandem affinity purification of Env-HBH from 293T cells transfected with ΔGP-HBH showed modest recovery of Env-HBH in western blot and silver stained gels. Comparisons with cells transfected with non-HBH tagged versions of Env showed relatively low levels of non-specific proteins bound and eluted from the second purification step. In the future ΔGP-HBH should be valuable in identifying candidate JSRV Env binding proteins by proteomics/mass spectrometry.

Introduction

Jaagsiekte sheep retrovirus (JSRV) is an ovine betaretrovirus that was identified as the etiological agent of a type of lung cancer in sheep called ovine pulmonary adenocarcinoma (OPA) (31). OPA infected sheep have large amounts of fluid build-up in their lungs in addition to tumor formation. Combination of these two symptoms causes severe respiratory distress for animals with end-stage disease (11). OPA is also histologically similar to a type of human lung cancer called adenocarcinoma in situ (AIS), formerly known as bronchiolo-alveolar carcinoma (BAC) (37). AIS/BAC is only weakly associated with smoking, which raised the possibility of other causes. Interestingly a polyclonal antibody against the capsid of JSRV was found to react with AIS/BAC lung tumors, suggesting a retroviral etiology for this type of human lung cancer (9). However, other studies (e.g. PCR-based tests for JSRV-related sequences in AIS/BAC) have not supported a role for a JSRV-like virus in these human cancers (13, 28, 40). Nevertheless JSRV-induced OPA is a reasonable animal model for analyzing AIS/BAC.

Purified JSRV collected from lung fluid of sheep with OPA was able to induce lung tumors within as little as 10 days post-inoculation when inoculated intratracheally into newborn lambs (38).This suggested that JSRV may be an acute transforming retrovirus with a viral oncogene. However, analysis of the JSRV genome did not reveal an apparent oncogene (10). Nevertheless transfection of JSRV DNA into various cells in culture resulted in the formation of foci of transformed cells, indicating that JSRV does indeed carry an oncogene (27). Sequential deletion within the JSRV genome showed that the viral envelope protein, Env, functions as the oncogene (27). JSRV Env transformation has been extensively studied in different cell lines, including rodent fibroblasts (1, 5, 25, 26, 30), canine epithelials (21, 24), and avian fibroblast cells (2). The two main signaling pathways important for JSRV Env transformation are considered to be the Akt/mTOR pathway (21, 22, 24, 26, 41) and the Ras/Raf/MAPK pathway (19, 25) as determined by pathway inhibitors. Although it is known that JSRV Env utilizes both the Akt/mTOR and Ras/Raf/MAPK pathways for transformation, JSRV Env does not seem to physically interact with known components of these two signaling pathways (15, 23). Therefore, JSRV Env may first interact with some other cellular protein(s) in order to activate these signaling pathways downstream. Identification of interacting proteins will help us better understand the mechanism of JSRV transformation.

Several candidate Env-interacting proteins were identified in a genetic approach, namely a yeast two-hybrid screen, and two of these, and their potential roles in JSRV transformation, were investigated in preceding chapters in this thesis. A disadvantage of the yeast two-hybrid system is that some protein interactions require post-translational modifications of the interacting proteins which may not be carried out in yeast (e.g. phosphorylation) and that it is a binary

system. As a result, the set of JSRV Env candidate interacting protein obtained from the two-hybrid screen is likely incomplete.

Proteomics/mass spectrometry (3) represents a biochemical approach to identifying JSRV Env-interacting proteins. A previous attempt in the laboratory employed pull-down of interacting proteins from 293T cells transfected with an expression construct for JSRV Env containing glutathione S-transferase (GST) fused to the cytoplasmic tail (CT). Cell lysates were passed over and eluted from glutathione-agarose columns. Proteolytic (tryptic) digestion of eluates followed by mass spectrometry to identify the eluted proteins gave a large number of cellular proteins, so the results were inconclusive. There was a high background of non-specific proteins; most if not all of the proteins identified were also detected in parallel eluates from cells transfected with control plasmids (e.g. untagged Env [ΔGP], or the backbone vector pcDNA3).

In this chapter, we generated an expression construct for JSRV Env containing a C-terminal HBH tandem affinity tag, consisting of a arginine-glycine-serine (RGS) hexahistidine-biotination site-hexahistidine-- ΔGP-HBH. This tag allows more stringent purification of the tagged Env along with associated cellular proteins, which should reduce the non-specific background signals that were found in the GST-CT purification procedure. The HBH tag was developed by our colleague Dr. Peter Kaiser (UCI), and has been used extensively in characterization of large intracellular protein complexes such as the proteasome (12, 36). Tandem affinity purification is an efficient way of purifying appropriately tagged proteins from cell lysates while reducing the non-specific binding of other proteins by extending the purification procedure to two tandem steps, with each step using a different affinity resin that will be efficiently bound by the epitope tag on the protein (35). The HBH tag shows high affinity to Ni^{2+}columns and streptavidin resin due to its hexahistidine and biotination motifs,

respectively (36). The high binding affinity by the HBH tag to the different resins makes the two-step purification of HBH tagged JSRV Env very efficient at purifying the tagged protein while reducing the non-specific interactions, which can help greatly during the mass spectrometry analysis of the candidate interacting proteins of JSRV Env. This can lead to identification of new interacting proteins, which can further expand our understanding of JSRV Env transformation.

Materials and Methods

Plasmids. The JSRV Env expression vector ΔGP and the Flag-tagged version have been described previously (26, 27). pEGFP-N1 was from BD Biosciences. The HBH tag vector was a gift from Dr. Peter Kaiser at UCI(36) and is available at Addgene. The HBH tag consists of a RGS 6x histidine motif linked to a biotinylation site and another 6x histidine. The HBH tag was amplified from pIRES-BARD1-HBH (gift of Dr. Peter Kaiser, University of California, Irvine) using the following primers: 5' – GTAGAACCGGTCCGACTACGATATACCCACA and 5' – TCGCGACCGGTTCATTAATGATGGTGGTGATG. HBH was cloned into the JSRV Env expression vector ΔGP(AgeI) (26)at the *Age*I site located at the *env* gene stop codon, by first digesting the PCR product and ΔGP(AgeI) with restriction enzyme AgeI (New England Biolabs). The products were gel purified and ligated together using the Rapid DNA Ligation Kit (Roche) to generate ΔGP-HBH.

Cell lines. Rat fibroblast 208F (16, 19)and human embryonic kidney cells 293T(17, 19, 26, 29, 32, 33)were grown in Dulbecco's modified Eagle's medium supplemented with 10% fetal bovine serum, penicillin (100 U/mL) and streptomycin (100 µg/mL).

Cell transformation assays. 208F cells were plated at 3 X 10^5 cells in 6 cm dishes. Cells were transfected with 5 µg of ΔGP-HBH or ΔGP using Fugene 6 Transfection Reagent (Promega) and incubated with the transfection reagent for 24 hours, the medium was then replaced with fresh medium. Cells were maintained for 5-6 weeks, then examined under phase-contrast microscopy and scored for foci. Individual foci were isolated with sterile cloning rings and subcultured further. The subcultures were plated at a low density (100 cells/150cm dish) to generate single cell clones, and single cell clones showing transformed phenotype were isolated by selective trypsinization in cloning rings. The presence of ΔGP or ΔGP-HBH in cloned transformants was confirmed with RT-PCR and western blot.

RT-PCR. Total RNA was isolated from cells using Trizol Reagent (Life Technologies) and 2 µg of RNA was digested with DNase I and converted to cDNA using qScript cDNA Synthesis Kit (Quantas) as per manufacturer's instructions. Resulting cDNAs were diluted to a final concentration of 20 ng/µL. Primers for amplification of target genes were as follows: ΔGP, 5' –TGCCGAAGCGCCGCGCTGGA and 5' –CTCATTCCAGGCGTAGCGCA; rat β-actin, 5' –CACCAGT TCGCCATGGATGACGAT and 5' –TCTCTTGCTCTGGGCCTCGTCG. Samples were resolved in a 2% agarose gel.

Western Blot. Cells were collected and lysed in RIPA Lysis Buffer [50mM Tris-HCl, 150mM NaCl, 1% NP-40, 0.5% sodium deoxycholate, 0.1% SDS with 1 tablet of Complete Mini EDTA Free protease inhibitor tablet (Roche)]. 10% of total cell lysate was loaded into a 10% SDS-polyacrylamide gel for electrophoresis. After wet transfer to PVDF membranes (Bio-Rad), blots were probed with mouse anti-RGS6xHis (Qiagen) then reprobed with rabbit anti-β Tubulin (Cell Signaling Technologies), followed by probing with secondary antibodies goat anti-mouse

HRP and goat anti-rabbit HRP (Pierce), respectively. Blots were visualized by chemiluminescence (SuperSignal West Femto Maximum Sensitivity Substrate, from Pierce).

Tandem affinity purification (TAP) under non-denaturing conditions. 293T cells were plated at 2 X 10^6 cells in 10 cm dishes. After 18 hrs they were transfected with 28 µg of ΔGP-HBH, ΔGP-FLAG, ΔGP, or pEGFP DNAs using CalPhos Mammalian transfection kit (Clontech) as per manufacturer's instructions. Cells were lysed in a 1% Triton X-100 Lysis Buffer [50mM NaH_2PO_4, 300mMNaCl, 10 mM imidazole, 0.05% Tween 20, 1% Triton X-100, and 1 tablet of Complete Mini EDTA Free Protease Inhibitor (Roche)], and the whole cell lysate was incubated with Ni-NTA Agarose (25 µL Ni^{2+}slurry / 1 mg of protein, beads were equilibrated by washing with 1% Triton X-100 Lysis Buffer twice) (Qiagen) for 2 hours at 4°C under rotation in Poly-Prep Chromatography Columns (Bio-Rad). The flow-through was collected and the Ni^{2+} beads were washed with10x bead volume of Ni^{2+}wash buffer 1 (50 mM NaH_2PO_4, 300 mM NaCl, 20 mM imidazole, 0.05% Tween 20, pH 8.0), then washed with 10x bead volume of Ni^{2+}wash buffer 2 (same as Ni^{2+}wash buffer 1, but 30 mM imidazole), and a final wash with 10x bead volume of Ni^{2+}wash buffer 3 (same as Ni^{2+}wash buffer 1, but 40 mM imidazole). All washes were pooled. Proteins were eluted with 5x bead volume of Ni^{2+}elution buffer (50 mM NaH_2PO_4, 300 mM NaCl, 250 mM imidazole, 0.05% Tween 20, 2 mM EDTA, pH 8.0). Ni^{2+}resins were checked for elution efficiency by boiling the resin in 2x Laemmli buffer. Part of Ni^{2+}eluate was retained for western blot analysis, while the rest of the eluate was incubated with streptavidin beads (15 µL of streptavidin slurry / 1 mg of protein, beads were equilibrated by washing with Ni^{2+}elution buffer twice) (Thermo Fisher) for 3 hours at 4°C under rotation. The flow-through was collected and the streptavidin beads were washed twice with 10x bead volume of Ni^{2+}elution buffer, and the beads were boiled in 2x Laemmli buffer for western

blot analysis. 5% of the total volume from each of the collected fractions was loaded onto a10% acrylamide gel for resolution by SDS-PAGE and blot transfer to PVDF membrane. Blots were first probed with primary antibodies mouse anti-RGS6xHis then re-probed with rabbit anti-FLAG antibody, and secondary antibodies goat anti-mouse HRP and goat anti-rabbit HRP. Blots were visualized by chemiluminescence. Silver staining of gels was done with Pierce Silver Stain for Mass Spectrometry (Thermo) as per manufacturer's instructions.

Tandem affinity purification under crosslinked-denaturing conditions. 293T cells were plated at 5.4 X 10^6 cells in 15 cm dishes. After 18 hrs they were transfected with 77 µg of ΔGP-HBH or pEGFP DNAs using CalPhos Mammalian transfection kit (Clontech) as per manufacturer's instructions. Cells were first washed with 1X PBS then crosslinked with formaldehyde (1% formaldehyde final concentration in PBS), then quenched with cold 1X PBS/0.125mM Glycine. Cells were scraped off the plates with cell lifters and pelleted by centrifugation at 1,200 RPM at 4°C for 5 mins in a tabletop centrifuge. The pellets were washed with cold 1X PBS, pelleted, then the wash was removed and replaced with lysis buffer A [8M urea, 300mM NaCl, 0.5% NP-40, 50mM NaH_2PO_4, pH8, with 1 tablet of Complete Mini EDTA Free (Roche)]. Cell pellets were resuspended and incubated in lysis buffer A for 5 mins on ice, then the remaining cell debris was pelleted by centrifugation at 14,000 RPM for 5 mins at 4°C. The supernatant consisted of whole cell lysate, which was then incubated with Ni-NTA Agarose (25 µL Ni^{2+}slurry / 1 mg of protein, beads were equilibrated by washing with lysis buffer A twice) (Qiagen) for 3 hours at 4°C under rotation in Poly-Prep Chromatography Columns (Bio-Rad). The flow-through was collected and the Ni^{2+} beads were washed twice with 5x bead volumes of lysis buffer A, then once more with 5x bead volumes of buffer B (same as lysis buffer A, but at pH6.3). Proteins were eluted with 5x bead volume of elution buffer (8M urea,

200mM NaCl, 2% SDS, 50mM NaH_2PO_4, 10mM EDTA, 100mM Tris, pH4.3, with 1 tablet of Complete Mini EDTA Free). The Ni^{2+}eluate was then incubated with streptavidin beads (15 µL of streptavidin slurry / 1 mg of protein, beads were equilibrated by washing with elution buffer twice) (Thermo) overnight at 4°C under rotation. The flow-through was collected and the streptavidin beads were first washed twice with 10x bead volumes of buffer D (8M urea, 200mM NaCl, 2% SDS, 100mM Tris, pH 8, with 1 tablet of Complete Mini EDTA Free), then washed twice with 10x bead volumes of buffer E (same as buffer D, but 0.2% SDS), then washed twice with 10x bead volumes of buffer F (same as buffer D, but no SDS). The streptavidin beads were prepared for mass spectrometry analysis by washing the beads three times with 10x bead volume of 50mM NH_4HCO_3, then kept in 50mM NH_4HCO_3 until sent for mass spectrometry analysis.

Results

Generation of HBH-tagged JSRV Env. The HBH tandem affinity tag consists of a RGS 6x Histidine peptide that will bind to nickel (Ni^{2+}) resin, a biotination site that is derived from *Propionibacteriumshermanii* transcarboxylase that is biotinated in mammalian cells (7), and another hexahistidine tag (Fig. 5.1). The HBH tag is 88 amino acids in length, larger than the commonly used epitope tags such as hemagluttin (HA) (9 amino acids) or FLAG tags (8 amino acids). The HBH tag was PCR amplified from the pIRES-BARD1-HBH plasmid (a gift from Dr. Peter Kaiser, University of California, Irvine), and then cloned in a modified version of the JSRV Env expression plasmid ΔGP with an Age I site at the 3' end of the Env coding sequence as described in Materials and Methods. The resulting plasmid was designated ΔGP-HBH.

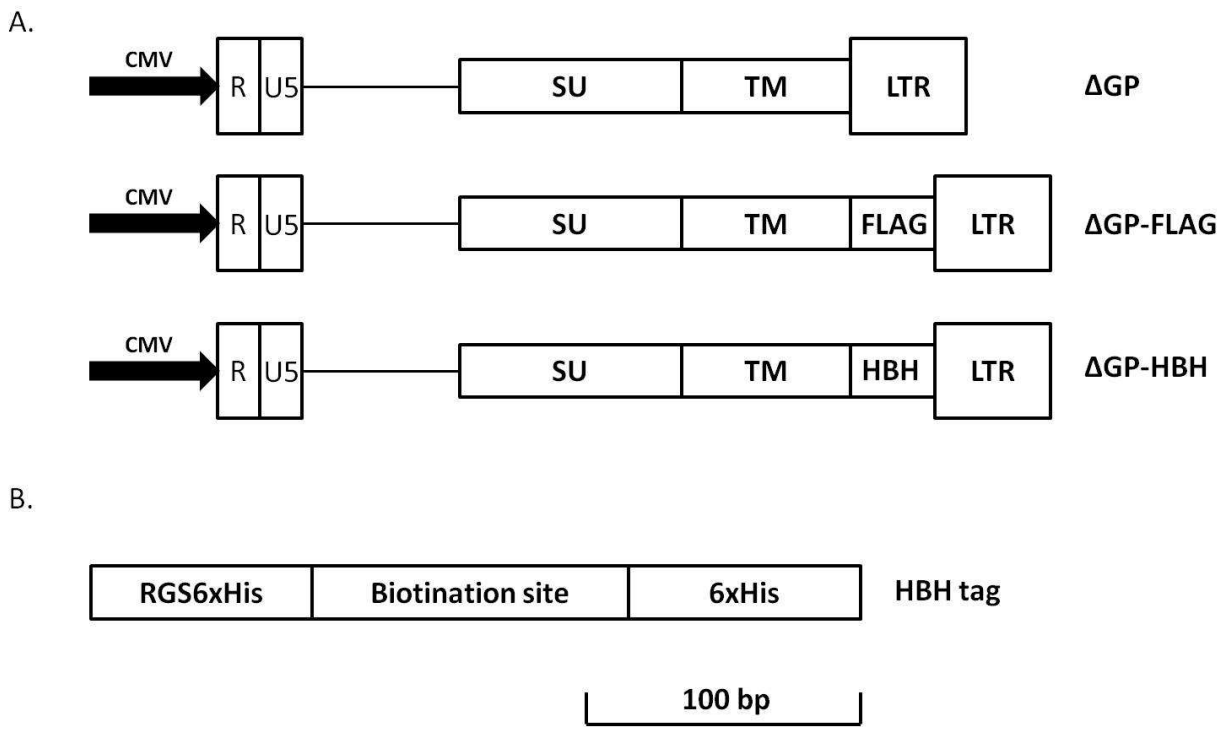

Fig. 5.1: JSRV Envelope expression constructs and the HBH tag. (A) All of the JSRV Env expression vectors are driven by the CMV immediate-early promoter, as indicated by the bold arrows. The location of the Env surface (SU) and transmembrane (TM) domains are shown, along with C-terminal epitope tags. The FLAG and HBH tags were attached at the end of the JSRV CT. LTR, long terminal repeat that contains U3, R and U5 regions. R, repeated sequences in viral LTR that also has the polyadenylation signal. U5, unique 5' region in viral LTR that has primer binding site. (B) The HBH tag consists of a RGS hexahistidine region, followed by a biotination site, and a second hexahistidine region. The hexahistidines interacts strongly with Ni^{2+} resin while the biotin interacts stongly with streptavidin resin.

ΔGP-HBH is able to transform 208F cells. A concern with attaching the relatively large HBH tag to JSRV Env was that it might abolish its transformation potential. To test this possibility ΔGP-HBH was transfected into rat 208F fibroblasts and the transfected cells were maintained in culture for 5-6 weeks. Starting at week 5, foci of transformed became visible. Transformed cells were recognizable by their rounded shape and the loss of contact inhibition, resulting in the cells piling on top of each other. Mature foci were observed one week later,

characterized by their opacity in the center of the foci and elongated cell shapes radiating from the center of the focus (Fig. 5.2 top panel). Transfection of rat RK3E epithelial cells with ΔGP-HBH also yielded transformed foci in two independent experiments (Fig 5.2 bottom panel). Thus the HBH-tagged JSRV Env protein retained the capacity to induce transformation.

While ΔGP-HBH was able to induce transformation in 208F and RK3Ecells, its transformation efficiency was reduced compared with native untagged JSRV Env encoded by the ΔGP expression vector. In a preliminary test 208F cells were transfected with ΔGP-HBH and ΔGP in parallel and incubated under focus forming conditions. 208F cells transformed with ΔGP or ΔGP-HBH showed 12 and 2 foci, respectively (Table 5.1). This represented approximately a 6 fold reduction in transformation efficiency, similar to the reductions observed when smaller HA or FLAG epitopes were added to the C-terminus of JSRV Env, showing 2 – 5 fold reductions, respectively (26). Subsequent trials showed 4-5 fold decrease in efficiency.

Thus despite the reduction in transformation efficiency, HBH-tagged Env is capable of transforming cells, so it presumably binds cellular proteins involved in transformation, and it should be useful for tandem affinity purification/proteomics characterization. Transformed foci were picked from the ΔGP and ΔGP-HBH transfected 208F cells and purified by cloning from single cells. The single cell clones were selected based on their phenotype, as transformed 208F cells have a long, elongated morphology demonstrated in Fig. 5.2. RNA from two randomly selected clones were converted to cDNA, and analyzed for the presence of JSRV Env using PCR with primers targeting the surface (SU) region of JSRV Env. PCR was able to detect ΔGP in each of these transformed clones, while untransformed parental 208F cells did not show any JSRV Env signals (Fig. 5.3A), demonstrating that these clones contained JSRV Env. In addition,

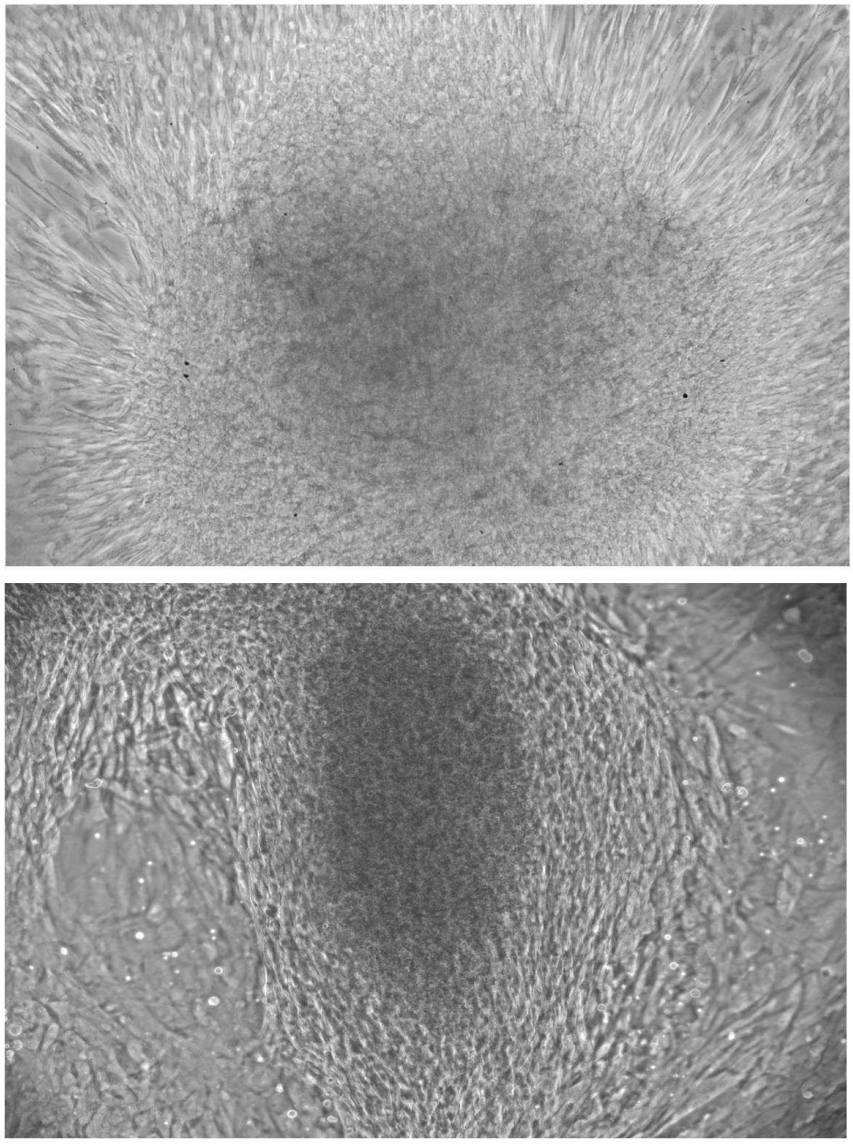

Fig. 5.2: Transformation of 208F and RK3E cells with ΔGP-HBH. Rat fibroblast 208F and rat epithelial RK3E cells were transfected with 5 μg of ΔGP-HBH and maintained in culture under conditions for focus formation for 5-6 weeks. Examples of the resulting foci for 208F (top) and RK3E (bottom) are shown. The transformed 208F focus on the culture plate showed opacity in the center of the focus and elongated cells extending from the center. The RK3E focus showed darker opacity in the center, with modest elongation of the cells around the center.

the ΔGP-HBH clones were found to be expressing the ΔGP-HBH protein via western blot (Fig. 5.3B). These ΔGP-HBH transformed cells should be useful in proteomics experiments.

Table 5.1. Transformation efficiency of ΔGP and ΔGP-HBH in 208F cells

	Foci formed:			
Plasmid used:	Trial 1	Trial 2	Trial 3	Trial 4
ΔGP	12	25	27	26
ΔGP-HBH	2	5	6	6

Rat fibroblast 208F cells were transfected with either ΔGP or ΔGP-HBH. The cultures were scored for transformed foci 5-6 weeks after transfection.

Tandem purification of ΔGP-HBH using nickel and streptavidin beads. To test for the purification efficiency of ΔGP-HBH, 293T cells were transfected with ΔGP-HBH and after 48 hr they were lysed by incubation in a lysis buffer containing 1% Triton X-100 that dissolved the plasma membrane as described in Materials and Methods. The subsequent TAP purification was done under non-denaturing conditions. The whole cell lysate was then incubated for 2 hr at 4 C with a nickel resin, packed into a 10 mL Poly-prep chromatography column and then the flow through from the column was collected. The resin was washed in monosodium phosphate buffer with increasing concentrations of imidazole in each subsequent wash step. The proteins were eluted from the washed resin by incubation in an elution buffer containing 2mM EDTA and 250mM imidazole and the eluate was collected. The eluate was then subjected to a second round of affinity purification by incubation for 3 hr with streptavidin agarose beads. The streptavidin agarose beads were washed then collected from the column; bound proteins were eluted from the collected streptavidin beads by boiling in Laemmli buffer (contain 10% SDS). Equal portions of the total cell lysates, non-bound fractions, washes and eluates from each step in the tandem affinity purification were analyzed by SDS-PAGE and western blot analysis with an anti-RGS6xHis antibody. As shown in Fig. 5.4 the first purification step with nickel resin

successfully retained the majority of the ΔGP-HBH protein, as shown by a weak signal in the flow-through fraction, no signals in the washes, and a strong ΔGP-HBH signal in the elution, and none retained on the beads (Fig. 5.4). The second purification step with streptavidin also showed even higher retention of ΔGP-HBH, with low to no signals in the non-bound and wash fractions. However a very faint signal was observed in the elution lane, even though the resin was boiled in buffer containing SDS and urea. This was observed in 3 independent trials, and we tentatively attribute this to the extremely high affinity of the biotin-streptavidin interaction (39). Nevertheless the results indicated Env-HBH showed very efficient binding to both nickel and streptavidin resins.

To investigate the specificity of the binding interaction by the HBH tag to nickel and streptavidin resin, 293T cells were also transfected with the original ΔGP lacking an epitope tag and with FLAG tagged ΔGP (ΔGP-FLAG), and subjected to tandem affinity purification over nickel and streptavidin resins. The ΔGP purification was undetectable on western blots due to a lack of an epitope tag to JSRV Env and there are no JSRV Env antibodies suitable for western

Fig. 5.3: JSRV Env in single cell clones of ΔGP and ΔGP-HBH transformed 208F cells. Rat fibroblast 208F cells were transfected with either ΔGP or ΔGP-HBH to induce cell transformation. Some of the resulting foci were isolated and subcultured, then plated at a very low concentration to generate single cell clones. The single cell clones that demonstrated transformed phenotype were isolated and subcultured further. (A) RNA from two ΔGP and ΔGP-HBH single cell clones, along with untransformed parental 208F cells, was collected. 20 ng of the resulting cDNA was used for RT-PCR, which was performed with primers targeting the SU region of JSRV Env and also with primers for β-actin as control. Replacement of cDNA with H_2O was used as internal control. Only the RNA from cells that were transformed with either ΔGP or ΔGP-HBH showed JSRV Env signals, while untransformed parental 208F and H_2O control lanes showed no JSRV Env signals. (B) Western blot of the single cell clones. 10% of the total lysates were loaded into 10% SDS-polyacrylamide gel. Blots were probed with anti-RGS6xHis then re-probed with anti-β-Tubulin. Names and sizes of the observed proteins are indicated on the sides of the blot.

A.

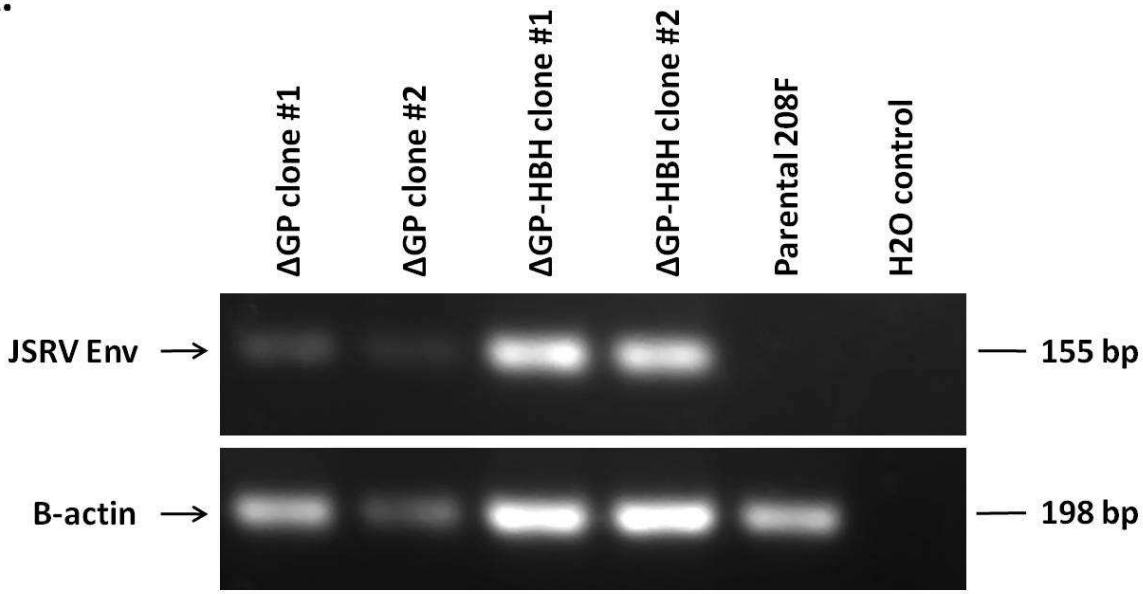
ΔGP clone #1
ΔGP clone #2
ΔGP-HBH clone #1
ΔGP-HBH clone #2
Parental 208F
H2O control
JSRV Env
155 bp
B-actin
198 bp

B.

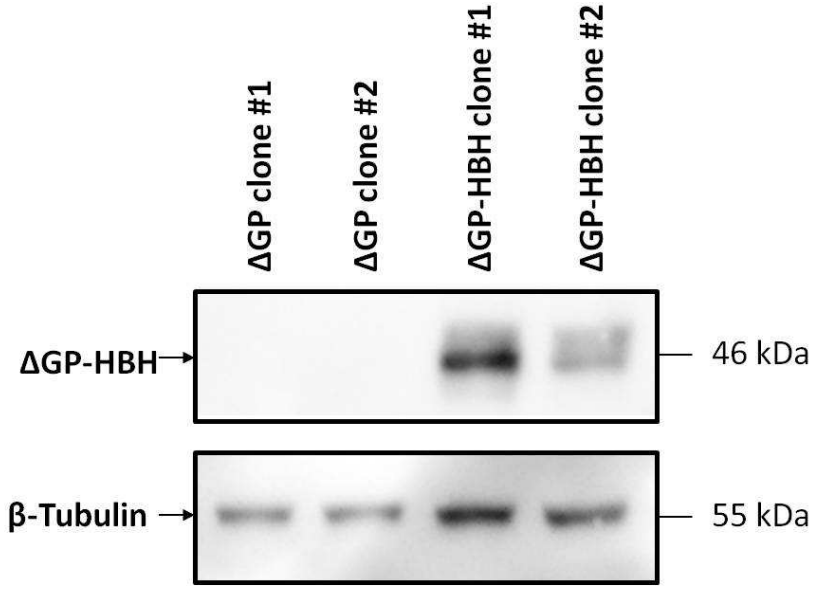
ΔGP clone #1
ΔGP clone #2
ΔGP-HBH clone #1
ΔGP-HBH clone #2
ΔGP-HBH
46 kDa
β-Tubulin
55 kDa

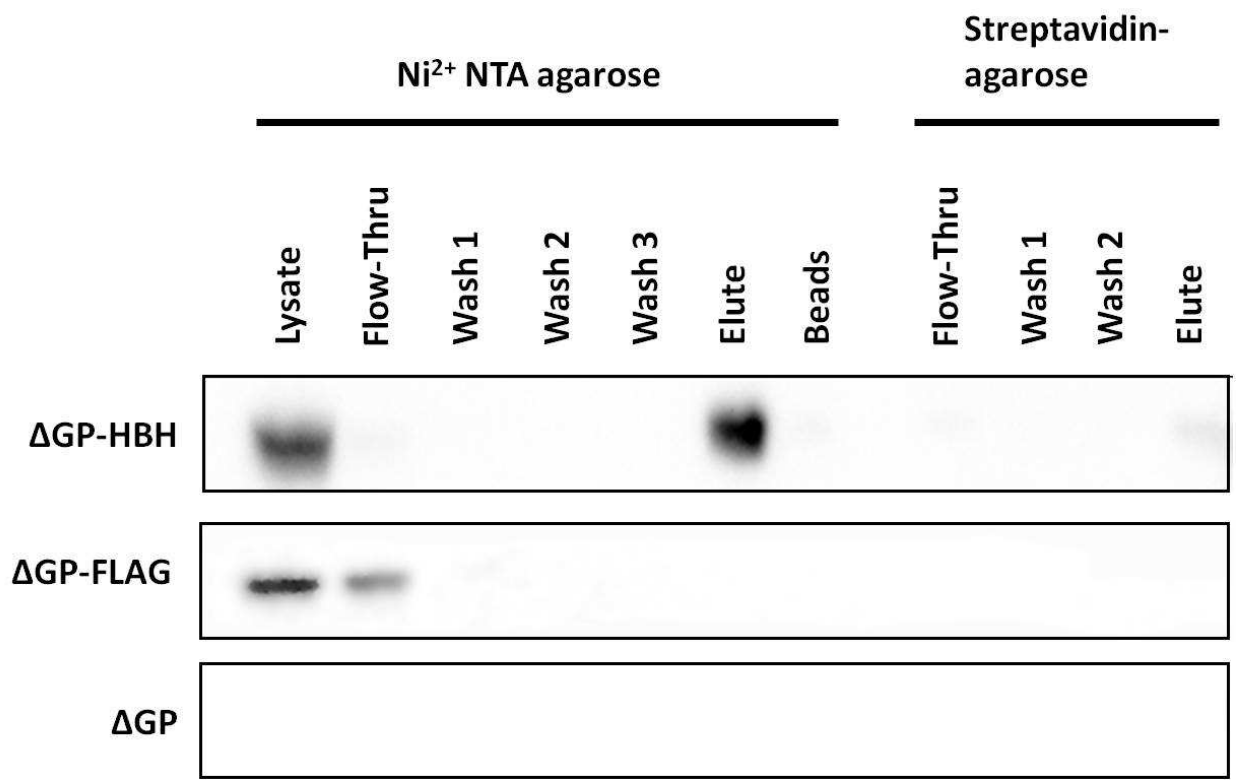

Fig. 5.4: Tandem affinity purification of ΔGP-HBH. HEK 293T cells were transfected with ΔGP, ΔGP-FLAG, or ΔGP-HBH expression vectors. Total cell lysates (Lysate) were incubated with Ni^{2+} resin and the unbound flow through (Flow-thru), washes (Wash 1, 2, and 3) were collected. The eluate from the Ni^{2+} resin (Elute) was collected with the remaining Ni^{2+} resin checked for elution efficiency (Beads). The Ni^{2+}eluate was incubated with streptavidin resin and the flow through, washes and eluate for the streptavidin purification was collected. Protein samples were loaded on 10% acrylamide gel for analysis. All blots were probed with anti-RGS6xHis then re-probed with anti-FLAG antibodies and visualized via chemiluminescence.

blotting (Fig. 5.4 bottom panel). The ΔGP-FLAG control purification showed that the majority of the Env-FLAG in the original cell lysate input was not retained by the nickel beads and was found in the original Flow-Through fraction (Fig. 5.4, middle panel). No more ΔGP-FLAG signal was detected in the subsequent steps of the purification. These results showed that binding of HBH was not only very efficient, but also extremely specific since Env proteins lacking HBH did not bind to or elute from the original nickel column.

To assess the specificity of the tandem affinity purification globally, SDS-PAGE gels of the different purification steps were analyzed by silver staining that would detect all proteins present. In addition to cells transfected with ΔGP-HBH, ΔGP-FLAG and ΔGP, cells transfected with a plasmid expressing enhanced jellyfish green fluorescence protein (EGFP) were analyzed. As shown in Fig 5.5, silver staining of the different purifications showed the large reduction of background signals in the final streptavidin elution as compared with nickel elution (Fig. 5.5), indicating the removal of non-specific signals. The specificity and efficiency of purification of HBH tagged Env was indicated by comparing the streptavidin eluates from 293T cells transfected with ΔGP-HBH vs. the other plasmids. In order to visualize the faint band in the streptavidin elution lane, the acrylamide gel was subjected to a more extensive development time during silver staining (25 min instead of the recommended 3-4 mins). A prominent silver-stained band with a molecular weight appropriate for HBH-tagged TM protein (TM-HBH) was evident only in the ΔGP-HBH transfected cells. Likewise a fainter signal with a molecular weight consistent with HBH-tagged Pr80 Env was specific for the ΔGP-HBH transfected cells.

Discussion

Here we report the construction of a JSRV Env expression vector containing the HBH tandem affinity purification tag (ΔGP-HBH) for use in purification of cellular proteins bound to JSRV Env. We demonstrated that ΔGP-HBH was able to transform rat 208F and RK3E cells, albeit with lower efficiency compared to native JSRV Env. Thus the HBH-tagged Env seem to retain the ability to bind cellular proteins involved in JSRV transformation, and JSRV Env was found in the transformed single cell clones through PCR and the HBH tag was detected by western blot. Tandem affinity purification over nickel affinity and streptavidin resins performed with the cell lysates from ΔGP-HBH transfected 293T cells indicated high efficiency and

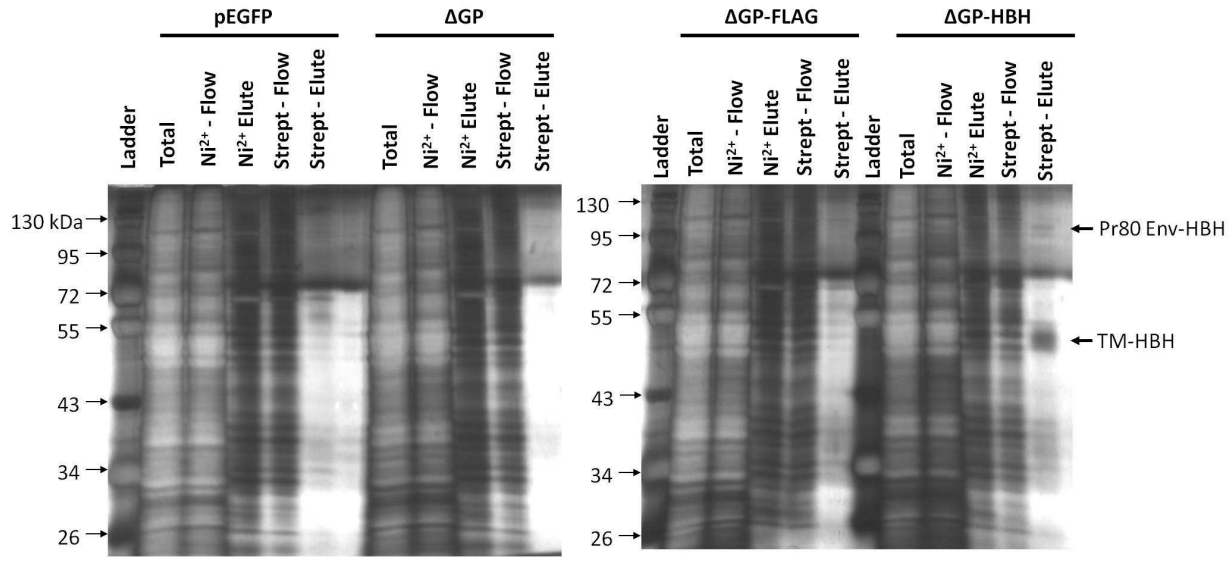

Fig. 5.5: Silver staining of the tandem affinity purified samples under non-deanturing conditions. The total cell lysates (Total) and samples collected from each of the steps of the tandem affinity purification as described in Fig. 5.4 were resolved on a 10% acrylamide gel and the gel was subjected to silver staining. The amount of non-specific background signals were reduced after each purification step. Most of the background proteins were found in the flow through (Ni^{2+} -Flow) in the first purification step using Ni^{2+} resin with some background proteins remaining in the eluate (Ni^{2+} -Elute). The remaining background proteins were found in the flow through after the second purification step using streptavidin resin (Strept-Flow), with faint signals in the eluates (Strept-Elute) that are mainly detectable only after long development time in silver staining. JSRV Env signal was found only in ΔGP-HBH, in the Strept-Elute lane.

specificity of Env-HBH binding and purification. Notably the second step in tandem affinity purification was able to greatly reduce the non-specific detection of cellular proteins observed when only one-step affinity purification was employed. The establishment of the ΔGP-HBH purification system will allow for more stringent purification of JSRV Env and associated proteins from cell lysates, which will be important for proteomic/MS identification of novel JSRV Env interacting proteins.

The tandem affinity purification (TAP) approach has been widely used in conjunction with proteomics/MS to identify proteins that interact with a protein of interested. TAP tags may

consist of epitope tags that bind to specific antibodies (e.g. FLAG or HA) or other tags that allow specific binding to an affinity resin. In comparison to one-step affinity purifications, effective TAP tags yield tagged proteins that bind with high binding affinity to different resins, and sequential binding to the resins results in more stringent purification of the target protein (and associated proteins) with reduces background of proteins that bind non-specifically to the resins. As shown in Fig. 5.5, use of the HBH tagged JSRV Env in native tandem affinity purifications over nickel and streptavidin columns resulted in reduction of non-specific binding proteins after the second affinity purification over streptavidin agarose. Silver staining indicated that a major component of the final eluate was Env protein, while many other proteins were evident in the eluate from the first nickel affinity column. Another feature of the HBH tag is that both the 6-His – Ni^{2+} and biotin-streptavidin interactions also occur in denaturing conditions (36). Thus complexes with HBH-tagged proteins can be purified under denaturing conditions (e.g. 8M urea) if the proteins are first cross-linked; this has been used to identify interactions with yeast Skp1, which is a core component of SCF-ubiquitin ligases and is known to form several distinct multiprotein complexes (34, 36). Thus if some of the cellular proteins important for JSRV transformation have weak or transient interactions with Env, it may be possible to identify them by formaldehyde crosslinking followed by tandem affinity purification under denaturing conditions.

In design of the ΔGP-HBH expression construct, the HBH tag was placed at the C-terminus of the Env protein. This location was chosen because we previously found that the ~10 C-terminal residues of Env (in the CT of TM protein) are not essential for transformation (18), and addition of HA or FLAG epitopes at this position yielded tagged Env proteins that could transform cells (25, 26). Indeed as shown in Fig. 5.2 the HBH-tagged Env protein could

transform rat 208F and RK3E cells, which validates use of this protein in future studies to identify Env-interacting proteins important for transformation. However transformation by ΔGP-HBH showed a ca. 4-6 fold decrease in efficiency compared with untagged ΔGP. This was not unexpected, as we previously found that other C-terminal epitope tagged versions of ΔGP also have lower transformation efficiency (26). The reduced transformation efficiency of ΔGP-HBH is similar to that for HA-tagged Env encoded by ΔGP-HA (ca. 5-fold) that we and others have used extensively in transformation studies (8, 16, 17, 20, 21, 25, 26, 29). In any event tandem affinity purification/proteomics approaches on cells transformed with ΔGP-HBH will be suitable for identifying cellular proteins interacting with the tagged Env in those cells.

One theoretical limitation in using the C-terminal HBH tagged Env protein for identification of associated cellular proteins is that the $Pr80^{env}$ precursor is cleaved during maturation into SU and TM proteins. Thus cellular proteins associated with the SU domain might not be efficiently identified in tandem affinity purification of proteins from ΔGP-HBH transformed cells unless the two subunits become cross-linked with formaldehyde. Indeed, we have previously shown that domains of SU also are important for JSRV transformation in addition to the CT of TM (16). On the other hand as shown in Chapter 3, the nuclear form of Env ($P70^{env}$) is important for transformation (and binding of Zfp111) and $P70^{env}$ is not cleaved into SU and TM. Thus cellular proteins associated with the SU domain of $P70^{env}$ would still be associated with HBH-tagged $P70^{env}$.

As shown in Fig 5.4, elution of HBH-tagged Env protein from the streptavidin agarose used in the second step of tandem affinity purification was rather inefficient. Indeed substantial amounts of the protein apparently even remained bound to the streptavidin agarose after boiling

in Laemmli sample buffer (10% SDS), since much of the HBH-Env was not present in either the non-bound fractions from the streptavidin agarose columns or in the eluate. This was presumably due to the high affinity of streptavidin-biotin binding that is resistant to strong denaturing conditions such as 6M Urea. Even if the HBH tagged Env protein is not efficiently eluted from the streptavidin agarose, it should still be useful for TAP and proteomics/MS. If trypsin digestion is conducted on the streptavidin beads prior to elution (as is often the case), it seems likely that peptides from proteins bound to HBH-tagged Env (as well as Env peptides) will be released from the streptavidin agarose during the proteolysis. In addition, streptavidin contamination was perpetually found in preliminary mass spectrometry results (not shown), due to trypsin digestion of the streptavidin beads. Neutravidin, which does not have the sugar moiety like streptavidin (14), should be more resistant to trypsin cleavage and reduce the levels of streptavidin contamination observed.

In collaboration with Dr. Paul Gershon (UCI), we have carried out three preliminary proteomic/MS experiments to identify proteins bound to HBH-tagged Env. In these experiments 293T cells were transiently transfected with ΔGP-HBH, non-tagged ΔGP or the backbone expression vector pcDNA3.1. Cell extracts were subjected to sequential TAP purification over Ni^{2+} NTA and streptavidin agarose resins. In the second affinity step the streptavidin agarose beads with bound proteins were incubated directly with trypsin, and the released peptides were analyzed by mass spectrometry by Dr. Gershon using the LTQ Velos Pro mass spectrometer. In the first two experiments, TAP was conducted under non-denaturing conditions while in the third experiment cell extracts were fixed with formaldehyde and the TAP purifications were conducted under denaturing conditions (8 M urea). A summary of the results of the three experiments is shown in Table 5.2. Multiple cellular proteins were identified in all samples. Of

Table 5.2. The number of ΔGP-HBH specific candidate proteins from three independent mass spectrometry analyses of TAP purified ΔGP-HBH.

	Experiment 1[A]		Experiment 2[A]		Experiment 3[B]	
	Number of candidates	Unique to ΔGP-HBH	Number of candidates	Unique to ΔGP-HBH	Number of candidates	Unique to ΔGP-HBH
pEGFP	152		130		63	
ΔGP-HBH	143	96	33	10	28	3

[A]TAP purification performed under non-denaturing conditions.
[B]TAP purification performed under crosslinked-denaturing conditions.

greatest interest were proteins that were identified in the ΔGP-HBH transfected cells but not present in TAP samples from control transfected cells. Most of the proteins were common to multiple samples, indicating that they were bound non-specifically to the TAP resins, or that they resulted from contamination of the samples (e.g. by keratins). In each experiment a small number of cellular proteins were uniquely detected in the ΔGP-HBH samples, which could make them candidates for proteins that bind JSRV Env (Table 5.2). However in the three experiments (with the exception of JSRV Env) different unique proteins in the ΔGP-HBH samples were detected. Thus it is unclear if any of these proteins represents genuine interacting partners of JSRV Env. The one protein that was consistently identified uniquely in TAP samples from ΔGP-HBH transfected cells was the JSRV Env protein itself, which was expected and reassuring. JSRV Env peptide sequences identified from mass spectrometry experiment trials showed both SU and TM peptides of JSRV Env (Table 5.3), suggesting that cellular interactors of SU could also be included in the candidates identified in that trial. In addition, one Env signal peptide (SP) sequence was also found. It is unclear why the SP sequence was also identified, as the SP portion of Env is presumably cleaved from the Env precursor polyproteins during translation (6).

Table 5.3. JSRV Env peptide fragments identified in Experiment 1 (in Table 5.2)[1]

Sequence	Residue location in Env	Part of Env
GEQVIIVK	335-342	SU
INTALSRPK	369-377	SU
GVAKGEQVIIVK	331-342	SU
YGDVGVTGFLYPR	281-293	SU
VEMLHMK	583-589	TM
VEMLHMK	583-589	TM
IQCHANYK	462-469	TM
LSALYDVVR	439-447	TM
VMGTQEDIDK	424-433	TM
VMGTQEDIDKK	424-434	TM
VMGTQEDIDKK	424-434	TM
VMGTQEDIDKK	424-434	TM
VLGEQVQSINFR	448-459	TM
NSLTHQMQR	18-26	SP

[1]JSRV Env is 615 residues long, with the SP region spanning residues 1-84, surface protein (SU) spanning residues 85-378, and transmembrane protein (TM) spanning residues 379-615 (4).

Unfortunately, none of the proteins identified by the yeast two-hybrid screening were identified in the preliminary TAP – proteomics/MS experiments, including Zfp111 and RRM2.

In the future, additional TAP purifications and proteomics/MS may lead to the identification of cellular proteins that interact with HBH-tagged JSRV Env. Optimizing the TAP conditions, combined with multiple repeats may eventually result in identification of cellular

proteins that are uniquely and consistently identified in extracts from ΔGP-HBH transfected cells. Improvement in the experimental technique to minimize contamination with keratin, according to existing protocols, will help to reduce this source of non-specific proteins. In addition, use of fixation followed by TAP under denaturing conditions may reduce non-specific binding of proteins. Indeed, in the pilot TAP experiments, fewer proteins were detected in the third experiment where fixation and TAP under denaturing conditions was employed. Finally, alteration in the TAP purification protocol may be advantageous: in the preliminary experiments, the samples for proteomics/MS were generated by trypsin digestion of the material bound to the streptavidin agarose beads; in this approach cellular proteins that bound non-specifically to the beads would also be released by trypsin and analyzed in the MS. As shown in Fig 5.5, the material eluted from the streptavidin beads showed substantially increased purity. Thus digestion of proteins after they are eluted from the streptavidin agarose resin could yield samples with fewer non-specific proteins. The trade-off is that elution from streptavidin-agarose is inefficient (Fig 5.4).

In summary, this chapter describes generation of an expression vector for HBH-tagged JSRV Env protein, ΔGP-HBH. This plasmid may be useful in future proteomics/MS experiments to identify novel cellular proteins that interact with JSRV Env. In light of the fact that multiple signaling pathways are activated during JSRV transformation (11, 15, 23), and there are both cytoplasmic and nuclear forms of Env (Chapter 3), it is likely that multiple cellular proteins that interact with Env are involved in transformation. TAP purification and proteomics/MS with the new form of Env may provide an efficient means to identify such proteins.

References

1. **Alberti, A., C. Murgia, S. L. Liu, M. Mura, C. Cousens, M. Sharp, A. D. Miller, and M. Palmarini.** 2002. Envelope-induced cell transformation by ovine betaretroviruses. J Virol **76:**5387-94.
2. **Allen, T. E., K. J. Sherrill, S. M. Crispell, M. R. Perrott, J. O. Carlson, and J. C. DeMartini.** 2002. The jaagsiekte sheep retrovirus envelope gene induces transformation of the avian fibroblast cell line DF-1 but does not require a conserved SH2 binding domain. J Gen Virol **83:**2733-42.
3. **Bensimon, A., A. J. Heck, and R. Aebersold.** Mass spectrometry-based proteomics and network biology. Annu Rev Biochem **81:**379-405.
4. **Caporale, M., F. Arnaud, M. Mura, M. Golder, C. Murgia, and M. Palmarini.** 2009. The signal peptide of a simple retrovirus envelope functions as a posttranscriptional regulator of viral gene expression. J Virol **83:**4591-604.
5. **Chow, Y. H., A. Alberti, M. Mura, C. Pretto, P. Murcia, L. M. Albritton, and M. Palmarini.** 2003. Transformation of rodent fibroblasts by the jaagsiekte sheep retrovirus envelope is receptor independent and does not require the surface domain. J Virol **77:**6341-50.
6. **Coffin, J. M., Hughes, S.H., Varmus, H.E., editors.** 1997. Synthesis and Organization of Env Glycoproteins. Retroviruses. Cold Spring Harbor (NY): Cold Spring Harbor Laboratory Press.
7. **Cronan, J. E., Jr.** 1990. Biotination of proteins in vivo. A post-translational modification to label, purify, and study proteins. J Biol Chem **265:**10327-33.
8. **Dakessian, R. M., Y. Inoshima, and H. Fan.** 2007. Tumors in mice transgenic for the envelope protein of Jaagsiekte sheep retrovirus. Virus Genes **35:**73-80.
9. **De las Heras, M., S. H. Barsky, P. Hasleton, M. Wagner, E. Larson, J. Egan, A. Ortin, J. A. Gimenez-Mas, M. Palmarini, and J. M. Sharp.** 2000. Evidence for a protein related immunologically to the jaagsiekte sheep retrovirus in some human lung tumours. Eur Respir J **16:**330-2.
10. **Fan, H., M. Palmarini, and J. C. DeMartini.** 2003. Transformation and oncogenesis by jaagsiekte sheep retrovirus. Curr Top Microbiol Immunol **275:**139-77.
11. **Griffiths, D. J., H. M. Martineau, and C. Cousens.** 2010. Pathology and pathogenesis of ovine pulmonary adenocarcinoma. J Comp Pathol **142:**260-83.
12. **Guerrero, C., C. Tagwerker, P. Kaiser, and L. Huang.** 2006. An integrated mass spectrometry-based proteomic approach: quantitative analysis of tandem affinity-purified in vivo cross-linked protein complexes (QTAX) to decipher the 26 S proteasome-interacting network. Mol Cell Proteomics **5:**366-78.
13. **Hiatt, K. M., and W. E. Highsmith.** 2002. Lack of DNA evidence for jaagsiekte sheep retrovirus in human bronchioloalveolar carcinoma. Hum Pathol **33:**680.
14. **Hiller, Y., J. M. Gershoni, E. A. Bayer, and M. Wilchek.** 1987. Biotin binding to avidin. Oligosaccharide side chain not required for ligand association. Biochem J **248:**167-71.
15. **Hofacre, A., and H. Fan.** 2011. Jaagsiekte sheep retrovirus biology and oncogenesis. Viruses **2:**2618-48.
16. **Hofacre, A., and H. Fan.** 2004. Multiple domains of the Jaagsiekte sheep retrovirus envelope protein are required for transformation of rodent fibroblasts. J Virol **78:**10479-89.
17. **Hofacre, A., T. Nitta, and H. Fan.** 2009. Jaagsiekte sheep retrovirus encodes a regulatory factor, Rej, required for synthesis of Gag protein. J Virol **83:**12483-98.
18. **Hull, S., and H. Fan.** 2006. Mutational analysis of the cytoplasmic tail of jaagsiekte sheep retrovirus envelope protein. Journal of virology **80:**8069-8080.
19. **Hull, S., J. Lim, A. Hamil, T. Nitta, and H. Fan.** 2012. Analysis of jaagsiekte sheep retrovirus (JSRV) envelope protein domains in transformation. Virus Genes.
20. **Johnson, C., S. Jahid, D. R. Voelker, and H. Fan.** 2011. Enhanced proliferation of primary rat type II pneumocytes by Jaagsiekte sheep retrovirus envelope protein. Virology **412:**349-56.

21. **Johnson, C., K. Sanders, and H. Fan.** 2010. Jaagsiekte sheep retrovirus transformation in Madin-Darby canine kidney epithelial cell three-dimensional culture. J Virol **84:**5379-90.
22. **Liu, S. L., M. I. Lerman, and A. D. Miller.** 2003. Putative phosphatidylinositol 3-kinase (PI3K) binding motifs in ovine betaretrovirus Env proteins are not essential for rodent fibroblast transformation and PI3K/Akt activation. J Virol **77:**7924-35.
23. **Liu, S. L., and A. D. Miller.** 2007. Oncogenic transformation by the jaagsiekte sheep retrovirus envelope protein. Oncogene **26:**789-801.
24. **Liu, S. L., and A. D. Miller.** 2005. Transformation of madin-darby canine kidney epithelial cells by sheep retrovirus envelope proteins. J Virol **79:**927-33.
25. **Maeda, N., W. Fu, A. Ortin, M. de las Heras, and H. Fan.** 2005. Roles of the Ras-MEK-mitogen-activated protein kinase and phosphatidylinositol 3-kinase-Akt-mTOR pathways in Jaagsiekte sheep retrovirus-induced transformation of rodent fibroblast and epithelial cell lines. J Virol **79:**4440-50.
26. **Maeda, N., Y. Inoshima, D. A. Fruman, S. M. Brachmann, and H. Fan.** 2003. Transformation of mouse fibroblasts by Jaagsiekte sheep retrovirus envelope does not require phosphatidylinositol 3-kinase. J Virol **77:**9951-9.
27. **Maeda, N., M. Palmarini, C. Murgia, and H. Fan.** 2001. Direct transformation of rodent fibroblasts by jaagsiekte sheep retrovirus DNA. Proc Natl Acad Sci U S A **98:**4449-54.
28. **Morozov, V. A., S. Lagaye, J. Lower, and R. Lower.** 2004. Detection and characterization of betaretroviral sequences, related to sheep Jaagsiekte virus, in Africans from Nigeria and Cameroon. Virology **327:**162-8.
29. **Nitta, T., A. Hofacre, S. Hull, and H. Fan.** 2009. Identification and mutational analysis of a Rej response element in Jaagsiekte sheep retrovirus RNA. J Virol **83:**12499-511.
30. **Palmarini, M., and H. Fan.** 2001. Retrovirus-induced ovine pulmonary adenocarcinoma, an animal model for lung cancer. J Natl Cancer Inst **93:**1603-14.
31. **Palmarini, M., H. Fan, and J. M. Sharp.** 1997. Sheep pulmonary adenomatosis: a unique model of retrovirus-associated lung cancer. Trends in microbiology **5:**478-483.
32. **Palmarini, M., J. M. Sharp, M. de las Heras, and H. Fan.** 1999. Jaagsiekte sheep retrovirus is necessary and sufficient to induce a contagious lung cancer in sheep. J Virol **73:**6964-72.
33. **Palmarini, M., J. M. Sharp, C. Lee, and H. Fan.** 1999. In vitro infection of ovine cell lines by Jaagsiekte sheep retrovirus. J Virol **73:**10070-8.
34. **Petroski, M. D., and R. J. Deshaies.** 2005. Function and regulation of cullin-RING ubiquitin ligases. Nat Rev Mol Cell Biol **6:**9-20.
35. **Puig, O., F. Caspary, G. Rigaut, B. Rutz, E. Bouveret, E. Bragado-Nilsson, M. Wilm, and B. Seraphin.** 2001. The tandem affinity purification (TAP) method: a general procedure of protein complex purification. Methods **24:**218-29.
36. **Tagwerker, C., K. Flick, M. Cui, C. Guerrero, Y. Dou, B. Auer, P. Baldi, L. Huang, and P. Kaiser.** 2006. A tandem affinity tag for two-step purification under fully denaturing conditions: application in ubiquitin profiling and protein complex identification combined with in vivocross-linking. Mol Cell Proteomics **5:**737-48.
37. **Travis, W. D., E. Brambilla, M. Noguchi, A. G. Nicholson, K. R. Geisinger, Y. Yatabe, D. G. Beer, C. A. Powell, G. J. Riely, P. E. Van Schil, K. Garg, J. H. Austin, H. Asamura, V. W. Rusch, F. R. Hirsch, G. Scagliotti, T. Mitsudomi, R. M. Huber, Y. Ishikawa, J. Jett, M. Sanchez-Cespedes, J. P. Sculier, T. Takahashi, M. Tsuboi, J. Vansteenkiste, I. Wistuba, P. C. Yang, D. Aberle, C. Brambilla, D. Flieder, W. Franklin, A. Gazdar, M. Gould, P. Hasleton, D. Henderson, B. Johnson, D. Johnson, K. Kerr, K. Kuriyama, J. S. Lee, V. A. Miller, I. Petersen, V. Roggli, R. Rosell, N. Saijo, E. Thunnissen, M. Tsao, and D. Yankelewitz.** 2011. International association for the study of

lung cancer/american thoracic society/european respiratory society international multidisciplinary classification of lung adenocarcinoma. J Thorac Oncol **6:**244-85.

38. **Verwoerd, D. W., A. L. Williamson, and E. M. De Villiers.** 1980. Aetiology of jaagsiekte: transmission by means of subcellular fractions and evidence for the involvement of a retrovirus. Onderstepoort J Vet Res **47:**275-80.
39. **Wilchek, M., and E. A. Bayer.** 1988. The avidin-biotin complex in bioanalytical applications. Anal Biochem **171:**1-32.
40. **Yousem, S. A., S. D. Finkelstein, P. A. Swalsky, A. Bakker, and N. P. Ohori.** 2001. Absence of jaagsiekte sheep retrovirus DNA and RNA in bronchioloalveolar and conventional human pulmonary adenocarcinoma by PCR and RT-PCR analysis. Hum Pathol **32:**1039-42.
41. **Zavala, G., C. Pretto, Y. H. Chow, L. Jones, A. Alberti, E. Grego, M. De las Heras, and M. Palmarini.** 2003. Relevance of Akt phosphorylation in cell transformation induced by Jaagsiekte sheep retrovirus. Virology **312:**95-105.

CHAPTER 6: CONCLUSIONS

Jaagsiekte sheep retrovirus is a betaretrovirus that causes ovine pulmonary adenocarcinoma (OPA) in sheep (34), which is histologically similar to a type of human pulmonary adenocarcinoma called adenocarcinoma in situ (AIS) (39). OPA forms very rapidly in newborn sheep (40), which suggest that JSRV is an acute transforming retrovirus that contains an oncogene. This was confirmed by the demonstration that JSRV can transform cells in culture, a feature of many retroviral oncogenes (8-10). Sequential deletion analysis of the JSRV genome was performed to identify the gene responsible for transformation (29), which revealed the *env* gene to be the oncogene. JSRV Env can transform a wide range of cell lines (2, 18, 23, 26, 33), and transformed cells show activation of two prominent oncogenic signaling pathways: PI3K-Akt-mTOR (1, 6, 27, 28, 32) and Ras-Raf-MEK-ERK1/2 (13, 21, 27). However, JSRV Env protein has not been found to interact directly with components of these two signaling pathways. Hence JSRV Env presumably first interacts with other cellular protein(s) to activate these downstream pathways. Through yeast two-hybrid screening, seven candidate cDNAs were identified based on their interactions with bait containing the JSRV Env cytoplasmic tail (CT) or whole Env (Chapter 2). This thesis was focused on identifying the role and importance of two of these candidate cDNAs, which exhibited strong interaction with the bait proteins and for which multiple independent clones were isolated in the yeast two-hybrid screen: ribonucleotide reductase subunit 2 (RRM2) and zinc finger protein 111 (zfp111). The role of Zfp111 in JSRV Env transformation was explored in Chapter 2. In the process of analyzing Zfp111's role in JSRV transformation, an unexpected finding was discovery of a smaller-sized, nuclear form of JSRV Env that was termed $P70^{env}$. The characteristics of $P70^{env}$were explored in Chapter 3 of the thesis. Chapter 4 was focused on analyzing the role of RRM2 in JSRV Env transformation.

In Chapter 5, a biochemical approach to identify cellular interacting partners of JSRV Env was established: utilizing tandem affinity purification (TAP) of proteins bound to TAP tagged JSRV Env (encoded by ΔGP-HBH) for use in mass spectrometry based identification of bound proteins. The major findings in Chapters 2-5 will be reviewed in this chapter, coupled with a discussion of their significance and future directions.

Chapter 2: The Role of Zfp111 in JSRV Env Transformation

Zfp111, a member of a subset of Cys_2/His_2 zinc finger proteins called Krüppel-like transcription factors(11), was the focus of chapter 2. Co-immunoprecipitation of Zfp111 and JSRV Env was observed, and in particular Zfp111 appeared to be interacting with a faster migration form of JSRV Env. To determine if Zfp111 plays a role in JSRV transformation, zfp111 was knocked down in rat fibroblast 208F cells via a lentiviral shRNA vector. Knockdown of zfp111 reduced JSRV Env transformation levels in these 208F cells by ca. 50%, while it did not affect the transformation by *v-mos*, an oncogene that utilizes transformation pathways different from those of JSRV Env (27). The specificity of zfp111 knockdown for JSRV transformation was verified by restoration of transformation efficiency with a zfp111 cDNA resistant to the shRNA in knockdown cells. Overexpression of zfp111 also led to an increase in JSRV Env transformation. Interestingly while zfp111 knockdown did not inhibit the proliferation of parental 208F cells, it reduced proliferation of JSRV Env transformed cells which suggested that the JSRV transformed cells have become dependent on Zfp111. The evidence presented in this chapter provide strong support for Zfp111 playing a role in JSRV transformation.

So far, only two cellular proteins have been previously found to physically interact with JSRV Env: hyaluronidase-2 (Hyal2) (36) and toll-like receptor 4 (TLR4) (A. Hofacre, J. Rassa, S. Ross and H. Fan, unpublished). Hyal-2 is the receptor for JSRV, and it has been reported to bind to (and block) signaling from the receptor tyrosine kinase RON in human cells (12). JSRV Env binding leads to down regulation of Hyal-2 and results in activation of downstream signaling pathways through the constitutive activation of RON. Signaling downstream of RON involves the PI3K-AKT-mTOR and Ras-Raf-MEK-MAPK pathways. However, rodent Hyal2 does not interact with JSRV Env at high affinity, so it is unlikely that JSRV Env transformation of rodent cell lines such as 208F involves activation of the Hyal-2/Ron axis. TLR4 is a component of innate immunity; upon binding of its ligand (bacterial lipopolysaccharide), a series of downstream interactions leads activation of NFkappaB signaling, and it is unclear if TLR4 binding is important for JSRV transformation. Importantly, several studies have shown the necessity of the JSRV Env cytoplasmic tail (CT) for transformation (2, 20, 24, 26, 33), which strongly suggests that transformation may involve interaction of intracellular proteins with the cytosolic CT (17, 36). Zfp111 is the first intracellular protein shown to interact with JSRV Env protein and it interacts with the CT alone and whole Env. Thus it could be one of the proteins interacting with the CT of JSRV Env at the plasma membrane. However as discussed below, the relevant interactions between Zfp111 and Env may be nuclear.

The results reported in Chapter 2 described the importance of Zfp111 for transformation of rat 208F fibroblasts. In the future it will be interesting to investigate if Zfp111 is important for JSRV transformation of other cell lines and systems. The experiments were conducted in 208F cells because the r1104 shRNA vector was relatively effective; comparably effective shRNA vectors for mouse Zfp111 were not successfully developed (3 vectors tested). In the

future the effects of Zfp111 over-expression on JSRV transformation could be tested in cells of other species where knockdown vectors are not currently available; enhancement of transformation would be consistent with a role for Zfp111 in transformation of those cells. Ideally it would be desirable to test the role of ovine Zfp111 on JSRV transformation of ovine lung epithelial cells. While an efficient *in vitro* transformation system have not been developed for ovine lung epithelial cells, it would be interesting to test OPA tumor tissues for enhanced expression of ovine Zfp111 protein since it seems possible that JSRV would stabilize that protein analogously to the apparent stabilization of Zfp111 in rat cells. Development of antisera capable of recognizing endogenous Zfp111 in immunohistochemistry and western blots will be important for future studies.

In the future it would also be interesting to investigate if Zfp111 may be involved in the etiology of non-viral cancers such as human lung cancer. We have screened human lung cancer cell lines (e.g. A549), and transcripts of the putative human homolog of Zfp111 (Znf226) were detectable at low levels. However gene expression databases of human tumors (e.g. Oncomine) have not reported expression of Znf226, although this may reflect the fact that this gene remains uncharacterized and unannotated. Epigenetic and proteomic surveys of human tumors may also be important in case Znf226 is over-abundant by stabilization, similar to how Zfp111 may stabilized be in JSRV transformation of 208F cells.

Analysis of the co-immunoprecipitation of Zfp111 and JSRV Env revealed two interesting observations: 1) intracellular Zfp111 levels were enhanced in cells co-transfected with JSRV Env and 2) the appearance of a faster migrating Env band $P70^{env}$. $P70^{env}$ was found to be the form of Env that co-immunoprecipitated with Zfp111 (Fig. 2.1). Although the two proteins co-immunoprecipitated *in vivo*, one question was to determine how a nuclear protein

such as Zfp111 can interact with a cytoplasmic protein such as JSRV Env. The observation that P70^{env} is a nuclear protein provided a rationale for the interaction. Characterization of P70^{env} was the focus of Chapter 3.

Chapter 3: Characterization of Nuclear Env (P70^{env}) and its Interaction with Zfp111

The identification of P70^{env} provided a clue to how Env and Zfp111 proteins can interact with each other, since both of these proteins are nuclear. Co-transfection of FLAG tagged JSRV Env plasmid (ΔGP-FLAG) and HA-tagged Zfp111 plasmid (Zfp111-HA) resulted in enhanced levels of both proteins, consistent with binding and co-stabilization. Cell fractionation experiments indicated that P70^{env} is nuclear.

The next question addressed was the molecular relationship between P70^{env} and Pr80^{env}, the polyprotein precursor for the virion Env proteins SU and TM. Viral envelope proteins undergo extensive post-translational modifications in the form of glycosylation during their passage from the endoplasmic reticulum through the golgi to the plasma membrane (7). Treatment of Pr80^{env} and P70^{env} with endoglycosidase F indicated that they share the same polypeptide backbone, around 60 kDa in size. Thus the difference between Pr80^{env} and P70^{env} was in their glycosylation levels. Chymotryptic digestion of Endo F-treated and -untreated Pr80^{env} was used to determine the regions and degrees of glycosylation for the two proteins. The N-terminal domains of both proteins were found to have similar levels of glycosylation, and they differed in the fact that P70^{env} lacked glycosylation downstream of residue 215, while approximately half of the glycosylation of Pr80^{env} was in this region (including the TM domain which is glycosylated).

The identification of P70^{env} brings new possibilities to studies on the JSRV transformation. Previous studies on JSRV transformation focused on signaling pathways that start in the cytoplasm, indicated by the fact that envelope proteins have been consdered to be at the plasma membrane or in the RER or Golgi (15, 17, 25, 38). However, the identification of the nuclear P70^{env} and its binding to Zfp111 (a likely nucleic acid binding protein) expands potential JSRV transformation mechanisms. JSRV Env may directly affect the gene expression in transformed cell, perhaps by interacting with transcriptional activators or suppressors such as Zfp111. It would be interesting to see if P70^{env} can interact with other nuclear proteins, which might be identified through experiments described in Chapter 5. The results of this chapter make searching for transcriptional differences between normal and JSRV-transformed cells attractive. Standard approaches would be to perform gene expression microarrays or deep RNA sequencing (RNAseq). Also, given the results of Chapters 2 and 3, it would be interesting to identify genes under direct transcriptional control of Zfp111 by chromatin immunoprecipitation (CHiP and CHiP-Seq) (35). Such genes could then be evaluated for roles in JSRV Env transformation by RNA interference or over-expression. Such experiments could uncover another level of transformation mechanisms for JSRV.

One important question is how P70^{env} is transported to the nucleus. One possibility could be that P70^{env} contains a nuclear localization signal (NLS) in its polypeptide sequence. In fact when JSRV Env polyprotein is initially translated, the signal peptide region (residues 1-83) is cleaved off and retained as a fuctional protein Rej, that is involved in Gag-Pro-Pol protein translation and unspliced viral RNA export from the nucleus (4, 19, 31). Rej contain an NLS, which is cleaved off the Env polypeptide during translation, so the Rej NLS is not present in Pr80^{env} and P70^{env} (7). Scanning the Pr80^{env}/P70^{env} polypeptide sequence did not reveal any

predicted NLS sites [T.H. unpublished data; scans performed with NucPred (3) and RNABindR v2.0 (41)]. However it is still possible that there an atypical NLS hidden in the Env sequence that is revealed by the changes in glycosylation of $P70^{env}$. Another possibility could result from specific glycosylation of $P70^{env}$. Previous work has shown that specific glycosylation markers can lead to the re-localization of cellular proteins into the nucleus (37). Large proteins (MW>40 kDa) that cannot normally pass through the nuclear pores can re-localize into the nucleus when parts of these proteins were modified with specific types of α-glucoside and α-mannoside moieties (37). It will be interesting to identify the types of glycosylation on $P70^{env}$ as compared with $Pr80^{env}$, and whether Zfp111 binding alters the glycosylation. The nature of the glycosylation could be studied by mass spectrometry of purified $P70^{env}$ or $Pr80^{env}$.

In the last part of this chapter, alanine scanning mutants of JSRV CT were used to characterize its binding to Zfp111. These mutants were previously characterized for their transformational abilities in rodent cells (20). The amount of Zfp111 co-immunoprecipitated with given mutants was found to correlate with to their respective transformation potentials. In the mutants with little or no transformation activity, Zfp111 co-immunoprecipitation signals were the weakest. The strongest interactions were found in mutants that showed WT JSRV CT transformation levels. However super-transformer mutants showed weaker interaction with Zfp111, perhaps because they were activating other (cytoplasmic) pathways. These co-immunoprecipitation assays also showed correlations between the signal strength of Zfp111 and $P70^{env}$, again supporting direct binding of these two proteins. While the two-hybrid screen and the studies with the CT alanine scanning mutants indicate a primary region of interaction between $P70^{env}$ and the TM cytoplasmic tail, it will be interesting to test if other domains are

important for Zfp111 binding. We have previously generated deletions and point mutations in SU and the ectodomains of TM which could be used for such studies (18, 21).

Studies of the alanine scanning mutants also suggested regions in the cytoplasmic tail important for Zfp111 binding (residues 583 - 596). The solution NMR structure of the CT has been solved in collaboration with Dr. Melanie Cocco (UC Irvine) and it will be interesting to relate the structure to both Zfp111 binding and transformation activity. NMR studies of isotopically labeled CT when Zfp111 is added would also provide information about the nature of the binding. The current Zfp111 cDNA plasmids might need to be optimized for high efficiency expression in bacterial systems for such experiments.

Chapter 4: The Role of RRM2 in JSRV Env Transformation

In Chapter 4, the other candidate from the yeast two-hybrid screen was analyzed for its role in JSRV Env transformation. RRM2 could be pulled down with GST-tagged JSRV Env CT. NIH 3T3 cells transfected with HA-tagged JSRV Env showed not only co-localization of the endogenous RRM2 with JSRV Env, but also a re-localization of the RRM2 from a diffuse, evenly spread, cytoplasmic staining to becoming concentrated at the cytoplasmic membrane where JSRV Env was found. A lentiviral shRNA vector led to up to 70% reduction in RRM2 RNA in 208F cells, and JSRV transformation assays in these cells showed a 50% decrease in transformation levels. The same cells also show a 30% decrease in transformation levels when transfected with *v-mos* oncogene. These results suggest that knockdown of RRM2 may have an oncogene-independent effect on cell transformation levels, but there should also be a specific effect of RRM2 knockdown on JSRV transformation. Cell proliferation asays showed that

RRM2 knockdown led to a significant decrease in proliferation, suggesting that this general decrease may cause the reduction in *v-mos* transformation in RRM2 knockdown cells.

If the general decrease in cell proliferation (and presumably) transformation levels resulting from RRM2 knockdown can be alleviated, the specific effect of RRM2 knockdown on JSRV Env transformation may be more critically evaluated. As discussed in Chapter 4, addition of exogenous deoxyribonuclotides has been reported to counteract the deoxyribonucleotide depletion in cells where ribonucleotide reductase was inhibited cells with hydroxyurea (22). We have encountered significant cytotoxicity when dA and dG were added to growth media for 208F cells and were not able to continue transformation assays (data not shown). Optimization of the exogenous purine deoxyribonucleosides addition may help to remove the general effects of RRM2 knockdown and identify additional specific effects of RRM2 knockdown on JSRV transformation. Alternatively other cells may be less sensitive to the dA/dG toxicity.

If RRM2 is confirmed to be involved in JSRV transformation, this would expand the list of cellular proteins that interact with JSRV Env and affect transformation beyond Zfp111. In comparison with Zfp111, RRM2's role in JSRV transformation was easier to envision, given that RRM2 is a cytoplasmic protein and known to be a potential target for therapeutic drugs (5, 16, 22, 42). In addition, RRM2 has been shown to be involved in the MAPK signaling pathways, in which overexpression of RRM2 leads to an increase in Raf proteins at the plasma membrane in *Ras* transformed cells (14). The results from existing studies on RRM2 and oncogenesis show many similarities with what we know to be happening in JSRV oncogenesis (e.g. RRM2 overexpressing transgenic mice show cancer in the lungs exclusively, RRM2 overexpression increases Raf proteins in the MAPK pathway).

Chapter 5: Tandem Affinity Purification of HBH-tagged JSRV Env.

Chapter 5 describes the development of a biochemical approach to identifying new and confirming JSRV Env interacting proteins namely mass spectrometry. The arginine-glycine-serine (RGS) hexahistidine-biotination site-hexahistidine (HBH) tag allows for tandem affinity purification (TAP) of the tagged protein under non-denaturing or denaturing conditions, and should theoretically help to remove much of the background/non-specific proteins. The HBH-tagged JSRV Env (ΔGP-HBH) could transform both RK3E and 208F cells, albeit with a 4-6 fold decrease in transformation efficiency as compared with untagged JSRV Env (ΔGP). Purification using Ni^{2+} and streptavidin beads showed high efficiency and specificity of ΔGP-HBH binding and purification, and the tandem affinity purification was effective in removing non-specific proteins binding after the 2^{nd} purification step from streptavidin beads. Candidate proteins from three independent purifications were identified, with 3 to 96 ΔGP-HBH unique candidates, depending on the experiment. However none of the unique candidates from one experiment overlapped with those of another with the exception of JSRV Env protein itself. The proteins identified from the initial yeast two-hybrid screen did not show up in the proteomic/MS analysis either. Interestingly, the SU domain of the JSRV Env was found to be in the purified ΔGP-HBH samples, consistent with interactions between the SU and TM proteins even after $Pr80^{env}$ cleavage (e.g. disulfide bridges). Moreover, western blot results show that $P70^{env}$ is not cleaved into SU and TM domains. This suggests that cellular interactors of SU would also be part of the candidates identified, in which some of these candidates could be ones that interact with $P70^{env}$.

Although the mass spectrometry analysis of the first 3 purification trials did not yield protein candidates that were common across the 3 trials, the results of this chapter lay the groundwork for future proteomic/MS identification of Env-interacting proteins. Refinement of

the TAP purifications (with and without denaturation) may lead to the identification of Env-interacting proteins that are consistently detected. Once such candidates are identified, they can be analyzed for binding to Env (SU or TM) and roles in JSRV Env transformation as described in Chapters 2-4. It may be particularly interesting to conduct experiments on cells co-expressing ΔGP-HBH and Zfp111, given the enhancement of Env and Zfp111 levels in such cells. Additional interacting proteins (including those bound to an Env-Zfp111 complex) might be identified in this case. Another direction would be to compare binding of cellular proteins to wild-type and mutant Env proteins -- e.g., the the alanine scanning mutants of the CT. Proteins whose binding is dependent on a particular CT residue could be identified by the use of differentially isotopically labeled tags [SILAC approaches (30)] of mutant and WT Env-transfected cells, in combination with TAP and MS.

References

1. **Alberti, A., C. Murgia, S. L. Liu, M. Mura, C. Cousens, M. Sharp, A. D. Miller, and M. Palmarini.** 2002. Envelope-induced cell transformation by ovine betaretroviruses. J Virol **76:**5387-94.
2. **Allen, T. E., K. J. Sherrill, S. M. Crispell, M. R. Perrott, J. O. Carlson, and J. C. DeMartini.** 2002. The jaagsiekte sheep retrovirus envelope gene induces transformation of the avian fibroblast cell line DF-1 but does not require a conserved SH2 binding domain. J Gen Virol **83:**2733-42.
3. **Brameier, M., A. Krings, and R. M. MacCallum.** 2007. NucPred--predicting nuclear localization of proteins. Bioinformatics **23:**1159-60.
4. **Caporale, M., F. Arnaud, M. Mura, M. Golder, C. Murgia, and M. Palmarini.** 2009. The signal peptide of a simple retrovirus envelope functions as a posttranscriptional regulator of viral gene expression. J Virol **83:**4591-604.
5. **Cerqueira, N. M., S. Pereira, P. A. Fernandes, and M. J. Ramos.** 2005. Overview of ribonucleotide reductase inhibitors: an appealing target in anti-tumour therapy. Curr Med Chem **12:**1283-94.
6. **Chow, Y. H., A. Alberti, M. Mura, C. Pretto, P. Murcia, L. M. Albritton, and M. Palmarini.** 2003. Transformation of rodent fibroblasts by the jaagsiekte sheep retrovirus envelope is receptor independent and does not require the surface domain. J Virol **77:**6341-50.
7. **Coffin, J. M., Hughes, S.H., Varmus, H.E., editors.** 1997. Synthesis and Organization of Env Glycoproteins. Retroviruses. Cold Spring Harbor (NY): Cold Spring Harbor Laboratory Press.
8. **Coffin, J. M., Hughes, S.H., Varmus, H.E., editors. .** 1997. A Brief Chronicle of Retrovirology. Retroviruses. Cold Spring Harbor (NY): Cold Spring Harbor Laboratory Press; 1997. .
9. **Coffin, J. M., Hughes, S.H., Varmus, H.E., editors. .** 1997. Growth and Assay of Pathogenic Retroviruses. Retroviruses. Cold Spring Harbor (NY): Cold Spring Harbor Laboratory Press; 1997. .

10. **Coffin, J. M., Hughes, S.H., Varmus, H.E., editors. .** 1997. Oncogenesis. Retroviruses. Cold Spring Harbor (NY): Cold Spring Harbor Laboratory Press; 1997. .
11. **Dang, D. T., J. Pevsner, and V. W. Yang.** 2000. The biology of the mammalian Kruppel-like family of transcription factors. Int J Biochem Cell Biol **32:**1103-21.
12. **Danilkovitch-Miagkova, A., F. M. Duh, I. Kuzmin, D. Angeloni, S. L. Liu, A. D. Miller, and M. I. Lerman.** 2003. Hyaluronidase 2 negatively regulates RON receptor tyrosine kinase and mediates transformation of epithelial cells by jaagsiekte sheep retrovirus. Proceedings of the National Academy of Sciences of the United States of America **100:**4580-4585.
13. **De Las Heras, M., A. Ortin, A. Benito, C. Summers, L. M. Ferrer, and J. M. Sharp.** 2006. In-situ demonstration of mitogen-activated protein kinase Erk 1/2 signalling pathway in contagious respiratory tumours of sheep and goats. J Comp Pathol **135:**1-10.
14. **Fan, H., C. Villegas, and J. A. Wright.** 1996. Ribonucleotide reductase R2 component is a novel malignancy determinant that cooperates with activated oncogenes to determine transformation and malignant potential. Proc Natl Acad Sci U S A **93:**14036-40.
15. **Griffiths, D. J., H. M. Martineau, and C. Cousens.** 2010. Pathology and pathogenesis of ovine pulmonary adenocarcinoma. J Comp Pathol **142:**260-83.
16. **Heidel, J. D., J. Y. Liu, Y. Yen, B. Zhou, B. S. Heale, J. J. Rossi, D. W. Bartlett, and M. E. Davis.** 2007. Potent siRNA inhibitors of ribonucleotide reductase subunit RRM2 reduce cell proliferation in vitro and in vivo. Clin Cancer Res **13:**2207-15.
17. **Hofacre, A., and H. Fan.** 2011. Jaagsiekte sheep retrovirus biology and oncogenesis. Viruses **2:**2618-48.
18. **Hofacre, A., and H. Fan.** 2004. Multiple domains of the Jaagsiekte sheep retrovirus envelope protein are required for transformation of rodent fibroblasts. J Virol **78:**10479-89.
19. **Hofacre, A., T. Nitta, and H. Fan.** 2009. Jaagsiekte sheep retrovirus encodes a regulatory factor, Rej, required for synthesis of Gag protein. J Virol **83:**12483-98.
20. **Hull, S., and H. Fan.** 2006. Mutational analysis of the cytoplasmic tail of jaagsiekte sheep retrovirus envelope protein. Journal of virology **80:**8069-8080.
21. **Hull, S., J. Lim, A. Hamil, T. Nitta, and H. Fan.** 2012. Analysis of jaagsiekte sheep retrovirus (JSRV) envelope protein domains in transformation. Virus Genes.
22. **Kwon, N. S., D. J. Stuehr, and C. F. Nathan.** 1991. Inhibition of tumor cell ribonucleotide reductase by macrophage-derived nitric oxide. J Exp Med **174:**761-7.
23. **Liu, S. L., F. M. Duh, M. I. Lerman, and A. D. Miller.** 2003. Role of virus receptor Hyal2 in oncogenic transformation of rodent fibroblasts by sheep betaretrovirus env proteins. J Virol **77:**2850-8.
24. **Liu, S. L., M. I. Lerman, and A. D. Miller.** 2003. Putative phosphatidylinositol 3-kinase (PI3K) binding motifs in ovine betaretrovirus Env proteins are not essential for rodent fibroblast transformation and PI3K/Akt activation. J Virol **77:**7924-35.
25. **Liu, S. L., and A. D. Miller.** 2007. Oncogenic transformation by the jaagsiekte sheep retrovirus envelope protein. Oncogene **26:**789-801.
26. **Liu, S. L., and A. D. Miller.** 2005. Transformation of madin-darby canine kidney epithelial cells by sheep retrovirus envelope proteins. J Virol **79:**927-33.
27. **Maeda, N., W. Fu, A. Ortin, M. de las Heras, and H. Fan.** 2005. Roles of the Ras-MEK-mitogen-activated protein kinase and phosphatidylinositol 3-kinase-Akt-mTOR pathways in Jaagsiekte sheep retrovirus-induced transformation of rodent fibroblast and epithelial cell lines. J Virol **79:**4440-50.
28. **Maeda, N., Y. Inoshima, D. A. Fruman, S. M. Brachmann, and H. Fan.** 2003. Transformation of mouse fibroblasts by Jaagsiekte sheep retrovirus envelope does not require phosphatidylinositol 3-kinase. J Virol **77:**9951-9.

29. **Maeda, N., M. Palmarini, C. Murgia, and H. Fan.** 2001. Direct transformation of rodent fibroblasts by jaagsiekte sheep retrovirus DNA. Proc Natl Acad Sci U S A **98:**4449-54.
30. **Mann, M.** 2006. Functional and quantitative proteomics using SILAC. Nat Rev Mol Cell Biol **7:**952-8.
31. **Nitta, T., A. Hofacre, S. Hull, and H. Fan.** 2009. Identification and mutational analysis of a Rej response element in Jaagsiekte sheep retrovirus RNA. J Virol **83:**12499-511.
32. **Palmarini, M., and H. Fan.** 2001. Retrovirus-induced ovine pulmonary adenocarcinoma, an animal model for lung cancer. J Natl Cancer Inst **93:**1603-14.
33. **Palmarini, M., N. Maeda, C. Murgia, C. De-Fraja, A. Hofacre, and H. Fan.** 2001. A phosphatidylinositol 3-kinase docking site in the cytoplasmic tail of the Jaagsiekte sheep retrovirus transmembrane protein is essential for envelope-induced transformation of NIH 3T3 cells. J Virol **75:**11002-9.
34. **Palmarini, M., J. M. Sharp, M. de las Heras, and H. Fan.** 1999. Jaagsiekte sheep retrovirus is necessary and sufficient to induce a contagious lung cancer in sheep. J Virol **73:**6964-72.
35. **Park, P. J.** 2009. ChIP-seq: advantages and challenges of a maturing technology. Nat Rev Genet **10:**669-80.
36. **Rai, S. K., F. M. Duh, V. Vigdorovich, A. Danilkovitch-Miagkova, M. I. Lerman, and A. D. Miller.** 2001. Candidate tumor suppressor HYAL2 is a glycosylphosphatidylinositol (GPI)-anchored cell-surface receptor for jaagsiekte sheep retrovirus, the envelope protein of which mediates oncogenic transformation. Proc Natl Acad Sci U S A **98:**4443-8.
37. **Rondanino, C., M. T. Bousser, M. Monsigny, and A. C. Roche.** 2003. Sugar-dependent nuclear import of glycosylated proteins in living cells. Glycobiology **13:**509-19.
38. **Swanstrom, R., Wills, J. W.** 1997. Synthesis, Assembly, and Processing of Viral Proteins. In: Coffin JM, Hughes SH, Varmus HE, editors. Retroviruses. Cold Spring Harbor (NY): Cold Spring Harbor Laboratory Press; 1997.
39. **Travis, W. D., E. Brambilla, M. Noguchi, A. G. Nicholson, K. R. Geisinger, Y. Yatabe, D. G. Beer, C. A. Powell, G. J. Riely, P. E. Van Schil, K. Garg, J. H. Austin, H. Asamura, V. W. Rusch, F. R. Hirsch, G. Scagliotti, T. Mitsudomi, R. M. Huber, Y. Ishikawa, J. Jett, M. Sanchez-Cespedes, J. P. Sculier, T. Takahashi, M. Tsuboi, J. Vansteenkiste, I. Wistuba, P. C. Yang, D. Aberle, C. Brambilla, D. Flieder, W. Franklin, A. Gazdar, M. Gould, P. Hasleton, D. Henderson, B. Johnson, D. Johnson, K. Kerr, K. Kuriyama, J. S. Lee, V. A. Miller, I. Petersen, V. Roggli, R. Rosell, N. Saijo, E. Thunnissen, M. Tsao, and D. Yankelewitz.** 2011. International association for the study of lung cancer/american thoracic society/european respiratory society international multidisciplinary classification of lung adenocarcinoma. J Thorac Oncol **6:**244-85.
40. **Verwoerd, D. W., A. L. Williamson, and E. M. De Villiers.** 1980. Aetiology of jaagsiekte: transmission by means of subcellular fractions and evidence for the involvement of a retrovirus. Onderstepoort J Vet Res **47:**275-80.
41. **Walia, R. R., C. Caragea, B. A. Lewis, F. Towfic, M. Terribilini, Y. El-Manzalawy, D. Dobbs, and V. Honavar.** 2012. Protein-RNA interface residue prediction using machine learning: an assessment of the state of the art. BMC Bioinformatics **13:**89.
42. **Zuckerman, J. E., T. Hsueh, R. C. Koya, M. E. Davis, and A. Ribas.** 2011. siRNA knockdown of ribonucleotide reductase inhibits melanoma cell line proliferation alone or synergistically with temozolomide. J Invest Dermatol **131:**453-60.